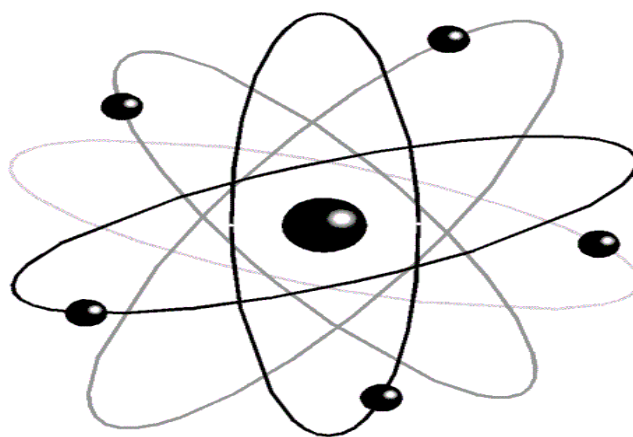People's Democratic Republic of Algeria
Ministry of Higher Education and Scientific Research
University Med Khider Biskra
Faculty of Exact Sciences and Sciences of Nature and Life

Department of Matter Sciences

Domain : Matter science

Spinneret: Chemistry

Field: Pharmaceutical Chemistry

Master's graduation thesis
Entitled:

Experimental, Spectral Characterization and Docking Studies of some bioactive agents.

Presented by:

Chikhaoui Abderrahime

Jury members:

*Mme:*Fettah Asma   *President*

*Mme:*Harkati Dalal   *Supervisor*

*Mr:*Boumedjane Youcef   *Examiner*

Acknowledgement

First and foremost, I owe a debt of gratitude to Almighty **Allah** who enlightens my path, and granted me the capability to proceed successfully.

At the outset, I would like to thank my supervisor Mme Harkati Dalal for her efforts, advice, and comments to achieve this work.

I wish to extend my sincere thanks to Mme Fettah Asma and Mr Boumedjane Youcef for accepting reading, and evaluating this research paper.

I would like also to thank all the teachers who support me with their continual incentives, and their encouraging advices and special thanks to Mr. Djani Fayssal who granted me support and strength I really needed

My deepest thanks go to all my friends who have constantly given me support and strength to continue this research and are extended to my colleagues who never refused to assist me. I am very grateful to Zineb Djoudi and Mariem Ghamri who gave me a helping hand during this research.

I wish also to thank my entire family for providing a loving environment for me.

Dedication

This Thesis is dedicated ….

To my wonderful parents who have raised me to be the

person I am today, to my beloved brother and sister; You have been with me

every step of the way, through good and bad times. Thank you for all the

unconditional love, guidance, and support that you have always given me.

To all my relatives and friends

And finally to you, dearest reader.

Abderrahime

CONTENTS

Chapter I: Background review

*Chapter II: Methods and Technique*s

Chapter III: Experimental assays

Chapter IV: Theoretical assays

Abstract

LIST OF ABBREVIATIONS AND ACRONYMS

AM1: Austin Model 1

Amber : Assisted Model Building with Energy Refinement

DFT: Density functional theory

DPPH: α, α-diphenyl-β-picrylhydrazyl

FTIR: Fourier-transform infrared spectroscopy

HOMO: Highest Occupied Molecular Orbital

IC50: Half maximal inhibitory concentration

LUMO: Lowest Unoccupied Molecular Orbital

MOE: Molecular operating envirenment

MVD: Molegro Virtual Docker

NMR: Nuclear magnetic resonance

PDB: Protein Data Bank

RMSD: Root-mean-square deviation

TLC: Thin-layer chromatography

TRPV1: The transient receptor potential cation channel subfamily V member 1

UV: Ultraviolet

LIST OF TABLES

CHAPTER III

CHAPTER VI

LIST OF FIGURES

CHAPTER I

CHAPTER II

CHAPTER III

CHAPTER VI

GENERAL INTRODUCTION

The questions of whether medicines discovered today are safer, more efficacious, and more affordable than generic medicines (whose patents have expired) or medicines that are centuries old could be answered "no" for most of the modern medicines. If so, then it is logical to revisit and revive these age-old medicines for the welfare of mankind. Curcumin is one such medicine. Its history goes back over 5000 years, to the heyday of Ayurveda (which means the science of long life). Turmeric derived from the rhizome of the plant *Curcuma longa* has been used by the people of the Indian subcontinent for centuries with no known side effects, not only as a component of food but also to treat a wide variety of ailments.

Turmeric is a spice of golden color that is used in cooking in the Indian subcontinent. Because of its color and taste, turmeric was named "Indian saffron" in Europe. Today, India is the primary exporter of turmeric (known as haldi in India). Although its ability to preserve food through its antioxidant mechanism, to give color to food, and to add taste to the food is well known, its health promoting effects are less well recognized or appreciated. It was once considered a cure for jaundice, an appetite suppressant, and a digestive. In Indian and Chinese medicines, turmeric was used as an anti-inflammatory agent to treat gas, colic, toothaches, chest pains, and menstrual difficulties. This spice was also used to help with stomach and liver problems, to heal wounds and lighten scars, and as a cosmetic.[1]

Curcumin has a diverse array of favourable properties including its capacity as an antioxidant, anti-inflammatory and anti-carcinogen.Furthermore, curcumin has generally been demonstrated to have low toxicity and is capable of crossing the blood brain barrier. However, this hydrophobic molecule displays low bioavailability, which is a particular challenge for treatment of central nervous system disorders. In spite of this limitation, the administration of curcumin has been shown to be effective in the treatment of neurodegenerative disorders such as Alzheimer's disease, Parkinson's disease, stroke and tardive dyskinesia, as well as other brain disorders such as multiple sclerosis, depression, and brain tumours. While curcumin's diverse mechanisms of action in the treatment of disease continue to be an enigma, its therapeutic usefulness and cost effectiveness make it a particularly valuable compound. [2]

On the other hand; Predicting and understanding the properties of a chemical compound are of great importance both from technological and academic points of view. In the same way the behaviour of the real material systems is also of great importance both form technical and academic point of view. The theoretical problems associated with these systems are quite complex. Quantum chemical computational methods have become a useful tool for solving interesting chemical problems and reaction mechanism. It has become a useful way to investigate materials to make predictions about the structure and properties of molecule and solids before running the actual experiments that are too difficult or too expensive.[3, 4]

This work will highlight some of curcumin potential properties using experimental and theoretical approaches for a better understanding of the implications of curcumin in our body system.

Our research is divided onto four chapters:

❖ The first chapter is devoted to a literature review covering some hand knowledge of curcumin as a natural component and see some generalities on the Transient Receptor Potential (TRP).

❖ The second chapter highlights the techniques and methods in both experimental and theoretical assays used or applied during our study.

❖ The third chapter aims to focus on the experimental assays starting with extraction and separation of curcumin, spectral FT-IR results investigation and finally an examination of antioxidant activity for the separated curcuminoids.

❖ The fourth chapter illustrates a theoretical approach including optimization and docking investigation of the chosen curcuminoids.

And finally a general conclusion that summarizes the essence of our research.

References

1. Aggarwal, B.B., Y.-J. Surh, and S. Shishodia, *The molecular targets and therapeutic uses of curcumin in health and disease*. Vol. 595. 2007: Springer Science & Business Media.

2. Sookram, C., et al., *CURCUMIN: IMPLICATIONS IN THE TREATMENT OF CENTRAL NERVOUS SYSTEM DISEASE.* Asia Pacific Journal of Life Sciences, 2012. **6**(2): p. 115.

3. Zerner, M., *Reviews in Computational Chemistry.* Vol. 2, Capítulo 8, pág. 313-365, KB Lipkowitz, DB Boyd Eds., VCH Publishers, Inc, 1991.

4. Lorenc, J., et al., *Crystal and molecular structure of 2‑amino‑5‑chloropyridinium hydrogen selenate—its IR and Raman spectra, DFT calculations and physicochemical properties.* Journal of Raman Spectroscopy, 2008. **39**(7): p. 863-872.

CHAPTER

1

BACKGROUND REVIEW

I. CURCUMIN BACKGROUND:

I.1. COMPOSITION OF TURMERIC:

Turmeric contains a wide variety of phytochemicals, including curcumin, demethoxycurcumin, bisdemethoxycurcumin, zingiberene, curcumenol, curcumol, eugenol, tetrahydrocurcumin, triethylcurcumin, turmerin, turmerones, and turmeronols.[1] Curcumin, demethoxycurcumin, and bisdemethoxycurcumin have also been isolated from *Curcuma mangga*,[2](**Figure I.1**).

Curcumin is the phytochemical that gives a yellow color to turmeric and is now recognized as being responsible for most of the therapeutic effects. It is estimated that 2–5% of turmeric is curcumin. Curcumin was first isolated from turmeric in 1815, and the structure was delineated in 1910 as diferuloylmethane. Most currently available preparations of curcumin contain approximately 77% diferuloylmethane, 18% demethoxycurcumin, and 5% bisdemethoxycurcumin. Curcumin is hydrophobic in nature and frequently soluble in dimethylsulfoxi de, acetone, ethanol, and oils. It has an absorption maxima around **420 nm**. When exposed to acidic conditions, the color of turmeric/curcumin turns from yellow to deep red, the form in which it is used routinely for various religious ceremonies.

I.2. CURCUMIN ANALOGUES:
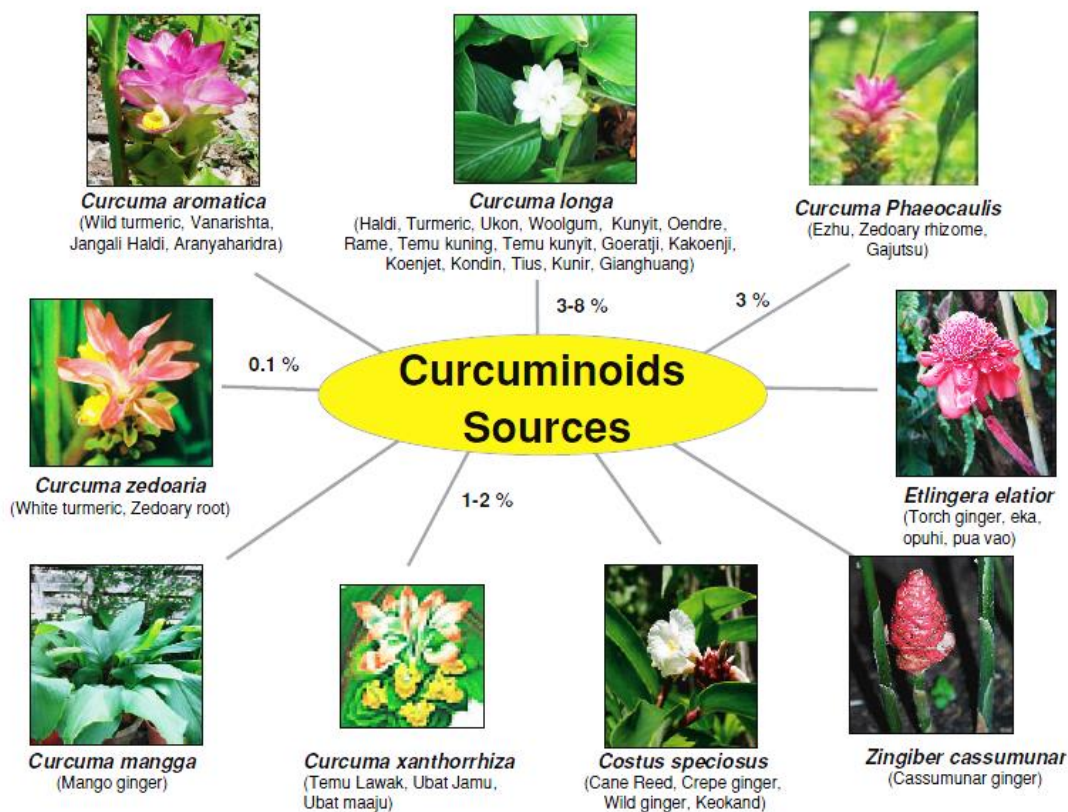
Figure I.1: Curcuminoids sources

As indicated earlier, turmeric contains three different analogues of curcumin (i.e., diferuloylmethane, also called curcumin, demethoxycurcumin, and bisdemethoxycurcumin (**Figure I.2**). Whether all three analogues exhibit equal activity is not clear. Although in most systems curcumin was found to be most potent, in some systems bisdemethoxycurcumin was found to exhibit higher activity. There are also suggestions that the mixture of all three is more potent than either one alone.

When administered orally, curcumin is metabolized into curcumin glucuronide and curcumin sulfonate. However, when administered systemically or intraperitoneally, it is metabolized into tetrahydrocurcumin, hexahydrocurcumin, and hexahydrocurcuminol. Tetrahydrocurcumin has been shown to be active in some Systems and not in others. Whether other metabolites of curcumin exhibit biological activity is not known.
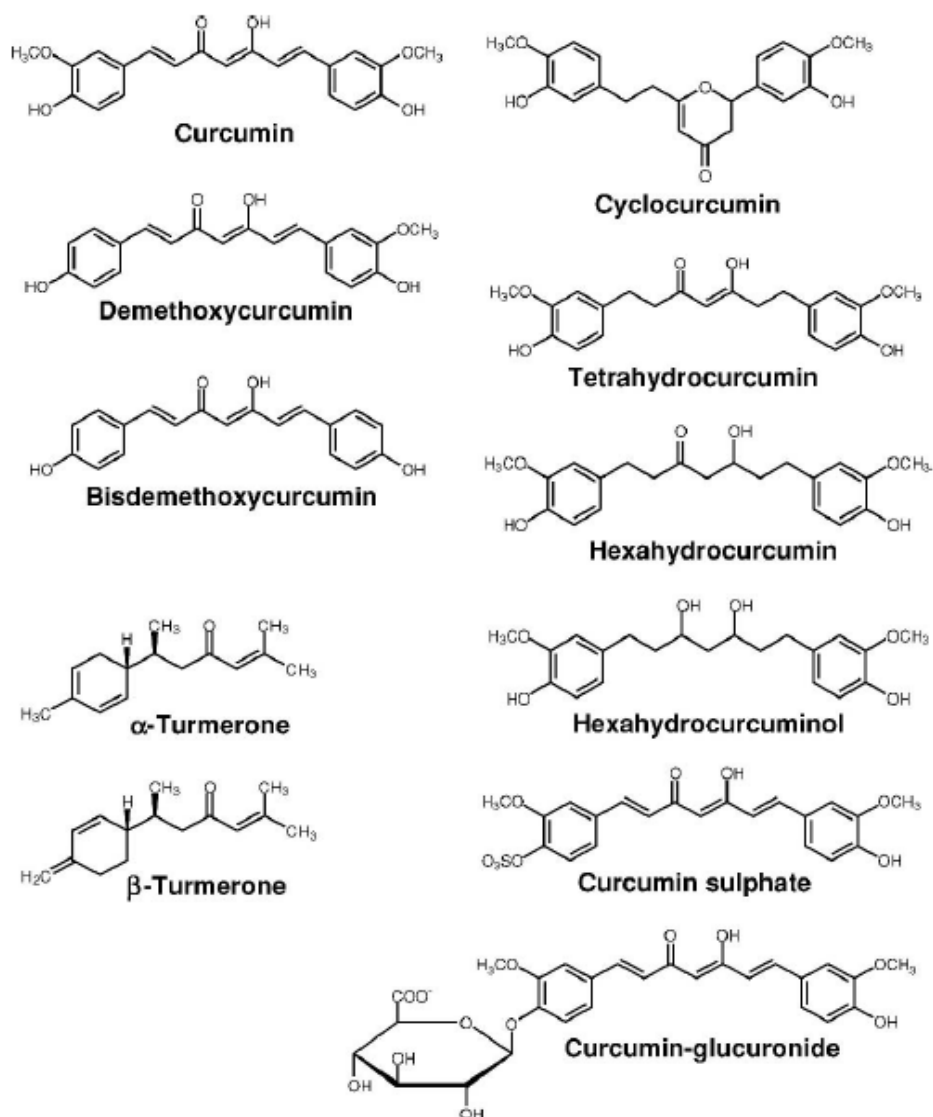
Figure I.2: Chemical structures of curcumin and its analogues

I.3. USES OF CURCUMIN:

The use of turmeric for health purposes is nothing new. As a folklore medicine, its use has been documented in both Indian and Chinese cultures. The long list of uses includes antiseptic, analgesic, anti-inflammatory, antioxidant, antimalarial, insectrepellant, and other activities associated to turmeric. Perhaps one of the most often prescribed uses is for wound-healing .It is now well recognized that most chronic diseases are the result of dysregulated inflammation.[3, 4]

Turmeric has been traditionally described as an anti-inflammatory agent. Recent scientific evidence has indeed demonstrated that turmeric, and curcumin in particular, exhibits potent anti-inflammatory activities as determined by a wide variety of systems. Therefore, it is not too surprising that turmeric displays activities against a variety of diseases. Because curcumin also exhibits potent antioxidant activity, whether the anti-inflammatory activity of curcumin is mediated through its antioxidant mechanism is not clear. Since most well-characterized antioxidants do not exhibit anti-inflammatory activity, it is unlikely that the anti-inflammatory activity of curcumin is due to its antioxidant activity.

I.4. MOLECULAR TARGETS OF CURCUMIN :

So many preclinical studies in vitro and in vivo have prompted various clinical trials in human subjects. among which many of them are already completed.These different clinical trials that are being conducted or already completed. In trials conducted with humans only minor side effects of curcumin, namely diarrhoea, have been reported, and it is considered safe and well tolerated.

In order to understand the health benefits of curcumin it is necessary to well-known its mechanisms of action based on the modulation of several molecular targets at this time it is described the molecular action of curcumin on the main molecular targets:

I.4.1. Curcumin Inhibits Transcription Factors :

Curcumin is a potent inhibitor of the activation of various transcription factors including nuclear factor-κB (NF-κB), activated protein-1 (AP-1), signal transducer and activator of transcription (STAT) proteins, peroxisome proliferator-activated receptor-g (PPAR-g), and β- catenin [5].

These transcription factors regulate the expression of genes that contribute to tumorigenesis, inflammation, cell survival, cell proliferation, invasion, and angiogenesis.

- NF-κB. Is one of the key transcription factors responsive to curcumin; many of the observed biological effects of curcumin involve processes that are NF-κB-dependent. For example, curcumin is capable to inhibit the survival and proliferation of diveses human tumor cell lines (myeloid leukaemia, B non-Hodgkin's lymphoma (NHL),embryonic kidney, mouse macrophage) by suppressing NF-κB-regulated gene products.[6]

- STAT proteins. They have an ubiquitous role in tumourigenesis; curcumin concretely inhibits STAT3 activation in human multiple myeloma [6] and Hodgkin and Reed-Sternberg lymphoma cells [7]. This protein is involved in dysregulation of cell growth, invasion, angiogenesis, metastasis and resistance to apoptosis.

- PPAR-g. Is a transcription factor that exerts anti-inflammatory, anti-cancer and insulin-sensitising actions. Curcumin is capable to induce the action of this receptor in rat liver cells[8].

- β-catenin. Is a central component of the cadherin cell adhesion complex. Curcumin induces activation of caspase-3, which in turn mediates cleavage of β –catenin and therefore impairs cell-cell adhesion pathways, resulting in cell cycle arrest at the G2/M phase and induction of apoptosis in in vitro models [9].

- AP-1. Is a transcription factor that is frequently associated with activation of NF-κB. Curcumin has been shown to inhibit the activation of AP-1 induced by tumour promoters[10].

- Response Element-Binding Protein. Along with histone acetyltransferases (HAT), have been implicated in cancer cell growth and survival. It has been proved that curcumin is a selective HAT inhibitor in vitro and in vivo [11].

I.4.2. Curcumin Down-regulates the Expression of p53 :

P53 is a tumour suppressor and transcription factor. It plays an important role as regulatorof many cellular processes, including cell signal transduction, cellular response to DNA damage, genomic stability, cell cycle control, and apoptosis. Curcumin has been shown to be a potent inhibitor of p53. In this molecular target the role of curcumin in complex, it has been shown that curcumin can inhibits P53 in immature B cell lymphoma mouse cell lines, a colon cancer cell line and myeloid leukaemic cells. On the contrary, other experiments show induction of p53 by curcumin. Therefore, it should take into account the different activity of curcumin in different types of cancer[12].

I.4.3. Cyclin

Cyclin D1 is a rate-limiting factor in progression of cells through the first gap (G1) phase of the cell cycle. Therefore, the loss of its regulation is a risk factor for cancer development. Curcumin down-regulates the expression of cyclin D1 at the transcriptional and posttranscriptional levels [13]

I.4.4. Inflammatory Enzymes:

- Cyclooxygenase-2 (COX-2). Is a form of prostaglandin H synthase regulated by mitogens, tumor promoters, cytokines, and growth factors. Curcumin exerts significant COX-2-inhibiting activity through suppression of NF-κB[14].
- Lipoxygenases (LOX). The family of lipoxygenases is responsible for several inflammatory processes such as asthma or allergy. Curcumin inhibits the activity of some LOX lisoenzymes and inhibits the release of compounds by LOX which promote inflammatory responses [15].

I.4.5. Curcumin Downregulates the Activity of Numerous Kinases :

A variety of tyrosine kinases are activated by mutations that contribute to the malignant transformation, growth, and metastasis of human cancers. Cellular experiments in vitro have shown that curcumin completely inhibits the activity of several protein kinases including phosphorylase kinase, protein kinase C (PKC), protamine kinase (cPK) , autophosphorylation activated protein kinase (AK), epidermal growth factor receptor (EGFR) .[14]

I.5. MEDICINAL PROPERTIES OF CURCUMIN:

The wealth of in vitro and pre-clinical data has provided a strong basis from which to progress to the trialling of curcumin in human subjects. In addition to the modulation of numerous metabolic pathways by curcumin in vitro assays, numerous studies carried out in rodents show that curcumin is active in numerous animal models for chronic diseases.

Pharmacokinetics and pharmacodynamics of curcumin have been also studied; first in rodents, and later in humans producing generally similar data. Results show that curcumin does not appear to be toxic to animals or humans even at high doses [16].

This safety allowed to conduct quite a lot human trials to test curcumin for chronic disease, several studies have been already completed and others are nowadays in development. Findings evidence that curcumin has the following benefits.

I.5.1. Anti-Inflammatory Activity:

Research shows curcumin is a highly pleiotropic molecule capable of interacting with numerous molecular targets involved in inflammation. Modulation of the inflammatory response by curcumin is carried out by down-regulating the activity of cyclooxygenase-2 (COX-2), lipoxygenase and inducible nitric oxide synthase (iNOS) enzymes; also by inhibiting the production of the inflammatory cytokines tumor necrosis factor-alpha (TNF-a) , interleukin (IL) -1, -2, -6, -8 and -12, monocyte chemoattractant protein (MCP), and migration inhibitory protein and down-regulating mitogen-activated and Janus kinases. [17]

I.5.2. Curcumin as Palliative Therapy for Cancerous Skin Lesions:

Curcumin could act similarly to corticosteroids in external sebaceous neoplasms. It improves lesions itching; odour, drying, pain and lesion size [14].

I.5.3. Curcumin Possibly Prevents Gallstone Formation:

A potential risk of gall bladder cancer is gallstone formation. Therefore, the emptying of gall bladder is a key factor in cancer prevention. Curcumin had shown this ability in a randomized, double-blind, crossover study involving 12 healthy volunteers[18]

I.5.4. Curcumin May Improve Cognitive Function in the Elderly:

Nowadays, several diseases in the elder stage of the life which diminish cognitive function are unfortunately becoming common. One of these diseases is the Alzheimer's disease (AD). Some natural antioxidants have been tested to treat AD without a great success.

Curcumin is several times more potent than vitamin E as a free radical scavenger, protects the brain from lipid peroxidation and scavenges NO-based radicals produced during inflammation. In the study of Limm et al. [19] they reported that the Indian spice curcumin suppresses indices of inflammation and oxidative damage in the brains of mice, factors that have been implicated in AD pathogenesis.

I.5.5. Curcumin Acts as Radiosensitizing and Radioprotective :

Curcumin have demonstrated to exert a dual mode of action after irradiation, depending on its dose. Curcumin could be useful in cancer treatment because of it protects various systems against the deleterious effects induced by ionizing radiation [20] and enhances the effect of this radiation in cancerous cells. [21]

I.5.6. Curcumin against Diabetes:

Curcumin is a potent antioxidant. It has been shown that curcumin is useful in preventing glucose-induced oxidative stress in the endothelial cells and in the heart of diabetic animals. It has also been observed that short-term treatment of diabetic rats with curcumin prevents diabetes-induced decreased antioxidant enzyme levels and kidney dysfunction; an important activity by the fact that diabetic nephropathy is a major cause of morbidity in diabetic patients [22].

I.5.7. Curcumin Diminish Symptoms of Irritable Bowel Syndrome

Two pilot studies demonstrated that curcumin, when given orally, reported benefit to patients with proctitis and Crohn's disease [23] or improved symptoms of irritable bowel disease after treatment [24].

All these effects are mediated by the fact that, as is mentioned above and well-known, curcumin can modulate a wide range of molecular targets. The anti-cancer properties of curcumin are mediated through its regulation of various transcription factors, growth factors, inflammatory cytokines, protein kinases, and other enzymes.

II. TRP CHANNELS:

For survival, all organisms depend on their ability to perceive, interpret and react to changes in their environment. Temperature sensing is an important element in the functioning of organisms, allowing for appropriate behavioural responses to changes in environmental temperature and the avoidance of prolonged contact with harmfully hot or cold objects. The mammalian sensory system is able to detect subtle changes in temperature through thermosensitive nerve terminals of primary afferent sensory neurons, which represent a fraction of the total of sensory afferents.

These thermosensitive nerve-endings express a subset of non-selective cationic ion channels of the Transient Receptor Potential (TRP) family, which respond to a range of different temperatures, spanning the whole range of the perceived temperature spectrum from burning hot to ice cold. Of these thermosensitive TRP channels.

II.1. ION CHANNELS:

Each cell is enclosed by a membrane, consisting of a double layer of phospholipids, which holds the essential cellular components together and separates them from the external environment. Due to the tight packing of lipid molecules, the bilayer is hydrophobic in nature and acts as a barrier to the diffusion of small charged molecules and ions such as Na^+, K^+, Ca^{2+} or Cl^-. For a proper and controlled regulation of ion flow, cell membranes contain specialized transmembrane proteins such as ion transporters and ion channels. Ion channels allow for the passive diffusion of ions, determined by a favourable electrochemical gradient, set up and maintained by ATP-driven ionic transporters that actively pump ions across the membrane.

When an ion channel opens, the ions rapidly diffuse through the channel pore, generating a flow of current and changing the membrane potential. Ion channels are found in the membranes of all cells, where they fulfil several essential functions.

These include controlling the resting membrane potential, shaping electrical signals in excitable cells and gating the flow of messenger Ca^{2+} ions [25].

Ion channels open and close their permeation pathway (i.e. pore) because of conformational changes of the channel protein, which is referred to as gating. Gating occurs by several mechanisms, such as the binding of a specific natural ligand or pharmacological compound, transmembrane voltage changes, mechanical perturbation of the membrane, light or temperature changes. A further defining feature of ion channels is their pore, the ion conductive pathway, which is selectively permeable and so allows only the passage of a certain class of ions.

Ion channels are classified by their gating mechanism, their ionic selectivity and by phylogenetic criteria like the homology of their amino acid sequences [25, 26].

II.2. THE TRP ION CHANNEL SUPERFAMILY:

Transient Receptor Potential (TRP) ion channels are an important superfamily of ion channels and derive their name from the phenotype of a mutant *Drosophila melanogaster* fly, the *Trp*-mutant. Measurements of the receptor potential response in the fly eye to visual stimuli, known as the electroretinogram, revealed that *Trp*-mutant flies display a transient negative receptor potential that quickly returns to baseline under continuous illumination, unlike their wild type counterparts in which the negative receptor potential is sustained [27]

TRP channels are non-selective cationic ionic channels, mediating the flow of Ca^{2+} and Na+ across the cell membrane. The opening of a TRP channel causes membrane depolarization, facilitating the generation of action potentials in excitable cells. In non-excitable cells, TRP channels can mediate a large fraction of Ca^{2+} entry upon stimulation.

The TRP superfamily has been found to display a greater diversity in gating mechanisms than any other group of ion channels, and it is this diversity that allow them to play critical roles in sensory physiology, which includes vision, hearing, olfaction, touch, thermo- and osmosensation, nociception, pheromone signaling and taste transduction [28]

II.2.1. TRP nomenclature and phylogenetic distribution:

The diverse cation channels that together make up the TRP superfamily vary markedly in their ion selectivity and gating mechanisms. However, they share significant sequence homology and therefore are classified based upon their protein sequence similarity [29] The

TRP superfamily is subdivided into seven subfamilies of which three (TRPC, TRPV and TRPM) are closely related to the classical TRP channel, whilst four additional subfamilies (TRPA, TRPML, TRPP and TRPN) are more divergent . Dependent on the organism in which they are expressed. **Figure I.3** represents a Sequence homology analyses that show how all TRP channels fall into seven subfamilies that comprise proteins with distinct channel properties.

Because TRPC2 is a pseudogene in humans and TRPNs are not present in mammals, mouse TRPC2 and fish TRPN1 were used to show relations between all subfamilies. The TRP subfamilies are represented by different colours [28].
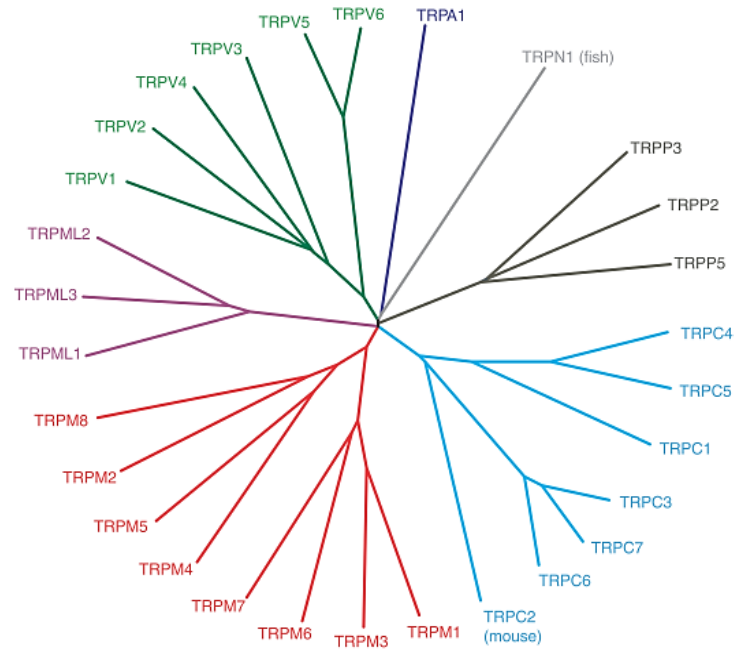
Figure I.3:Phylogenetic tree of human TRP channels

Briefly, the TRPC ('Canonical') subfamily consists of 7 members and is closely related to the TRP originally described in *Drosophila* [30]; [31] . It was the first TRP subfamily reported in mammals   [32]. A homolog of the TRPC2 gene exists in humans, but is non-functional. The TRPM ('Melastatin') subfamily has 8 members and is named after its first identified member, TRPM1, which was previously called melastatin [33] .

By using the vanilloid compound capsaicin as a ligand, the first member of the TRPV ('Vanilloid') subfamily was discovered [34] The TRPV subfamily includes 6 members. The TRPA ('Ankyrin') subfamily consists of only one member in mammals, and its name refers to the numerous ankyrin repeats in its N-terminus. The TRPP ('Polycystin') subfamily contains 3 members that are also known as polycystic kidney disease (PKD) proteins. Mutations in TRPP1 and TRPP2 underlie the most common form of hereditary kidney disease [35] The TRPML ('Mucolipin') subfamily encompasses 3 members, and mutations in TRPML1 are associated with mucolipidosis type IV, a neurodegenerative lysosomal storage disorder [36] Finally, the TRPN ('NOMP-C') is named after the NO-mechano-potential C channel in *Caenorhabditis elegans* and is absent in mammals. In vertebrates, the only animals known to express TRPN are the zebrafish *Danio rerio* and the frog *Xenopus laevis* [37]; [38]

II.2.2. General TRP structure and permeability

TRP proteins consist of six putative transmembrane (6TM) segments (S1-S6) (**Figure I.4**) with large intracellular amino- (N) and carboxyl- (C) termini. It is thought that most TRP proteins assemble as homotetramers to form cation-permeable pores, just as voltage gated K+ channels whose three dimensional structure they resemble [39] .Some heteromultimeric channels are reported to form between members of the same subfamily or different subfamilies, although their biological relevance remains unclear [40].The reported interaction between subunits of the TRPV1 and TRPA1 ion channel is the latest example of the formation of a functional heteromultimeric TRP channel [41]

In a typical TRP channel, the four centre-facing 2TM elements, S5 and S6, form the gate and selectivity filter of the channel. The re-entrant loop between S5 and S6 forms the pore of the channel, while the extracellular side of the pore loop shapes a selectivity filter for the exclusive permeation of certain ions The cytoplasmic ends of S6 form the lower gate, which opens and closes to regulate cation entry into the channel (a,b.). The elements that are outside of the S5-S6 region either function as linkers to elements that control gating or are associated with subunit association [39] .A significant number of TRP channels are weakly voltage dependent, and gating occurs by the movement of charged elements upon a change in the transmembrane potential.

The location of the voltage sensor in TRP channels remains unclear. However, in a recent structural study of TRPV1, S1 to S4 remain stationary upon channel activation, suggesting a less active role in gating [39] .

By performing charge reversal mutations, another group concluded that S4 does not have a separate role in the gating of TRPM8, but rather that voltage sensitivity depends upon an interaction between S3 and S4 [42] .
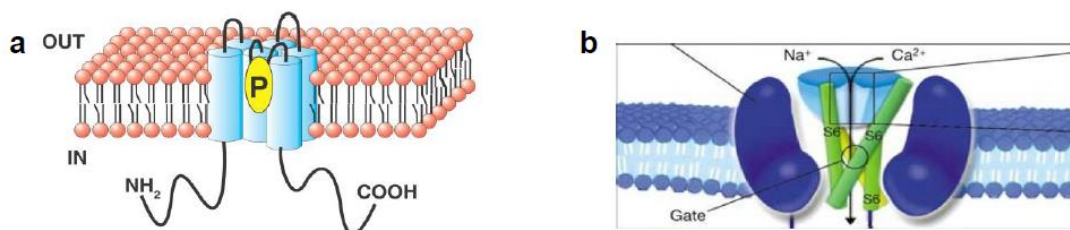
Figure I.4: All TRP-proteins contain six transmembrane segments (S1 to S6) with a putative pore region (P) between S5 and S6. Amino- and carboxyl-termini are variable in length and contain different sets of domains. b) The selectivity filter formed by the extracellular side of the pore loop (light blue) and the cytoplasmic parts of S6 which shape the lower gate shown in more detail. S5 is not shown

II.2.3. Gating, expression and function: TRP channels as ideal polymodal sensors:

As stated earlier, an enormous variety of gating mechanisms have been described within the TRP superfamily. They include voltage-, ligand-, mechano- and temperature-gated TRP channels, as well as constitutively active channels. Moreover, many TRP channels are polymodal, which means that the channel can be gated by several different stimuli.

Because TRP channels are expressed in nearly all mammalian cell types, they are thought to play important roles in a large variety of biological processes. In particular, by virtue of their multiple gating mechanisms, TRP channels are highly suited to function in receptor cells and thus in sensory physiology. Indeed, they are found to act as sensors to a broad range of environmental and endogenous stimuli, such as temperature, chemical irritants, osmolarity, pheromones and growth factors.

In brief, several TRP channels are involved in chemosensation, which is a broad class by definition and involves multiple sensory modalities, such as smell, taste and the detection of chemical compounds. Chemosensation is important for the detection of irritant and poisonous chemicals and as such has a protective or defensive function. TRPA1 is a preeminent example of a TRP channel that is activated by reactive chemicals, and among its chief ligands are a large variety of natural pungent chemicals, such as mustard oil, allicin and cinnemaldehyde.

TRPA1 activation is responsible for the pungent feel of many foods[43] In the taste buds of the tongue, TRPM5 is involved in the downstream taste transduction of sweet, bitter and umami receptors [44] Furthermore it has been implicated in the detection of signaling molecules such as pheromones in mouse olfactory sensory neurons.

Figure I.5 , represents Hypothetical correspondence between activation of TRP channels, body surface temperature and evoked sensations. Upper part: Schematic representation of the thermal activation profile of various TRP channels when expressed in recombinant systems. All of them have been located in sensory neurons and/or skin cells. [45]. Middle part: Schematic representation of impulse activity in various cutaneous sensory receptors during application to their receptive fields of temperatures indicated in the thermal scale. Lower part: Quality of sensations evoked in humans by application to the skin of different temperature values. [46]
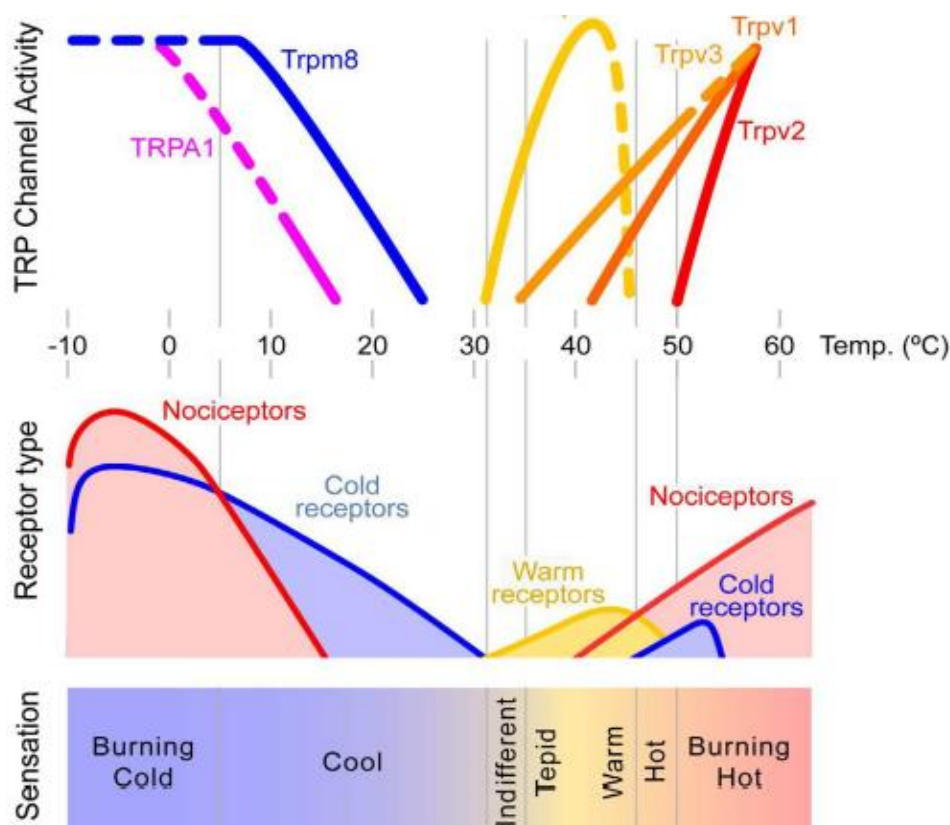
Figure I.5:Hypothetical correspondence between activation of TRP channels, body surface temperature and evoked sensations

II.3. TRP CHANNELS AND DISEASE:

Mutations and misregulation of some TRP channels have been linked to pathophysiology and disease, which is perhaps unsurprising considering their large diversity and association with a multitude of biological processes.

When TRP-related diseases are considered, one can distinguish between TRP channelopathies, as diseases caused by channel malfunction are called, and diseases in which TRPs are involved due to their nature as targets for irritants, inflammation products and toxins. To date, mutations in at least six members of the TRP family have been identified as TRP-channel related channelopathies in humans [47] .Misregulation of TRP channels, such as changes in the number of expressed TRP channels and channel (de)sensitization, can lead to diminished or potentiated responses to stimuli, and may result in disease. Mechanism through which misregulation lead to disease include disruptions in calcium signaling, which plays an important role in many processes, mistuning of sensory input, disturbances in calcium and magnesium homeostasis, disturbed organelle function, trafficking and dysfunctions in the control of cell proliferation and growth.

Diseases caused by dysfunction and misregulation of TRP channels make them promising targets for pharmacological modulation. However, the lack of knowledge about the function of many TRP channels and the limited number of available selective modulators has hindered the development of approved drugs that target TRP channels [48];[47]

II.4. THERMOTRPS:

The ability of an organism to sense ambient temperature and to avoid harmful extremes is essential to its survival. Thermosensitive ion channels in free nerve endings of peripheral sensory neurons that innervate the skin and mucosa are crucial to temperature sensation, the most notable being a small group of TRP channels that stand out by their extreme sensitivity to temperature. A way to quantify the temperature sensitivity of an ion channel is by measuring the temperature coefficient (Q_{10}), which is the change in the rate of gating by a change in temperature of 10°C. Typical ion channels have a Q_{10} around 3, similar to the effect of temperature on other enzymatic reactions [25].However, temperature sensitive TRP channels have Q_{10} values ≥ 5. Due to their high temperature dependence, these thermosensitive TRP channels were dubbed thermoTRPs [45].

References

1. Chattopadhyay, I., et al., *Turmeric and curcumin: Biological actions and medicinal applications.* CURRENT SCIENCE-BANGALORE-, 2004. **87**: p. 44-53.

2. Abas, F., et al., *A Labdane Diterpene Glucoside from the Rhizomes of Curcuma m angga.* Journal of natural products, 2005. **68**(7): p. 1090-1093.

3. Kumar, A., et al., *Nuclear factor-κB: its role in health and disease.* Journal of molecular medicine, 2004. **82**(7): p. 434-448.

4. Aggarwal, B.B., et al., *Nuclear transcription factor NF-kappa B: role in biology and medicine.* 2004.

5. Bharti, A.C., N. Donato, and B.B. Aggarwal, *Curcumin (diferuloylmethane) inhibits constitutive and IL-6-inducible STAT3 phosphorylation in human multiple myeloma cells.* The Journal of Immunology, 2003. **171**(7): p. 3863-3871.

6. Chen, A., J. Xu, and A. Johnson, *Curcumin inhibits human colon cancer cell growth by suppressing gene expression of epidermal growth factor receptor through reducing the activity of the transcription factor Egr-1.* Oncogene, 2006. **25**(2): p. 278.

7. Chiu, J., et al., *Curcumin prevents diabetes-associated abnormalities in the kidneys by inhibiting p300 and nuclear factor-κB.* Nutrition, 2009. **25**(9): p. 964-972.

8. Epstein, J., I.R. Sanderson, and T.T. MacDonald, *Curcumin as a therapeutic agent: the evidence from in vitro, animal and human studies.* British journal of nutrition, 2010. **103**(11): p. 1545-1557.

9. Huang, T.-S., S.-C. Lee, and J.-K. Lin, *Suppression of c-Jun/AP-1 activation by an inhibitor of tumor promotion in mouse fibroblast cells.* Proceedings of the National Academy of Sciences, 1991. **88**(12): p. 5292-5296.

10. Goel, A., A.B. Kunnumakkara, and B.B. Aggarwal, *Curcumin as "Curecumin": from kitchen to clinic.* Biochemical pharmacology, 2008. **75**(4): p. 787-809.

11. Hatcher, H., et al., *Curcumin: from ancient medicine to current clinical trials.* Cellular and Molecular Life Sciences, 2008. **65**(11): p. 1631-1652.

12. Bundy, R., et al., *Turmeric extract may improve irritable bowel syndrome symptomology in otherwise healthy adults: a pilot study.* Journal of Alternative & Complementary Medicine, 2004. **10**(6): p. 1015-1018.

13. Jurenka, J.S., *Anti-inflammatory properties of curcumin, a major constituent of Curcuma longa: a review of preclinical and clinical research.* Alternative medicine review, 2009. **14**(2).

14. Balogun, E., et al., *Curcumin activates the haem oxygenase-1 gene via regulation of Nrf2 and the antioxidant-responsive element.* Biochemical Journal, 2003. **371**(Pt 3): p. 887.

15. Jaiswal, A.S., et al., *β-catenin-mediated transactivation and cell–cell adhesion pathways are important in curcumin (diferuylmethane)-induced growth arrest and apoptosis in colon cancer cells.* Oncogene, 2002. **21**(55): p. 8414.

16. Aggarwal, B.B. and B. Sung, *Pharmacological basis for the role of curcumin in chronic diseases: an age-old spice with modern targets.* Trends in pharmacological sciences, 2009. **30**(2): p. 85-94.

17. Kumar, A., et al., *Curcumin (diferuloylmethane) inhibition of tumor necrosis factor (TNF)-mediated adhesion of monocytes to endothelial cells by suppression of cell surface expression of adhesion molecules and of nuclear factor-κB activation.* Biochemical pharmacology, 1998. **55**(6): p. 775-783.

18. Mackenzie, G.G., et al., *Curcumin induces cell‐arrest and apoptosis in association with the inhibition of constitutively active NF‐κB and STAT3 pathways in Hodgkin's lymphoma cells.* International journal of cancer, 2008. **123**(1): p. 56-65.

19. Sebastià, N., et al., *Assessment in vitro of radioprotective efficacy of curcumin and resveratrol.* Radiation Measurements, 2011. **46**(9): p. 962-966.

20. Shishodia, S., M.M. Chaturvedi, and B.B. Aggarwal, *Role of curcumin in cancer therapy.* Current problems in cancer, 2007. **31**(4): p. 243-305.

21. Singh, A.K., et al., *Curcumin inhibits the proliferation and cell cycle progression of human umbilical vein endothelial cell.* Cancer Letters, 1996. **107**(1): p. 109-115.

22. Soni, K. and R. Kuttan, *Effect of oral curcumin administration on serum peroxides and cholesterol levels in human volunteers.* Indian journal of physiology and pharmacology, 1992. **36**: p. 273-273.

23. Rasyid, A. and A. Lelo, *The effect of curcumin and placebo on human gall-bladder function: an ultrasound study.* Alimentary Pharmacology and Therapeutics, 1999. **13**(2): p. 245-250.

24. Roughley, P.J. and D.A. Whiting, *Experiments in the biosynthesis of curcumin.* Journal of the Chemical Society, Perkin Transactions 1, 1973: p. 2379-2388.

25. Hille, B., *Ion channels of excitable membranes*. Vol. 507. 2001: Sinauer Sunderland, MA.

26. Berridge, M.J., P. Lipp, and M.D. Bootman, *The versatility and universality of calcium signalling.* Nature reviews Molecular cell biology, 2000. **1**(1): p. 11.

27. Cosens, D. and A. Manning, *Abnormal electroretinogram from a Drosophila mutant.* Nature, 1969. **224**(5216): p. 285.

28. Nilius, B. and G. Owsianik, *The transient receptor potential family of ion channels.* Genome biology, 2011. **12**(3): p. 218.

29. Montell, C., et al., *A unified nomenclature for the superfamily of TRP cation channels.* Molecular cell, 2002. **9**(2): p. 229-231.

30. Montell, C. and G.M. Rubin, *Molecular characterization of the Drosophila trp locus: a putative integral membrane protein required for phototransduction.* Neuron, 1989. **2**(4): p. 1313-1323.

31. Hardie, R.C. and B. Minke, *The trp gene is essential for a light-activated Ca2+ channel in Drosophila photoreceptors.* Neuron, 1992. **8**(4): p. 643-651.

32. Wes, P.D., et al., *TRPC1, a human homolog of a Drosophila store-operated channel.* Proceedings of the National Academy of Sciences, 1995. **92**(21): p. 9652-9656.

33. Duncan, L.M., et al., *Down-regulation of the novel gene melastatin correlates with potential for melanoma metastasis.* Cancer research, 1998. **58**(7): p. 1515-1520.

34. Caterina, M.J., et al., *The capsaicin receptor: a heat-activated ion channel in the pain pathway.* Nature, 1997. **389**(6653): p. 816.

35. Wu, G., et al., *Somatic inactivation of Pkd2 results in polycystic kidney disease.* Cell, 1998. **93**(2): p. 177-188.

36. Sun, M., et al., *Mucolipidosis type IV is caused by mutations in a gene encoding a novel transient receptor potential channel.* Human molecular genetics, 2000. **9**(17): p. 2471-2478.

37. Sidi, S., R.W. Friedrich, and T. Nicolson, *NompC TRP channel required for vertebrate sensory hair cell mechanotransduction.* Science, 2003. **301**(5629): p. 96-99.

38. Shin, J.-B., et al., *Xenopus TRPN1 (NOMPC) localizes to microtubule-based cilia in epithelial cells, including inner-ear hair cells.* Proceedings of the National Academy of Sciences of the United States of America, 2005. **102**(35): p. 12572-12577.

39. Cao, E., et al., *TRPV1 structures in distinct conformations reveal activation mechanisms.* Nature, 2013. **504**(7478): p. 113.

40. Schaefer, M., *Homo-and heteromeric assembly of TRP channel subunits.* Pflügers Archiv, 2005. **451**(1): p. 35-42.

41. Fischer, M.J., et al., *Direct evidence for functional TRPV1/TRPA1 heteromers.* Pflügers Archiv-European Journal of Physiology, 2014. **466**(12): p. 2229-2241.

42. Kühn, F.J., et al., *Surface expression and channel function of TRPM8 are cooperatively controlled by transmembrane segments S3 and S4.* Pflügers Archiv-European Journal of Physiology, 2013. **465**(11): p. 1599-1610.

43. Viana, F., *Chemosensory properties of the trigeminal system.* ACS Chem Neurosci, 2011. **2**(1): p. 38-50.

44. Chandrashekar, J., et al., *The receptors and cells for mammalian taste.* Nature, 2006. **444**(7117): p. 288.

45. Patapoutian, A., et al., *ThermoTRP channels and beyond: mechanisms of temperature sensation.* Nature Reviews Neuroscience, 2003. **4**(7): p. 529.

46. Belmonte, C. and F. Viana, *Molecular and cellular limits to somatosensory specificity.* Molecular pain, 2008. **4**(1): p. 14.

47. Moran, M.M., et al., *Transient receptor potential channels as therapeutic targets.* Nature reviews Drug discovery, 2011. **10**(8): p. 601.

48. Nilius, B., et al., *Transient receptor potential cation channels in disease.* Physiological reviews, 2007. **87**(1): p. 165-217.

1

CHAPTER

2

METHODS AND TECHNIQUES

I. MOLECULAR MODELING TECHNIQUES:

A key requirement in molecular modelling is to be able to calculate the energy of an arrangement of atoms and/or molecules in 3D space. There exist a variety of methods that can be used to perform such calculations.

The most 'fundamental' way to tackle this problem is to use *quantum mechanics*, where in the Schrödinger equation is solved for the distribution of electrons and atoms in the system in order to derive a wave function from which other properties can be derived

Quantum mechanical methods have some clear advantages in that they are much less reliant on empirical parameters and provides some other valuable properties like electronic. However, they do have the significant drawback of being relatively time consuming to perform and so are rarely used for calculations involving large systems and/or for those on large numbers of molecules.

Empirical force field methods (also known as *molecular mechanics*) ignore the electronic motions in the system and calculate the energy solely as a function of the positions of the atoms. The method uses a very simple model of the intra- and intermolecular interactions within a molecular system with the energy being partitioned into contributions from processes such as the stretching of bonds, bending of angles, rotations about single bonds, and steric and electrostatic interactions between pairs of no bonded atoms (**Figure II.1**). The simplest type of force field encountered in drug design applications contains just these four contributions; a common functional form is as follows:

$$E = \sum_{bonds} \frac{k_i}{2}(l_i - l_{i,0})^2 + \sum_{angles} \frac{k_i}{2}(\theta_i - \theta_{i,0})^2 + \sum_{torsions} \frac{V_n}{2}(1 + \cos(n\omega - \gamma))$$

$$+ \sum_{i=1}^{N}\sum_{j>i}^{N}\left(4\varepsilon_{ij}\left[\left(\frac{\sigma_{ij}}{r_{ij}}\right)^{12} - \left(\frac{\sigma_{ij}}{r_{ij}}\right)^{6}\right] + \frac{q_i q_j}{4\pi\varepsilon_0 r_{ij}}\right) \tag{1}$$
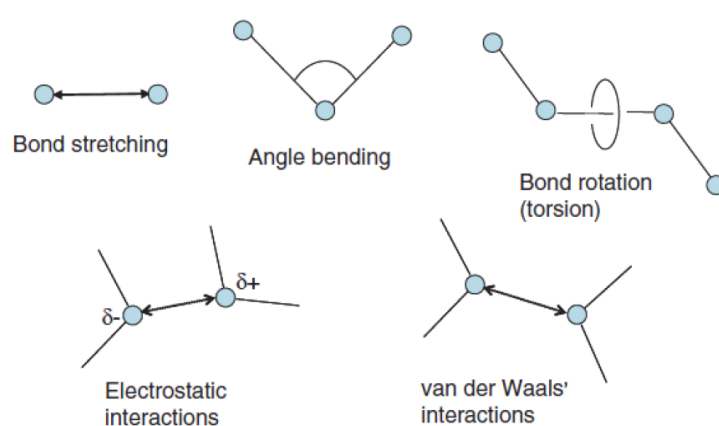
Figure II.1: An illustration of the various terms that contribute to a typical force field

The greatest appeal of quantum mechanical methods is that they can, in principle, be used to calculate the entire range of properties that are necessary to understand the characteristics of a molecule which are responsible for all its properties and that allow its recognition by and activation of receptors.

Quantum mechanical calculations are also able to extrapolate and predict properties of basically any compound without prior knowledge or parameterization, as mentioned above. This is in contrast to other computational methods like for example the classical force fields, which require extensive and complex parameterization and can only interpolated within the boundaries of that parameterization. However, quantum mechanics techniques are computationally very intensive and require significantly more specialist expertise for the correct and meaningful interpretation of the data they generate then do conventional molecular mechanics or force field methods.[1] This significant difference in required expertise combined with a lack of understanding of the potential of quantum mechanical calculations in the wider chemistry community and particular in medicinal chemistry may perhaps be responsible for the apparent underutilization of these very powerful methods.

I.1. THEORETICAL BACKGROUND FOR QUANTUM MECHANICAL CALCULATIONS:

The QM approach postulates the fundamental principles and then uses these postulates to deduce experimental results. For the definition of the state of a system in QM, the function of the coordinates of particles is referred as the wave function or state function Ψ.

In general, the state changes with time, thus for one-particle, one dimensional system, $\Psi=\Psi$ (x, t). The wave function contains all possible information about a system.[2]

Suppose there is a single particle (e.g., an electron of mass m) which is moving through space (given by a position vector $r = x_i + y_j + z_k$) under the influence of an external potential ϑ. In order to find the future state of a system from the knowledge of its first state, an equation is needed that tells how the wave function changes with time (t). Schrödinger's time dependent equation describes the particle by a wave function Ψ (r, t):

$$\left[-\frac{\hbar^2}{2m}\left(\frac{\partial^2}{\partial x^2} + \frac{\partial^2}{\partial y^2} + \frac{\partial^2}{\partial z^2} \right) + V \right] \Psi(r,t) = i\hbar \frac{\partial \Psi(r,t)}{\partial t} \qquad \textbf{(2)}$$

(where, $\hbar = h/2\pi$, h is the Planck's constant and $i^2 = -1$)

When the external potential ϑ is independent of time, then the wave function can be written as the product of a spatial part and a time part; $\Psi(r,t) = \psi(r)T(t)$. In many applications of QM, the potential is considered as independent of time, thus the time dependent Schrödinger equation can be written in the more familiar, time-independent form [2-4]

$$\left[-\frac{\hbar^2}{2m}\nabla^2 + V \right]\Psi(r) = \text{E}\Psi(r) \tag{3}$$

Where, E is the energy of the particle and $\nabla^2 = \left(\frac{\partial^2}{\partial x^2} + \frac{\partial^2}{\partial y^2} + \frac{\partial^2}{\partial z^2} \right)$

Usually $-\frac{\hbar^2}{2m}\nabla^2 + V$ is abbreviated as Hamiltonian operator H. Thus, Schrödinger equation is reduced to $H\Psi=E\Psi$. In order to solve the Schrödinger equation for manybody systems, Hartree-Fock (HF) and density functional theory (DFT) are the commonly used approaches in the QM calculations. In the HF approximation, instead of calculating repulsions between electrons in the system explicitly, repulsions are calculated between one electron and the average field of all of the other electrons. In the DFT approximation, the total electron density is decomposed into one-electron densities, which are constructed from one-electron wave functions. [5, 6]

I.1.1. Ab Initio Methods [7]:

The term *ab initio* implies a rigorous, nonparameterized molecular orbital treatment derived from first principles. This is not completely true. A number of simplifying assumptions are used in *ab initio* theory as it is currently implemented; but the calculations are more complete, and therefore more expensive with respect to computer time, than those of the empirical or semi empirical methods. It is possible to obtain chemical accuracy via *ab initio* calculations, but the cost in computer time is enormous, and only small systems can be treated this accurately at present. In practice most calculations are performed at lower levels of theory than would be considered definitive, and then the shortcomings are taken into account when higher level calculations are performed. Like the semi empirical calculations, *ab initio* theory makes use of the Born-Oppenheimer approximation. The nuclei are regarded as fixed on the time scale of electron movement, the electronic wave function is unaffected by nuclear motion. This is a very good approximation in almost all cases.

Only for an extremely flat potential surface, as in some Jahn-Teller systems for instance, does significant coupling exist between the vibrational and electronic wave functions.

In contrast to the NDDO methods, many different possible choices for the sets of atomic orbitals (the *basis set)* are available. Almost all modern *ab initio* calculations employ *Gaussian type orbital* (GTO) basis sets. These basis sets, where each atomic orbital is made up of a number of Gaussian probability functions, have considerable advantages over other types of basis sets for the evaluation of-one-and two-electron integrals. They are much faster computationally than equivalent Slater orbitals, for instance. The GAUSSIAN series of programs deal, as the name implies, exclusively with Gaussian-type orbitals and include several optional GTO basis sets of varying size. The use of Gaussians is one of the main advantages of such a widely distributed program system. The methods and basis sets used almost become a standard, and a direct comparison with other literature data is often possible. The simplest of the optional basis sets is the STO-nG basis set, where STO-3G is the only one to have found wide use, although the basis sets STO-2G to STO-6G were originally tested.[8] The STO-nG is an abbreviation for Slater-Type Orbitals simulated by n Gaussian functions. This means that each atomic orbital consists of n Gaussian functions added together.

The coefficients of the Gaussian functions are selected to give an optimum fit to the corresponding Slater-type orbitals. The STO-3G uses a *minimal basis* set. This means that it has only as many orbitals as are necessary to accommodate the electrons of the neutral atom.

The greatest problem of any minimal basis set is its inability to expand or contract its orbitals to fit the molecular environment because the exponent is fixed. One solution to the problem is to use *split-valence* or *double zeta* basis sets. In these basis sets the atomic orbitals are split into two parts: an inner, compact orbital and an outer, more diffuse one. The coefficients of these two types of orbitals can be varied independently during construction of the molecular orbitals in the self-consistent field (SCF) procedure. Thus, the size of the atomic orbital that contributes to the molecular orbital can be varied within the limits set by the inner and outer basis functions. Split-valence basis sets split only the valence orbitals in this way, whereas double zeta basis sets also have split-core orbitals ("double zeta" simply implies two different exponents).

The split-valence basis set most widely used for the early calculations was 4-31 G. This nomenclature means that the core orbitals consist of 4 atomic orbitals, and the inner and outer valence orbitals of 3 and 1 Gaussian functions, respectively.

The advent of optimization procedures that use an analytical gradient led to the development of split-valence basis sets with fewer primitive Gaussians than 4-31G. The basis set used most commonly for geometry optimizations is now 3-21G. It uses three primitive Gaussians for the core orbitals and a two/one split.

The next step to improve a basis set is usually the addition of d-orbitals for all heavy (non-hydrogen) atoms. For most organic compounds these do not function as d-orbitals in the normal sense of being involved in bond formation as in transition-metal compounds. Their purpose is to allow a shift of the center of an orbital, a p-orbital for instance, away from the position of the nucleus. Mixing the d-orbital with the p-orbital results in a deformation of the resulting orbital to one side of the atom. This adjustment is particularly important for compounds containing small rings and for compounds of the second-row elements.

The most commonly used polarization basis set (i.e involving d-orbitals) is 6-31 G·. This basis set uses six primitive Gaussians for the core orbitals, a three/one split for the s- and p-valence orbitals, and a single set of six d-functions (indicated by the asterisk). Six d-functions (equivalent to five d-and one s-orbital) are used for computationalconvenience, although the GAUSSIAN programs can also handle basis sets with five real d-orbitals. A further development is the 6-31G basis set. A set of p-orbitals has been added to each hydrogen in the 6-31 G· basis set.

One additional type of basis set, the *diffuse function* augmented basis, is intended for use in calculations on anions or molecules that require very good descriptions of nonbonding electron pairs. These basis sets are obtained by adding a single set of very diffuse S-and p-orbitals to the heavy atoms in a standard basis such as 6-31 G·, The purpose of the diffuse functions is to improve the basis set at large distances from the nucleus, and thus to better describe the high-energy electron pairs associated with anions.

The number of basis functions rises rapidly with an increasing sophistication of the basis set. This is important for two reasons: first, because the number of basis functions the program can handle is limited, and second, because the computer time required is approximately proportional to the fourth power of the number of basis functions.

 After selection of an appropriate basis set for the problem is made (usually the largest Practical), the type of calculation to be performed is chosen. The normal practice for *ab initio*

calculations differ from that used with semi-empirical methods. Almost all calculations are performed with full geometry optimization.

Because of the cost of *ab initio* calculations and the possibility of improving the basis set, it is often necessary to optimize the geometry with a small basis set and then perform single-point calculations with a better basis set or with a correction for electron correlation. This practice allows energy calculations at levels of theory that are too high for practical full geometry optimization. Usually the results are good approximations to those that would be obtained through a full geometry optimization at the higher level. However, in some cases the inclusion of d-orbitals can lead to large changes in the structure so that single-point calculations on a geometry obtained with a nonpolarization basis set may sometimes be misleading.

I.1.2. Density Functional Theory Methods [9]:

DFT is founded in the theorems of Hohenberg and Kohn, who demonstrated a unique relationship between the electron density, r, and the total energy of the ground state, E_0:

$$E_0 = E(\rho) \qquad\qquad \textbf{(4)}$$

This deceptively simple equation implies that if r is known, then all the complicated quantum mechanical exchange and correlation contributions to E_0 are known. The latter – i.e. correlation – is a particular problem for wave function methods like Hartree–Fock (**HF**) theory which only provides an averaged correlation energy. Of course, it is possible to recover the missing correlation energy via post-HF methods but these methods do not scale well and rapidly become prohibitively expensive. In contrast, DFT promises a much cheaper but still accurate alternative.

However, the reality is not perfect. Most practical implementations of DFT are based on the Kohn–Sham (KS) formulation that expresses the density in terms of one-electron functions – orbitals. The 'trick' of KS-DFT is to compute the exact kinetic energy of a set of hypothetical non-interacting electrons, which has the same density as the true ρ, and fold away the difference between this model kinetic energy and the true kinetic energy into the exchange-correlation term, E_{XC}.

Unfortunately, while an inspired and elegant solution to the problem of a practical formulation of DFT, the exact form of E_{XC} is unknown in general so while DFT is exact in principle, in practice we need to formulate approximate functionals to describe the exchange and correlation energies.

However, an exact solution of the KS-DFT equations exists for the special case of the uniform electron gas. In this case, exchange and correlation can be separated and the value of each at a given point in space depends only on the local value of the density at that point. This construct is therefore referred to as the local density approximation (LDA). The LDA exchange energy E_X^{LDA}, for example, depends simply on the 4/3 root of ρ:

$$E_X^{LDA} = \frac{-3}{2}\left(\frac{3}{4\pi}\right)^{1/3} \int \rho(r)^{4/3}\, dr \qquad (5)$$

The expression for the correlation energy is more complex and is replaced by an interpolation scheme developed by Vosko, Wilk and Nusair (VWN) who computed correlation energies numerically for a range of ρ values. The LDA is simple, relatively efficient and remarkably accurate for molecular systems where the density is far from uniform. However, the LDA typically overbinds. In response, corrections that depend on the gradient of ρ were added to the base LDA that engendered a whole slew of new Generalised Gradient Approximation (GGA) functionals. The problem here is that systematic mathematical improvement of functionals is extremely challenging.

Thus, many have resorted to a healthy dose of empiricism in an attempt to 'fit' functionals to experimental and/or numerical data. Becke, for example, developed a gradient corrected exchange functional based on reproducing the exact exchange energies of noble gas atoms.[10] The Becke exchange energy E_X^B is given by:

$$E_X^B = E_X^{LDA} - \beta \sum_\sigma \int \rho_\sigma^{4/3} \frac{x_\sigma^2}{\left(1 + 6\beta x_\sigma \sinh^{-1} x_\sigma\right)} d^3 r \qquad (6)$$

Where σ refers to the spin (either up or down), β is an empirically determined constant (0.0042 **a.u.**), and x_σ is a dimensionless ratio which depends on the gradient of the spin density, ∇_{ρ_σ} ,viz.:

$$x_\sigma = \frac{\left|\nabla_{\rho_\sigma}\right|}{\rho_\sigma^{4/3}} \qquad (7)$$

31

Becke's continuing quest for yet better functionals soon led him to develop what has become the most popular form of DFT – the so-called hybrid functional.

Becke reasoned that the shortcomings of LDA exchange could be corrected by mixing local density exchange with 'exact' HF exchange. By empirically adjusting the amount of LDA exchange, his earlier gradient corrected exchange, E_X^B, and HF exchange plus adding LDA and gradient corrected correlation, a generally superior functional could be developed.

Although Becke used a different correlation functional, the general notion was adopted by the developers of the Gaussian program system who, as described in this research [11] implemented the B3LYP hybrid functional with the following form:

$$E_{XC}^{B3LYP} = (1-a)E_X^{LDA} + aE_X^{HF} + b\Delta E_X^B + (1-c)E_C^{LDA} + cE_C^{LYP} \qquad \textbf{(8)}$$

Where a, b and c are empirical constants.

On the one hand, we could use a more sophisticated wave function method such as MP2 but at some cost in terms of additional computational resource. Moreover, MP2 tends to over bind stacked aromatic systems. Alternatively, we can simply add an empirical dispersion correction to an existing (gradient corrected) DFT functional to generate, for example, BLYP-D. Dispersion forces are treated by an inter-atomic potential of the form C_6R^{-6} which is both strongly damped and scaled.[12] The latter smooths out any dependence on the choice of functional.

In such cases it is clearly desirable that the chosen computational method not only predicts the correct ground spin state but also the energy of the excited spin state.

Here, the performance of various functionals is patchier. 'Standard' B3LYP with 20% HF exchange does not perform well for first-row Transition Metal species.(as an example) [9].However, according to this research [13]they found a linear relationship between the amount of exact (i.e. HF) exchange and the high-spin/low-spin energy difference for a series of Fe-sulfur complexes prompting them to propose the B3LYP functional with only 15% HF exchange as a reasonable choice for first-row complexes. Conversely, Sorkin et al.12 report that 'standard' B3LYP performs the best out of a set of GGA and hybrid functionals for Fe_2 , Fe_2^- and FeO^+ .

Also , a recent study by Ye and Neese [14] concludes that still more complex, so-called, double-hybrid functionals are necessary just for qualitatively correct results although, in the author's opinion, this is something of an exaggeration in that most functionals give the correct ranking of complexes as a function of spin state and simply differ as to the position where the spin state changes.[15].In summary, modern DFT is an extremely useful tool for modelling molecular systems. However, any quantum chemical method, even DFT, is relatively compute-intensive and thus the type of drug discovery problem that is amenable to a quantum treatment is limited. Comprehensive conformational searching and vHTS, which may require many millions of individual calculations, are challenging for QC and faster methods are generally required.

Semi-empirical molecular orbital theory offers a possible alternative. It is certainly significantly more efficient than, say, 'full' DFT but developing suitable parameters for Transition Metal Systems for example centres is very challenging and the resulting accuracy can be a little variable.

I.1.3. Semi empirical Methods:

The development of semi-empirical techniques has a long history; over the past decades, SMs (**Semi empirical Methods**) have been widely used in organic chemistry, biochemistry and drug design. The accuracy of SMs has been continuously improved, new algorithms for treatment of very large systems have been suggested. This makes SMs suitable for modelling various systems, where specific electrostatic interactions, hydrogen bonds, and solvent dynamics are of particular importance.

This category of methods has been developed in parallel with ab initio methods based on the realization that further simplifications were needed in order to be able to perform calculations on larger molecular systems and reactions. The main difference between semi empirical and ab initio as well as DFT is the additional use of parameters derived either empirically or from high-level ab initio calculations in place of the explicit calculation of some molecular integrals. The Free Electron molecular-orbital (FE MO), Huckel molecular-orbital (HMO),and Pariser-Parr-Pople (PPP)[16, 17] methods treat only planar conjugated molecules and only the π electrons. However, other semi-empirical methods such as AM1, PM3, CINDO, and MINDO can be applied to most molecules and treat all the valence electrons Semi-empirical MO methods can be classified into two main categories:

❖ Those using a Hamiltonian, which is the sum of one-electron terms found in Huckel theory

❖ The other uses a Hamiltonian of two-electron-terms in addition to one electron terms found in PPP.

Many two-electron semi-empirical MO generalizations of the PPP method, such as, CNDO, INDO, and NDDO methods, were developed that apply to planar and non-planar molecules.

I.1.3.a. The Pariser-Parr-Pople (PPP) Method:

The PPP [16, 17]method is generally considered to be the most reliable method in predicting the wavelength of maximum absorption (λ_{max}) of large conjugated molecules and considering interatomic effects. Unlike all other semi-empirical methods, the PPP method incorporates only π-orbital effects and neglects sigma (σ) effects. When compared to other methods, such as CNDO, INDO, etc…

it has the following advantages:

- ability to accommodate heteroatomic systems effectively,
- ability to distinguish molecular geometry (e.g. cis from trans isomers)
- ability to distinguish between singlet and triplet state.

The PPP method uses the same assumptions as the Huckel molecular orbital (HMO) method, i.e., that each molecular orbital is a linear combination of the individual atomic orbitals. However, the only difference is that in the case of the PPP method the energy quantities α and β defined in the secular determinant include the effects of electronic interactions.

In the case of CNDO and INDO, however, the energy quantities α and β refer to electrons localized on an atom or sitting in the region of overlap of two atomic orbitals in the absence of any other π- electrons. Linear combination of the atomic orbitals furnishes the molecular orbitals, which can be expressed as a secular.

I.1.3.b. Complete Neglect of Differential Overlap (CNDO) Method:

The complete neglect of differential overlap method was reported in 1965 by Pople, Santry and Segal. This model treats the overlap of atomic orbitals (AOs) in a manner such that only the Coulomb one-center and two-center two-electron integrals remain. In this regard, the differential overlap of atomic orbitals on the same atom is neglected.

For instance, in the case of formaldehyde, all overlap sets of atomic orbitals $<$ SA|SC $>$, $<$ SA|SB $>$, $<$ SA|SP $>$, $<$ SA|SPC(x, y) $>$, $<$ SA|SPO(x, y) $>$ etc., are zero (**Figure II.2**). PPP is a CNDO approximation in which only π- electron are treated.
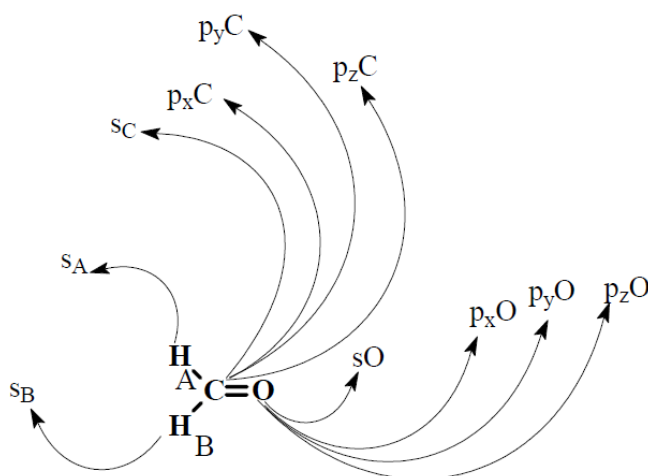
Figure II.2:Overlap integrals of atomic orbitals in formaldehyde

I.1.3.c. **Intermediate Neglect of Diatomic Overlap (INDO):**

The intermediate neglect of differential overlap (INDO) method was developed by Pole, Beveridge, and Dobosh in 1967. Like CNDO, INDO treats the valence electrons explicitly . INDO, however, is an improvement on CNDO in that the differential overlap between AOs on the same atom is not neglected in one center electron–repulsion integrals. However, all two-center electron-repulsion integrals that are not a Coulomb type, are still neglected. In terms of utilities, both CNDO and INDO give good bond lengths predictions, fair electronic spectra and bond angle predictions, but poor dissociation energy and dipole moment predictions . CNDO and INDO methods [18, 19] are considered obsolete now due to advances in other semi-empirical methods [20]

I.1.3.d. **Modified Neglect of Diatomic Orbitals (MNDO):**

The modified neglect of diatomic overlap was developed by Dewar [21-23] and was parameterized for compounds containing H, B, C, N, O, F, Al, Si, Ge, Sn, Pb, P, S, Cl, Br, I, Zn, and Hg. The parameters were taken from atomic and molecular spectra

I.1.3.e. **Austin Model 1 (AM1):**

The AM1 method was developed by Dewar and co-workers, and was parameterized for compounds containing H, B, Al, C, Si, Ge, Sn, N, P, O, S, F, Cl, Br, I, Zn, and Hg using 100 model compounds. [24] The differences between AM1 and MNDO are that the Slater type valence orbital exponents of s and p on the same atom are allowed to differ [2]

I.1.3.f.   Parametrized Method 3 (PM3):

Stewart (69) reparametrized the AM1 method to give this method, (methods 1 and 2 are MNDO and AM1, respectively). In the case of PM3, one-center electron repulsion integrals are optimized, rather than being found empirically from atomic spectra data. PM3 is parameterized for more atoms (H, C, Si, Sn, Pb, N, P, As, Sb, O, S, Se, Te, F, Cl, Br, I, Al, Ga, In, Tl, Be, Mg, Zn, Cd, and Hg) using 657 compounds[25-27]

I.1.3.g.   Common Limitations to MNDO, AM1, and PM3:

Some general limitations to these three methods are:

- Poor prediction of intermolecular interactions such as van der Waals forces or hydrogen bonds. This limitation suggests that either the interaction is weak or the calculated energy minimum (molecular geometry) is incorrect.

- Poor prediction of the rotational barriers for bonds having double bond character. This is observed for compounds having amide linkages. In enable for semi-empirical MO methods to account for rotational barriers, a force field term was added to bring the calculated value in line with the experimental value. Similarly, rotational barrier prediction around the central bond in butadiene is also underestimated. It is calculated to be 0.2-0.5 kcal/mol whereas the experimental value is 5.9 kcal/mol[28]

- In the case of nitrosyl compounds, the bond length of N-N is underestimated. For instance, the N-N bond length in N_2O_3 is calculated to be ~0.7 A°, which is much shorter than the experimental value[28]

- In the case of metal-containing compounds, errors in calculations are likely since the parameters for metals in AM1, PM3, and MNDO are based only on very limited experimental data. For instance, all PM3 parameters are only based on data collected from X-ray data due to the lack of reliable energetic data for transition metals.

I.1.4. Molecular Mechanics or Force Field Methods: [29]

I.1.1.a.   Molecular Mechanics:

Molecular mechanics (MM) is a non-quantum mechanical computational method of determining the energy and structure of a molecule*[30]*. MM treats motion of particles within the classical (Newton) physics instead of quantum physics. Atoms are pictured as balls and bonds as springs.

MM is tremendously less computational demanding than QM and thus allows treating molecular systems containing tens of thousands of atoms. Each interaction between all atoms is parameterized empirically.

There are parameters for the interactions between atoms separated by one or several bonds (i.e., bonded interactions) and between atoms through space independently of the existence of bonds between them (i.e., non-bonded interactions). The collection of all these parameters is one part of the so-called force field. The second part of the force field is the set of equations that are used to calculate the potential energies and ultimately the forces by derivation. The function assembling this set of equations to calculate the total energy in the case of a force field can be given as:

$$Vtotal = Vbonded + Vnon-bonded$$

$$Vbonded = Vbond + Vangle + Vdihedral$$

$$Vnon-bonded = Velectrostatic + Vvan\ der\ Waals$$

❖ **Bonded interactions:**

Interactions between atoms separated by bonds consist of three types. Bond stretching describes energetic dependence vs length rij of a bond between atoms i and j by a harmonic potential $Vbond$ (**Figure II.1**):

$$V_{bond}(r_{ij}) = \frac{1}{2} k_{ij}^b (r_{ij} - b_{ij})^2 \qquad \textbf{(9)}$$

where k_{ij}^b is the force constant of the "spring" and bij the equilibrium bond length.

The energetic variation vs the angle θijk formed by three atoms are also usually described by a harmonic potential $Vangle$:

$$V_{angle}(\theta_{ijk}) = \frac{1}{2} k_{ijk}^\theta (\theta_{ijk} - \theta_{ijk}^0)^2 \qquad \textbf{(10)}$$

where $k_{ij}^{b\theta}$ is the force constant and $k\theta_{ijk}^0$ 0 the equilibrium angle.

Finally, dihedral angles are defined as the angle $\varphi ijkl$ formed by four atoms around a bond. One must distinguish (i) proper dihedrals, usually used to describe the periodic rotation around a single bond, and (ii) improper dihedrals, useful in out-of-plane motion in rings.

$$Vdihedral = Vproper + Vimproper$$

Dihedral angles are important parameters in the conformation of a molecule as the rotation of a single bond can dramatically impact the tridimensional structure and thus on molecule properties. In some case, it has to be carefully reparameterized.

❖ **Non-bonded interactions:**

Whether two atoms are within a molecule or not, non-bonded interactions always affect them. They are weak and rather long distance (several Ångströms) interactions being responsible for numerous physical, chemical or biological processes. For instance, ebullition temperature, chemical reactivity and the existence of lipid bilayer membranes are directly driven by non-bonded interactions.

There are three main types of non-bonding interactions: electrostatic (or Coulombic), Van der Waals and hydrogen bond interactions. Electrostatic interactions (between charges) are described by the classical Coulombic interaction given by:

$$V_{electrostatic}(r_{ij}) = \frac{1}{4\pi\varepsilon_0}\frac{q_i q_j}{\varepsilon_r r_{ij}} \qquad \textbf{(11)}$$

Where rij is the distance between atoms i and j, qi is the charge of atom i, and εr is the relative dielectric constant.

The van der Waals interaction corresponds to the dispersion interactions (fluctuating dipole - fluctuating dipole and higher order interactions). It is usually well described by the Lennard- Jones potential V_{LJ} :

$$V_{LJ}(r_{ij}) = \frac{C_{ij}^{(12)}}{r_{ij}^{12}} - \frac{C_{ij}^{(6)}}{r_{ij}^{6}} \qquad \textbf{(12)}$$

Hydrogen bond interactions have a strong electrostatic character, therefore being often sufficiently well described by the electrostatic potential. However, some force fields of the AMBER or OPLS-AA families also include a specific description of hydrogen or halogen bonding [31, 32]This is performed either by fine-tuning electrostatic and van der Waals parameters for halogens and polar hydrogens or by introducing special potentials for these atom types.

Whereas bonded interactions are roughly proportional to the number of molecules, non-bonded interactions scale to N $(N-1)/2$, N being the number of atoms.Thus, as the system size increases the number of non-bonded interactions to compute becomes very large.

However, the non-bonded interactions between two atoms further apart than 1.4 nm is small. Therefore, in order to reduce computational time, the non-bonded interactions between two atoms separated by more than a certain distance (i.e., a cutoff) are not directly evaluated. Depending on the force field, this cutoff can be set from 0.9 to 1.4 nm for Coulombic and van der Waals interactions.

In order to account for small contributions to the potential energy of atoms further than the cutoff, long range corrections have to be applied. They consist of an additional potential energy term calculated in 3D space. The most popular implementation of long-range correction to electrostatic potential is the Particle-mesh Ewald (PME)[33]. In this method, point charges are transformed into Gaussian charge potentials and reported on a 3D grid. This grid or mesh is then Fourier transformed, so that the Poisson equation calculating the potential from the charges can be solved much more easily in reciprocal space. PME has the advantage of scaling to $N \cdot \log N$ thanks to efficient Fourier transform algorithms.

I.1.1.b. Force Fields[30]:

There have been many force fields developed over the past few decades. A discussion of the general approaches of all force fields is presented here rather than an attempt to review all such efforts. And here is a list and description of well-known and often used force fields:

LIST OF FORCE FIELDS

❖ **AMBER:** 'Assisted Model Building with Energy Refinement'. The most popular force field for modeling proteins and nucleic acids. AMBER was developed by the Kollman research group at University of California at San Francisco. [34, 35]

❖ **CHARMm:** "Chemistry at Harvard Macromolecular Mechanics.This is both the name of the force field and the name of the program which manipulates it.They were designed by Karplus to model macromolecular structure and proteins in particular[36, 37]

❖ **CFF93:** This force field was designed by Hagler for accurate definitions of both small and large molecules, and is designated a "Class II' force field by it's creators because it contains parameters for anharmonicity and coupling between different distortions. This approach leads to higher accuracy at the expense of greater complexity, and a very large number of parameters are required for the force field. In addition, seven scaling parameters are introduced. The force field has its roots in the earlier consistent force field, CFF.[38]

❖ **OLPS:** 'Optimized Potentials for Liquid Simulations'. Designed to model proteins in solution.

❖ **COSMIC:** 'Computation and Structure Manipulation in Chemistry'. COSMIC is the name of both a force field and a molecular mechanics package designed to manipulate it, and was designed to be a general purpose force field.[39]

❖ **DREIDING:** A simple generic force field for predicting the structures and dynamics of organic, biological and main-group inorganic molecules.[40]

❖ **ECEPP:** 'Empirical Conformational Energy Program for Peptides'. Developed by Scheraga. [41]

❖ **GROMOS:** Groningen Molecular Simulation. A general molecular mechanics force field. [42]

❖ **KOLLMAN:** Developed specifically to simulate nucleic acids and proteins. This later evolved into the Amber force field. [34]

❖ **MM2:** Developed by Allinger and coworkes at the University of Georgia, it is designed to work with small molecules (500 atoms or less). [43] This force field is very popular and is a benchmark by which other force fields are sometimes judged.

❖ **MM3:** This force field corrects some of the weaknesses of MM2, particularly concentrating on vibrational frequencies, which MM2 does not reproduce very well. While similar to MM2 in many respects, new parameters were added, which increased the complexity and accuracy for systems for which the new force field was designed. [44]

❖ **MM4:** A further increase in complexity and accuracy over MM3, concentrating on vibrational frequencies and rotational barriers, which are particularly difficult to calculate precisely. [45]

❖ **MMFF94:** Merck Molecular Force Field.[46, 47] It was designed based on high level *ab initio* calculations to work well for both small molecules and large macromolecules.

❖ **Tripos:** The force field from Tripos Associates used in the Sybyl software. It was developed mainly for treating small organic molecules and biomolecules. Its design was based on COSMIC, and White's force field.

❖ **UFF:** 'Universal Force Field'. The parameters for this force field are based only on Force fields describe chemical bonds by stretching, bending, and torsional potentials. Ab initio data at the Hartree-Fock level is used to determine the parameters for the bonded interaction. Electrostatic interactions are addressed by calculating and assigning partial charges to the atoms.

The energy, E, of a molecule derived from a force field is given by a sum of energy contributions. The earliest MM models used force fields that added only three energy terms: the contribution from the energy in a bond (E_{bonds}), the contribution from each bonding angle (E_{angles}), and the energy of van der Waals forces (E_{vdw}).[48-50] However, later it was determined that a term for the torsion angles, $E_{torsion}$, was important. Energy contributions from charge interactions, E_{charge}, were also found to be necessary for the force field to function properly for molecules with electronegative groups.

Most force fields use these energy terms, and follow the general pattern shown in the expression below Force fields are often individualized by additional terms as well (E_{misc}).

$$E_{MM} = E_{bonds} + E_{angles} + E_{vdw} + E_{torsion} + E_{charge} + E_{misc}$$

A review of different force field approaches was published as early as 1956, in which Hendrickson accurately predicted that "machine computation" would be the future of molecular mechanics calculations.

E_{bonds} is the first term in the force field expressions, dealing with the bond stretching energy.

As described in **Figure II.3**, the bond is treated as a spring. The energy can be described by Hooke's law approximation, which gives a harmonic energy curve. The energy, E_{bonds}, is the square of the displacement of the two atoms ($l - l_o$), multiplied by the "spring constant" (k):

$$\mathbf{E_{bonds} = k_1 \ (\ l - l_o \ )^2} \qquad \qquad \mathbf{(13)}$$
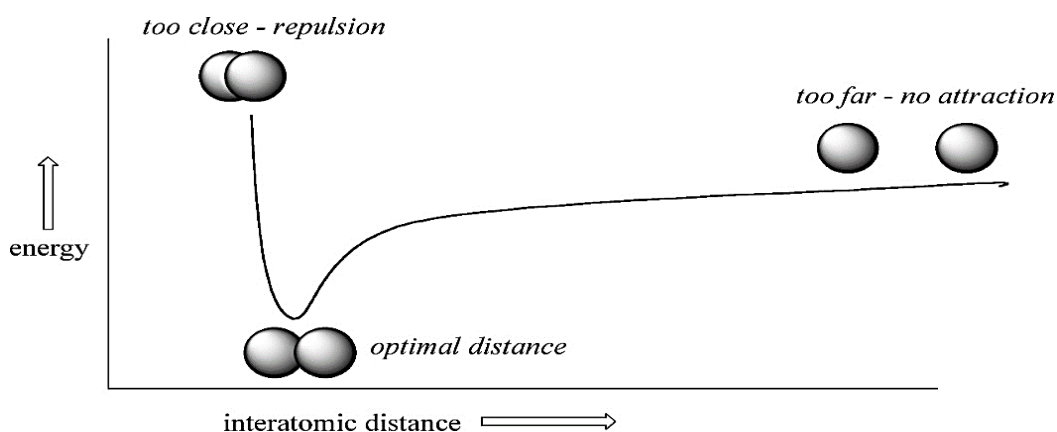
Figure II.3: A chemical bond is treated as a spring. The plot below shows change of energy with bond length, and Hooke's Law approximation

As can be seen from the **Equation 13**, the energy increases during both compression and stretching of the bond. Hooke's Law approximation would dictate that the energy continually increase as the bond stretching is increased.

However, in real bonds the attraction between atoms will eve naturally deviate from the "spring constant" value, k, and the bond will be broken. A distance dependant k value is therefore sometimes implemented for E_{bonds} calculations, with the values being determined by X-ray diffraction and infra-red spectroscopy. There are large databases of such information, from which force fields can obtain their parameters.

The bending of a bond angle between two atoms (E_{angles}), can be described by **Equation 14**, where the energy is dependent on the square of the displacement from equilibrium (**Figure II.4**):

$$E_{angles} = k_\theta \ (\theta \ - \ \theta_0 \ )^2 \qquad (14)$$
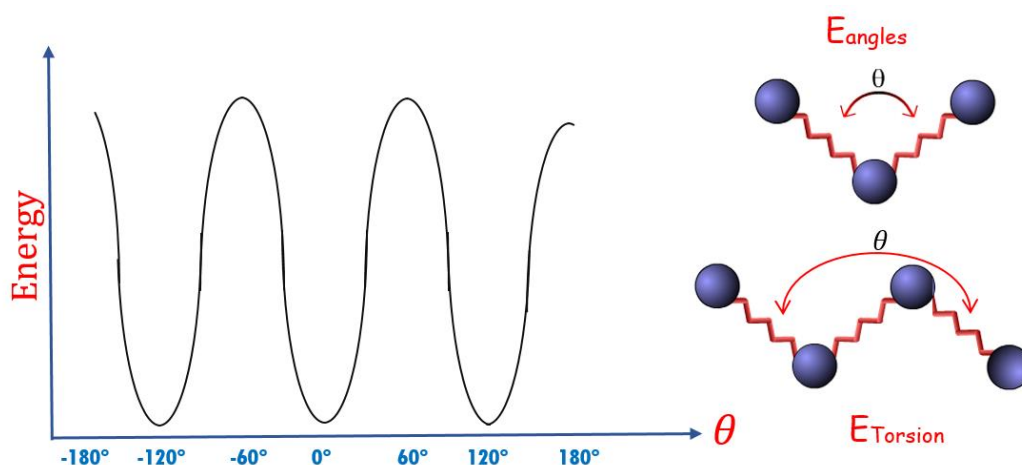
Figure II.4: Angle bending of atoms (a) is shown. The constraining of a torsion angle (b) creates a barrier to rotation, as shown in a typical plot of energy vs. rotational angle, θ.

The torsional angle energy ($E_{torsion}$) is also shown represented in **Figure II.4**. Energy barriers to rotation occur as molecules rotate along single bonds. This energy can be calculated by a partial Fourier series:

$$E_{torsion} = V_1/2 \ (1 \ + \ cos \ \theta \ ) + V2/2 \ (1 \ - \ cos \ 2\theta \ ) + V1/2 \ (1 \ + \ cos \ 3\theta \ ) \qquad (15)$$

where (θ) is the torsion angle between the four atoms involved. These rotation barriers parameters are found in databases of experimental data from microwave spectroscopy and NMR measurements.

Atoms behave as though they have a definite size, and the van der Waals radius is a measure of this. As atoms approach each other at very close ranges, the energy goes up very

quickly. The van der Waals radius is usually estimated from X-ray diffraction experiments. The kinetic theory of gases also allows for cross-sectional areas to be calculated. The energy of van der Waals interactions (E_{vdw}) is a measure of the interaction between atoms that are separated by three or more bonds. This is because the E_{angle} and $E_{torsion}$ already deal with the closer interactions. The Lennard-Jones potential uses a 1/r12 term, and various force fields use this in expressions for E_{vdw} and give similar results.

Usually estimated from X-ray diffraction experiments. The kinetic theory of gases also allows for cross-sectional areas to be calculated. The energy of van der Waals interactions (E_{vdw}) is a measure of the interaction between atoms that are separated by three or more bonds. This is because the E_{angle} and $E_{torsion}$ already deal with the closer interactions. The Lennard-Jones potential uses a **$1/r^{12}$** term, and various force fields use this in expressions for E_{vdw} and give similar results. And here are the expression for E_{vdw} and other energy terms:

❖ **E_{bonds} : energy of a bond stretched or compressed from its natural bond length:**

$$Ebonds = \sum all\ bonds\ 0.5 * k_{b,i} * (\ d_i\ - d_i^0\ )^2$$

where:

di : the length of the i-th bond (Å)

d_i^0 : the equilibrium length of the i-th bond (Å)

$k_{b,i}$: the bond stretching force constant (kcal/(mole)(Å)^2)

❖ **E_{angles} : energy of bending bond angles from their natural values:**

$$E_{angles} = \sum all\ angles\ 0.5 * k_{\theta,i} * (\theta_i - \theta_i^0)^2$$

where:

θ_i : the angle between two adjacent bonds (degrees)

θ_i^0 : the equilibrium value for the i-th angle

$k_{\theta,i}$: the angle bending force constant (kcal/(mole)(degrees)^2)

❖ **$E_{torsion}$: energy of bending planar atoms out of the plane:**

$$E_{torsion} = \Sigma\ all\ trigonal\ atoms\ 0.5 * k_{torsion,i} * d_i^2$$

where:

d_i : the distance between the center atom and the plane of its substituents (Å)

$k_{torsion,i}$: the out of plane bending constant (kcal/(mole)(degrees)^2)

E_{tors} : torsional energy due to twisting about bonds.

$$E_{tors} = \Sigma \text{ all torsions } 0.5 * V_{\Omega,i} * [\ 1 + S_i * cos\ (\ |n_i| * \Omega_i\ ]$$

where:

$V_{\Omega,i}$: the torsional barrier (kcal/mole)

S_i : +1 for staggered minimum energy and -1 for eclipsed minimum energy

$|n_i|$: the periodicity

Ω_i : the torsion angle

Coulomb's Law is used to calculate the energy of electrostatic attractions and repulsions (**Equation 16**). Charge-charge interactions are determined via a partial charge assigned to every atom

$$E_{charge} = \frac{1}{4\pi\varepsilon}\ \frac{q_1 q_2}{r} \qquad\qquad \textbf{(16)}$$

The partial charges from the two atoms are included in Equation 16 as q_1 and q_2. The attractive or repulsive force between the two charged particles has a $1/r^2$ dependance, and the energy has a $1/r$ dependance. ε is the dielectric constant. Calculation of the partial charges is frequently accomplished by considering their electronegativity, as used in a technique developed by Gasteiger et al.[51]

The number of calculations needed to determine E_{charge} rises exponentially with the number of atoms to address. E_{charge} must be calculated by adding up the resulting energies for all pairs of atoms. For a molecule with N atoms, there are N^2 interactions to consider. A common approach is to specify a cut-off distance, where atoms separated by this distance or more are considered to have no interaction.

Most force fields also apply additional energy consideration terms to the calculation of E_{MM}. For example, the stretching of a bond may also affect the bending of that bond. These effects are usually added into the E_{misc} term to improve force field results.

I.1.5. Application of Quantum Mechanical Calculations to Medicinal Chemistry and Drug Design [52]:

One of the major challenges for computer-aided drug design is that it is not governed by the clear-cut rules of design in engineering, and hence.

These methods do not produce a finished product by a fully prescribed procedure. The limitations of the rational computer-aided drug design approach arise because of the complexity of the biological processes involved in drug actions and metabolism at the molecular level and the level of approximation that must be used in describing molecular properties. However, there is clear evidence in the literature that molecular modelling and computer-aided drug design methods and also data analysis and chemoinformatics approaches have become very important tools for drug discovery and that they have been successfully applied to medicinal chemistry, particularly hit and lead generation as well as at the lead development stages. Accepting that molecular modelling and chemoinformatics are useful techniques does however not sufficiently explain why one needs quantum mechanical methods.

This has been done by Clark in a recent review, where he indicates that calculational techniques used to describe molecules should be able to describe the intermolecular interactions adequately. He points out that this can only be achieved if the molecular electrostatics and the molecular polarizability are described well.

The former is responsible for strong interactions and the latter is directly related to dispersion and other weak interactions. Therefore, following this argument, molecular interactions of any type can only be described adequately and accurately by using quantum mechanical calculations.

I.2. COMPUTATIONAL DOCKING [53]:

Generally speaking, molecular docking comprises the process of generating a model of a complex based on the known 3D structures of its components, free or complexed with other species. Pioneered during the early 1980s, it remains a field of vigorous research, having become a useful tool in drug discovery efforts, and a primary component in many drug discovery programs. In particular, protein–ligand docking occupies a very special place in the general field of docking, because of its applications in medicine.

From the initial efforts involving the docking of both protein and ligand as rigid bodies, protein–ligand docking has evolved to a level where full or at least partial flexibility on the ligand is commonly employed. Over the last years, several important steps beyond this point have been given. Handling the flexibility of the protein receptor efficiently is currently considered one of the major challenges in the field of docking.

The fact that proteins are in constant motion between different conformational states with similar energies is still often disregarded in docking studies, even though protein flexibility is known to allow increased affinity to be achieved between a given drug and its target. Furthermore, binding site location and binding orientation can be greatly influenced by protein flexibility.

In terms of protein–ligand docking methods, the docking problem can be rationalized as the search for the precise ligand conformations and orientations (commonly referred as posing) within a given targeted protein when the structure of the protein is known or can be estimated. The binding affinity prediction problem addresses the question of how well the ligands bind to the protein (scoring). Docking protocols can be described as a combination of a search algorithm and a scoring function. The search algorithm should allow the degrees of freedom of the protein–ligand system to be sampled sufficiently as to include the true binding modes. Naturally, the two critical elements in a search algorithm are speed and effectiveness in covering the relevant conformational space.

Among other requirements, the scoring function should represent the thermodynamics of interaction of the protein–ligand system adequately as to distinguish the true binding modes from all the others explored, and to rank them accordingly. Furthermore, it should be fast enough to allow its application to a large number of potential solutions.

Logically, the ideal solution would be to combine the best searching algorithm with the best scoring function. However, several studies have shown that the performance of most docking tools is highly dependent on the specific characteristics of both the binding site and the ligand to be investigated, and that establishing which method would be more suitable in a precise context is almost impossible.

I.2.1. Docking procedures[54]:

I.2.1.a. Manual docking:

Both the ligand and the protein remain in the same conformation throughout the process and so this is a rigid fi t. Once a molecule has been docked successfully, fit optimization is carried out. This is essentially the same as energy minimization, but carried out on the ligand–target protein complex. Different conformations of the molecule can be docked in the same way and the interaction energies measured to identify which conformation fits the best.

I.2.1.b. Automatic docking:

A variety of docking programs now exist that can automatically dock ligands into a binding site with the minimum of input from an operator. (**Like MOE**) They have the advantage that they do not depend on any preconceived ideas that the operator may have on how a particular ligand should bind and, as a result, they can reveal unexpected binding modes.

They are also amenable to studying many different molecules automatically. Indeed, an important application of automatic docking programs is to carry out virtual screening of hundreds of different molecules with the aim of identifying new lead compounds that will interact with the target. Virtual screening can be seen as complementary to biological screening in that the former can identify the structures from a chemical 'library' that are most likely to bind to the target. These can then be given priority for biological screening, making the latter more efficient. For virtual screening to be effective it has to use efficient algorithms which not only dock each molecule realistically, but also give an accurate 'score' of the relative binding energies of the molecules concerned. Moreover, for each molecule studied, the docking program is likely to generate several different orientations or binding modes. It is necessary to score all of these in order to identify the most likely binding mode in terms of how well it fits the space available and how many intermolecular interactions it can form with the binding site.

The calculations required for docking and scoring have to be rapid in order to process the number of molecules involved in a reasonable time period, but they also have to be accurate enough to give a good measure of relative binding energies. This is a difficult compromise to make as increasing the speed at which an algorithm operates involves assumptions or short cuts that inevitably reduce the accuracy of the calculation. As a result, this is an area of intense research interest in the development of new and improved docking programs. For reasons of space, it is not possible to go into the mathematical details of docking algorithms.

The simplest approach to automatic docking is to treat the ligand and the macromolecular target as rigid bodies. This is acceptable if the active conformation of the ligand is known or if the ligand is a rigid cyclic structure. At the next level of complexity, the target is still considered as a rigid body, but the ligand is allowed to be flexible and can adopt different conformations. The most complex situation is where both the target and the ligand are considered to be flexible. This last situation is extremely expensive in terms of computer time, and most docking studies are carried out by assuming a rigid target.

I.2.1.c. Defining the molecular surface of a binding site:

In order to carry out docking calculations, it is necessary to know the structure of the protein target and the nature of the binding site. This can be obtained from an X-ray crystal structure of the protein which can be downloaded onto a computer. The amino acids lining the binding pocket can then be identified. The next step is to define the molecular surface of the binding site. One could do this by defining each atom within the binding site by its van der Waals radius, but this results in an extensive surface area, much of which would be inaccessible to a ligand (**Figure II.5**).
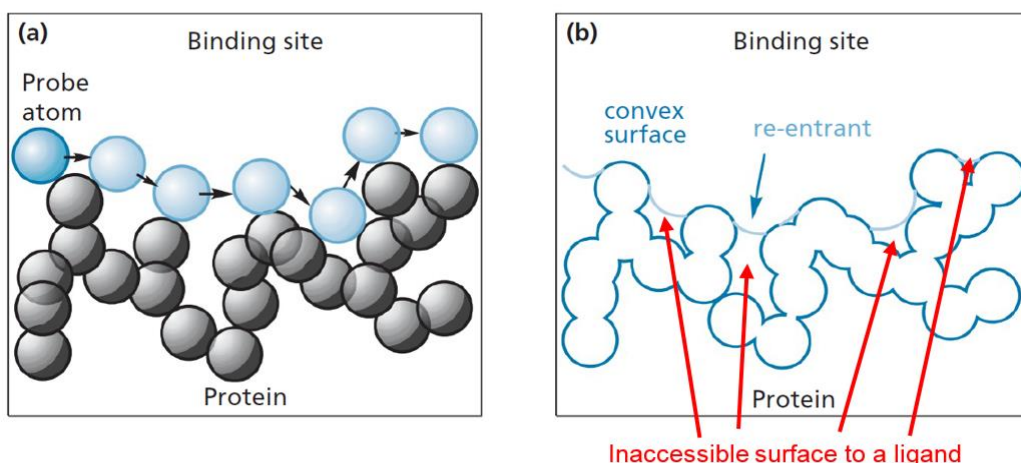
Figure II.5 : Defining the Connolly surface of :(a) binding site with a probe atom. (b) The Connolly surface shown in blue

The probe atom can access the space between the atoms of the binding site. In this area, the probe is in contact with two or three atoms. This kind of molecular surface is also referred to as a Connolly surface. The surface is actually represented by a regular distribution of points or dots, and the crucial ones for docking are those on the convex surfaces. Each one of these has a vector associated with it which points into the binding site. The direction of the vector corresponds to the normal of the surface at that point and so it is a mathematical indication of curvature.

I.2.1.d. Rigid docking by shape complementarity:

The first problem with any docking program is how to position the ligand within the binding site. If you or I were handed real models of the target and the ligand, we would consider the space available in the binding site, eye up the ligand, and judge how we could place it into the binding site before we actually do it. In other words, humans have a spatial awareness, which includes the ability to assess the shape of an empty space.

This does not come naturally to computers, and the empty space of a binding site has to be defined in a way that a computer program can understand before ligands can be inserted.

The DOCK program was one of the earliest programs to tackle this problem. The Connolly surface is first defined, then the empty space of the binding site is defined by identifying a collection of differently sized spheres which will fill up the space available and give a 'negative image' of the binding site (**Figure II.6**).
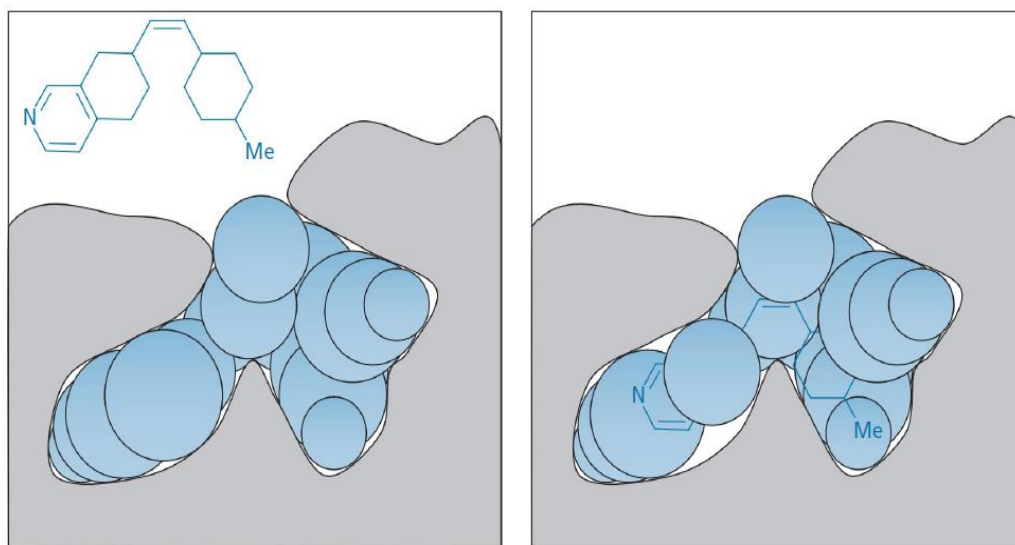
Figure II.6: The DOCK program

For each dot representing the molecular surface, spheres are constructed that touch that dot plus one other dot on the molecular surface. Therefore, if there are in dots representing the molecular surface, n–1 spheres will be created at each of the dots. This represents a massive number of spheres and so it is necessary to whittle these down. The number of spheres can be reduced significantly as follows:

❖ for each dot on the molecular surface, the sphere of smallest radius touching it is chosen. This ensures that none of the spheres chosen intersects the molecular surface .

❖ there are several dots associated with the surface of a particular atom and each of these now has one sphere associated with it. The next filtering process is to select the sphere with the largest radius. Once this has been completed, the number of spheres left is the same as the number of atoms lining the binding site. Spheres are allowed to overlap and the centre of each sphere accurately defines a unique position of 3D space within the binding site.

Each sphere representing the binding site can be considered as a pseudoatom and so it is now possible to carry out an overlay operation, where ligand atoms are matched with pseudoatoms then overlaid. However, how does the programme decide which ligand atom and pseudoatom should be matched?

One could try out every possible combination, but this would take up far too much computer time. Instead, a systematic matching operation takes place called distance matching or clique searching. Firstly, the distances between each of the ligand atoms are measured.

This is repeated for all of the pseudoatoms. These distances are then used to identify which ligand atoms and pseudoatoms can be matched up. The operation takes place as follows. A graph is prepared where each ligand atom (1, 2, 3, …) is matched to each of the receptor spheres (A, B, C, …) to give a list of paired atom/pseudoatoms (1A, 1B, 1C…, 2A, 2B, 2C….3A, 3B, 3C…, etc.). The next stage is to identify whether two of these pairs are compatible, for example is the pairing 1A possible at the same time as the pairing 2C? This is done by comparing the distance between the ligand atoms 1 and 2, with the distance between the receptor spheres A and C. If the distances are similar, then they are compatible. This process is now repeated for further pairings to see if they are compatible with those already identified.

The minimum number of pairings required for an acceptable docking is four. The whole procedure is repeated systematically for each ligand atom to find a variety of matches which will eventually lead to different docking modes.

I.2.1.e. Rigid docking by matching hydrogen bonding groups:

Rigid docking by shape complementarity is based on whether a ligand has the right shape to fit into the binding site and takes no account of possible binding interactions. This is ideal for ligands that take up most of the space available in the binding site, but is less satisfactory for ligands which are small in comparison with the size of the binding site.

An alternative method of docking is to use the same '**clique technique'** described inI.**2.1.d**) , but this time to match up hydrogen bonding groups in the binding site with complementary hydrogen bonding groups present on the ligand. There are two important factors to take into account. Firstly, a hydrogen bonding group on the ligand must be the correct distance from a hydrogen bonding group in the binding site. Secondly, the two groups concerned must have the correct orientation with respect to each other. It is, therefore, necessary to identify positions in space within the binding site where ligand atoms can be

positioned to satisfy these criteria. These positions are defined by interaction points as follows.

Firstly, a sphere is created around each hydrogen bonding group in the binding site (**Figure II.7**). The surface of the sphere represents the optimum distance at which a complementary group on the ligand should be placed in order to form a good hydrogen bond. A series of uniformly spaced points is placed over the surface of the sphere to define the surface. These are the interaction points onto which complementary binding groups on the ligand will be positioned during the docking process. However, not all of the points are feasible positions for a good hydrogen bonding interaction and so a filtering process takes place which:

❖ removes the points that are not accessible in the binding site

❖ removes the points which would not allow a bonding angle (α) greater than 90°.

The interaction points that survive this filtering procedure are now used as 'targets' for the matching operation with suitable ligand atoms.

This method is used in the Directed Dock algorithm alongside the matching algorithm based on shape complementarity. This means that it is possible to carry out a docking which takes into account both hydrogen bonding interactions and shape complementarity.
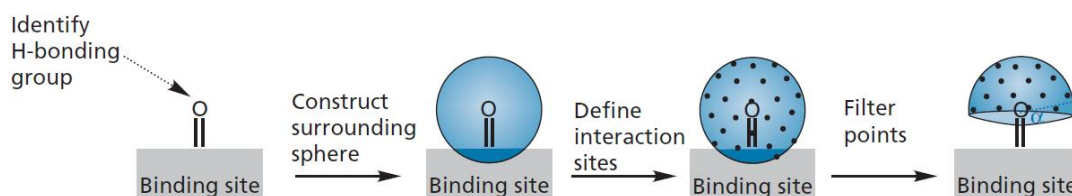
Figure II.7 : Identifying interaction sites for hydrogen bonding groups in the binding site.

II.   EXPERIMENTAL TECHNIQUES:

II.1. CHROMATOGRAPHY:

Chromatography (from Greek χρῶμα *chroma* "color" and γράφειν *graphein* "to write") is one term that describes set of laboratory techniques for the separation of mixtures. For this method mixture has to be dissolved in a fluid called the mobile phase, which carries it through other part of chromatography system which is holding another material called the stationary phase.

The various compounds of the mixture travel with different speeds, and that way they are being separated. There are couple of ways to divide existing chromatography methods, but most common division is the one based on physical state of mobile phase [55, 56]

II.1.1. Column Chromatography[56, 57]:

II.1.1.a. Principle and Theory:

Chromatography is a technique in which compounds to be separated are distributed between a mobile phase and a stationary phase. In such a system, different distributions based on selective adsorption give rise to separation. There are different types of chromatography, such as paper, thin layer, or column chromatography, each with its own strengths and weaknesses.

Column chromatography is one of the most useful methods for the separation and purification of both solids and liquids when carrying out small-scale experiments. The separation can be liquid/solid (adsorption) or liquid/liquid (partition) in column chromatography. The stationary phase, a solid adsorbent, is usually placed in a vertical glass column and the mobile phase, is added from the top and let flow down through the column by either gravity or external pressure (**Figure II.8**).

Column chromatography is advantageous over most other chromatographic techniques because it can be used in both *analytical* and *preparative* applications. It can be used to determine the number of components of a mixture and as well as the separation and purification of those components.
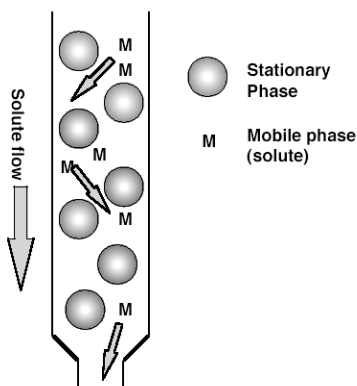
Figure II.8: Column chromatography involves a mobile phase flowing over a stationary phase.

Column chromatography is advantageous over most other chromatographic techniques because it can be used in both *analytical* and *preparative* applications. It can be used to determine the number of components of a mixture and as well as the separation and purification of those components.

Column chromatography isolates desired compounds from a mixture in such a way that the mixture is applied from the top of the column. The columns are usually glass or plastic with sinter frits to hold the packing. The liquid solvent (eluent) is passed through the column by gravity or by the application of air pressure. The eluent, instead of rising by capillary action up a thin layer, flows down through the column filled with the adsorbent. Equilibrium is established between the solute adsorbed on the adsorbent and the eluting solvent flowing down through the column. Stationary phases are almost always adsorbents. Adsorbent is a substance that causes passing molecules or ions to adhere to the surface of its particles. The mobile phase is a solvent that flows past the stationary phase, dissolving the molecules of the compounds to be separated some of the time.

Because the different components in the mixture have different interactions with the stationary and mobile phases, they will be carried along with the mobile phase to varying degrees and a separation will be achieved. The individual components, or elutants, are collected as solvent drips from the bottom of the column.

Many compounds are not visible to the eye when dissolved in a solvent or adsorbed on a adsorbent. Visualization processes make these substances visible. The used techniques for this purpose include UV lights that cause fluorescence or phosphorescence and chemical reactions that give colored compounds.

II.1.1.b. Adsorbent:

Silica gel (SiO_2) and alumina (Al_2O_3) are two adsorbents commonly used by organic chemists for column chromatography. These adsorbents are sold in different mesh sizes, indicated by a number on the bottle label: "silica gel 60" or "silica gel 230-400" are a couple of examples. This number refers to the mesh of the sieve used to size the silica, specifically, the number of holes in the mesh or sieve through which the crude silica particle mixture is passed in the manufacturing process. If there are more holes per unit area, those holes are smaller, thus only smaller silica particles are allowed to pass the sieve. The larger the mesh size, the smaller the adsorbent particles are.

Adsorbent particle size affects the way the solvent flows through the column. Smaller particles (higher mesh values) are used for flash chromatography; larger particles (lower mesh values) are used for gravity chromatography.

Alumina is quite sensitive to the amount of water which is bound to it; the higher its water content, the less polar sites it has to bind organic compounds, and thus the less "sticky" it is. This stickiness or activity is designated as I, II, or III with I being the most active. Alumina comes in three forms: acidic, neutral, and basic. The neutral form of activity II or III, 150 mesh, is most commonly employed.

II.1.1.c. Solvent:

The polarity of the solvent, which is passed through the column, affects the relative rates at which compounds move through the column. Polar solvents can more effectively compete with the polar molecules of a mixture for the polar sites on the adsorbent surface and will also better solve the polar constituents. Consequently, a highly polar solvent will move even the highly polar molecules rapidly through the column. If a solvent is too polar, movement becomes too rapid, and little or no separation of the components of a mixture will result. On the other hand, if a solvent is not polar enough, no compounds will elute from the column. Proper choice of an eluting solvent is thus crucial for a successful application of column chromatography as a separation technique since compounds interact with the silica or alumina largely due to polar interactions.

II.1.1.d. Elution Chromatography

Elution involves transporting a species through a column by continuous addition of fresh mobile phase. Single portion of sample contained in the mobile phase is introduced from the top of the column whereupon the components of that sample distribute themselves between two phases. Introduction of additional mobile phase (the *eluent*) forces the solvent containing a part of the sample down the column where further partition between the mobile phase and fresh portions of the stationary phase occurs (time t_1).

Simultaneously, partitioning between the fresh solvent and the stationary phase takes place at the site of the original sample. Continued additions of solvent carry solute molecules move down the column in a continuous series of transfers between the mobile and the stationary phases. Because the movement of the sample can occur in the mobile phase, however, the average rate at which a solute zone migrates down the column depends upon

the fraction of time it spends in that phase. This fraction is small for solutes that are strongly retained by the stationary phase and it is large where retention in the mobile phase is more likely.

Ideally the resulting differences in rates cause the components in the mixture to separate into bands, or zones located along the length of the column (t_2). Isolation of the separated species is then accomplished by passing a sufficient quantity of mobile phase through the column to cause the individual zones to pass out the end, where they can be detected or collected (times t_3 and t_4) .(**Figure II.9)**
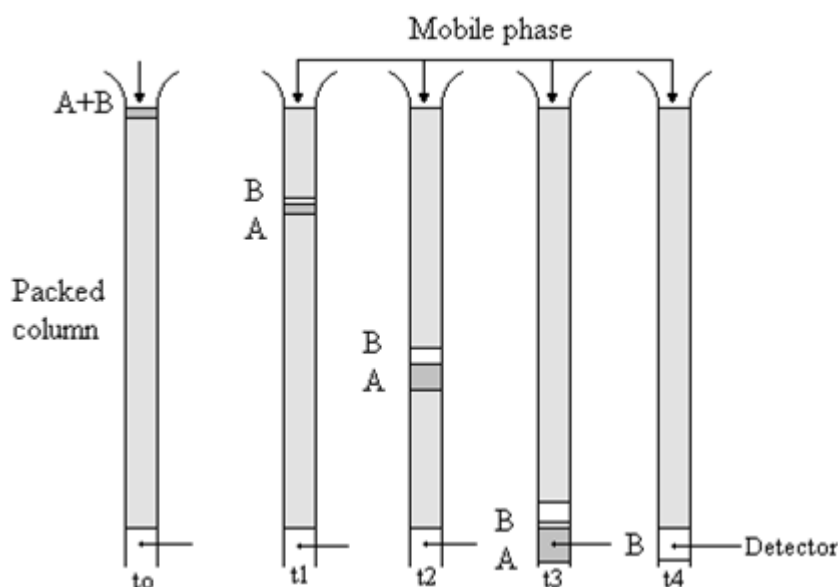
Figure II.9 : Elution Chromatography

II.1.2.   THIN LAYER CHROMATOGRAPHY:

Thin layer chromatography (TLC) is a chromatography technique used to separate mixtures. Chromatography was discovered by M. Tswett in 1906.

Thin layer chromatography is performed on a sheet of glass, plastic, or aluminium foil, which is coated with a thin layer of adsorbent material, usually silica gel, aluminium oxide, or cellulose (blotter paper). This layer of adsorbent is known as the stationary phase. After the sample has been applied on the plate, a solvent or solvent mixture (known as the mobile phase) is drawn up the plate via capillary action. Because different analytes ascend the TLC plate at different rates, separation is achieved.

Thin layer chromatography can be used to: Monitor the progress of a reaction, identify compounds present in a given substance, determine the purity of a substance. Separation of compounds is based on the competition of the solute and the mobile phase for binding places on the stationary phase. For instance, if normal phase silica gel is used as the stationary phase it can be considered polar. Given two compounds which differ in polarity, the more polar compound has a stronger interaction with the silica and is therefore more capable to dispel the mobile phase from the binding places.Consequently, the less polar compound moves higher up the plate (resulting in a higher *Rf* value). If the mobile phase is changed to a more polar solvent or mixture of solvents, it is more capable of dispelling solutes from the silica binding places and all compounds on the TLC plate will move higher up the plate. Practically this means that if you use a mixture of ethyl acetate and heptane as the mobile phase, adding more ethyl acetate results in higher R_f values for all compounds on the TLC plate. Changing the polarity of the mobile phase will normally not result in reversed order of running of the compounds on the TLC plate.[58]

II.1.3. Principle of TLC [59] :

Thin layer chromatography uses a thin glass plate coated with either aluminium oxide or silica gel as the solid phase. The mobile phase is a solvent chosen according to the properties of the components in the mixture. The principle of TLC is the distribution of a compound between a solid fixed phase (the thin layer) applied to a glass or plastic plate and a liquid mobile phase (eluting solvent) that is moving over the solid phase. A small amount of a compound or mixture is applied to a starting point just above the bottom of TLC plate.

The plate is then developed in the developing chamber that has a shallow pool of solvent just below the level at which the sample was applied. The solvent is drawn up through the particles on the plate through the capillary action, and as the solvent moves over the mixture each compound will either remain with the solid phase or dissolve in the solvent and move up the plate. Whether the compound moves up the plate or stays behind depend on the physical properties of that individual compound and thus depend on its molecular structure, especially functional groups. The solubility rule "Like Dissolves Like" is followed. The more similar the physical properties of the compound to the mobile phase, the longer it will stay in the mobile phase. The mobile phase will carry the most soluble compounds the furthest up the TLC plate. The compounds that are less soluble in the mobile phase and have a higher affinity to the particles on the TLC plate will stay behind.

II.1.4. R_f values:

The behaviour of an individual compound in TLC is characterized by a quantity Known as R_f and is expressed as a decimal fraction. The R_f is calculated by dividing the distance the compound travelled from the original position by the distance the solvent travelled from the original position (the solvent front).

$$R_f = \frac{Distance\ of\ centre\ of\ spot\ from\ starting\ point}{Distance\ of\ solvent\ front\ from\ starting\ point}$$

The R_f value is a constant for each component only under identical experimental condition. It depends upon number of factors as:

- **Nature of adsorbent**: Different adsorbents will give different R_f value for same solvent. Reproducibility is only possible for given adsorbent of constant particle size and binder. Plates should be stored over silica gel in desiccators before use and the sample should be applied quickly so that the water vapour in the atmosphere is not adsorbed by the plate. Because of the difficulties associated with activation procedures, it is far better to use plates stored at room temperature and not to activate them.

- **The mobile phase**: The purity of solvents and quantity of solvent mixed should be strictly controlled. It should be made freshly for each run if one of the solvents is very volatile or hygroscopic. Example- acetone.

- **Temperature**: Although precise control of temperature is not necessary, the tank should be kept away from sources of heat, direct sunlight etc. As the temperature is increased, Volatile solvents evaporate more quickly, solvents run faster, and R_f values generally decrease slightly.

- **Thickness of layer**: Standard plates approximately 250 micrometre is the preferable thickness of layer. Below 200, the R_f values vary considerably. The layers may be of higher or lower thickness in individual compounds.

- **Developing tank**: It is important that saturated conditions are attained for running TLC plates. This is best accomplished by using small tanks with filter paper liners and sufficient solvent, and by leaving the tank to equilibrate for at least 30 minutes before running the plates. A well-fitting lid is essential.

- **Mass of sample**: Increasing the mass of sample on the plate will often increase the R_f of drug, especially if it normally tails in the system. However, if a plate is grossly

overloaded, this too will give a tailing spot and will have the effect of apparently decreasing the R_f value. The two situations are normally easy to distinguish by the intensity of the spot.

- **Chromatographic Technique**: Depending upon the development technique used i.e. ascending, descending, horizontal … etc., the R_f value change for the same solvent system.

II.1.5. Plate preparation [59]:

TLC plates are usually commercially available, with standard particle size ranges to improve reproducibility. They are prepared by mixing the adsorbent, such as silica gel, with a small amount of inert binder like calcium sulfate (gypsum) and water. This mixture is spread as thick slurry on an unreactive carrier sheet, usually glass, thick aluminium foil, or plastic. The resultant plate is dried and activated by heating in an oven for thirty minutes at 110 °C. The thickness of the adsorbent layer is typically around 0.1- 0.25 mm for analytical purposes and around 0.5- 2.0 mm for preparative TLC.

- ➤ **Capillary spotters:** Place a melting point capillary and in the dark blue part of the Bunsen burner flame. Hold it there until it softens and starts to sag. Quickly remove the capillary from the flame and pull on both ends to about 2-3 times its original length. If you pull the capillary inside the flame, you will have a "piece of art", but not a good spotter. Allow the capillary to cool down, and then break it in the middle. Make sure to break off the closed end on one of them.

- ➤ **Spotting the plate:** The thin end of the spotter is placed in the dilute solution; the solution will rise up in the capillary (capillary forces). Touch the plate briefly at the start line. Allow the solvent to evaporate and spot at the same place again. This way you will get a concentrated and small spot. Try to avoid spotting too much material, because this will deteriorate the quality of the separation considerably ('tailing'). The spots should be far enough away from the edges and from each other as well. If possible, you should spot the compound or mixture together with the starting materials and possible intermediates on the plate.

- ➤ **Location of spots:** The position of various solutes separated by TLC can be located by various methods. Coloured substances can be seen directly when viewed against stationary phase, while colourless substances can be detected only by making them

visible by making use of some spraying agent, which produces coloured areas in the region which they occupy.

Specifically, in TLC following can be used for spraying the invisible spots:

- Being purely inorganic in nature, corrosive agents may also be used for spraying on the invisible spots.
- Dilute solution of Potassium dichromate in concentrated sulfuric acid. In the process, potassium dichromate (yellow) is reduced to chromic sulfate (green) by most of the organic compounds, particularly used for sugars.
- Vapours of sulfur trioxide, produced on warming fuming sulfuric acid, chars organic compound and makes them visible as dark spots.
- Solution of potassium permanganate.
- Iodine vapours.

Other common reagents include saturated solution of hydrogen sulphide, 0.2N aqueous ammonium sulphide, 0.1% alcoholic quercetin, 0.2% methanolic 1-(2-pyridylazo)-2- napthol, 1% methanolic oxine , and 0.5% aqueous sodium rhodizonate. If the adsorbent used for the TLC plate contains a fluorescing material, the solutes can be viewed under ultraviolet light.

II.1.6. Development solvents [59]:

The choice of a suitable solvent depends upon: Nature of substance, and adsorbent used on the plate. A development solvent should be such that, does not react chemically with the substances in the mixture under examination. Carcinogenic solvents (benzene …etc.) or environmentally dangerous solvents (dichloromethane …etc.) should always be avoided.

Solvent systems range from non-polar to polar solvents. Non-polar solvents are generally used; as highly polar solvents cause the adsorption of any component of the solvent mixture. Commonly used development solvents are petroleum ether, carbon tetrachloride, pyridine, glycol, glycerol, diethyl ether, formamide, methanol, ethanol, acetone, and n-propanol.

II.1.7. Mobile Phase:

For silica gel chromatography, the mobile phase is an organic solvent or mixture of organic solvents. As the mobile phase moves pass the surface of the silica gel it transports the analyte pass the particles of the stationary phase. However, the analyte molecules are only free to move with the solvent if they are not bound to the surface of the silica gel. Thus, the fraction of the time that the analyte is bound to the surface of the silica gel relative to the time it spends in solution determines the retention factor of the analyte. The ability of an analyte to bind to the surface of the silica gel in the presence of a particular solvent or mixture of solvents can be viewed as at the sum of two competitive interactions. First, polar groups in the solvent can compete with the analyte for binding sites on the surface of the silica gel. Therefore, if a highly polar solvent is used, it will interact strongly with the surface of the silica gel and will leave few sites on the stationary phase free to bind with the analyte. The analyte will, therefore, move quickly pass the stationary phase. Similarly, polar groups in the solvent can interact strongly with polar functionality in the analyte and prevent interaction of the analyte with the surface of the silica gel.

This effect also leads to rapid movement of the analyte pass the stationary phase. The polarity of a solvent to be used for chromatography can be evaluated by examining the dielectric constant (å) and dipole moment (ä) of the solvent. The larger these two numbers, the more polar is the solvent. In addition, the hydrogen bonding ability of the solvent must also be considered. For example, methanol is a strong hydrogen bond donor and will severely inhibit the ability of all but the most polar analytes to bind the surface of the silica gel.

II.1.8. Developing a Plate [59]:

A TLC plate can be developed in a beaker or closed jar. Place a small amount of solvent (mobile phase) in the container. A small spot of solution containing the sample is applied to a plate, about one centimetre from the base. The plate is then dipped in to a suitable solvent, such as hexane or ethyl acetate, and placed in a sealed container. The solvent moves up the plate by capillary action and meets the sample mixture, which is dissolved and is carried up the plate by the solvent. Different compounds in the sample mixture travel at different rates due to the differences in their attraction to the stationary phase, and because of differences in solubility in the solvent. By changing the solvent, or perhaps using a mixture, the separation of components (measured by the $\mathbf{R}_f$ value) can be adjusted.

The solvent level has to be below the starting line of the TLC, otherwise the spots will dissolve away. The lower edge of the plate is then dipped in a solvent. The solvent (eluent) travels up the matrix by capillarity, moving the components of the samples at various rates because of their different degrees of interaction with the matrix (stationary phase) and solubility in the developing solvent. Non-polar solvents will force non-polar compounds to the top of the plate, because the compounds dissolve well and do not interact with the polar stationary phase. Allow the solvent to travel up the plate until ~1 cm from the top. Take the plate out and mark the solvent front immediately. Do not allow the solvent to run over the edge of the plate. Next, let the solvent evaporate completely.

Precautions during sample application;

✓ Sample should be dissolved in a nonpolar solvent as polar solvent has a tendency to spread out the starting spot.

✓ Solvent used for dissolving sample should be volatile.

✓ While applying sample, the surface of the adsorbent should not be disturbed as this distorts the shapes of the spots on subsequent developed chromatogram, hindering the accuracy of quantitative measurements.

✓ The sample spot should be within 2-5 mm in diameter.

An example is shown below:
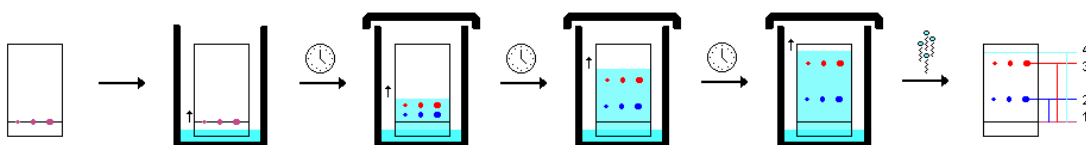
II.1.9. Visualization:

When the solvent front has moved to within about 1 cm of the top end of the adsorbent (after 15 to 45 minutes), the plate should be removed from the developing chamber, the position of the solvent front marked, and the solvent allowed to evaporate. If the components of the sample are coloured, they can be observed directly. If not, they can sometimes be visualized by shining ultraviolet light on the plate or by allowing the plate to stand for a few minutes in a closed container in which the atmosphere is saturated with iodine vapour. Sometimes the spots can be visualized by spraying the plate with a reagent that will react with one or more of the components of the sample.

II.1.10. Analysis:

The components, visible as separated spots, are identified by comparing the distances they have travelled with those of the known reference materials. Measure the distance of the start line to the solvent front. Then measure the distance of center of the spot to the start line. Divide the distance the solvent moved by the distance the individual spot moved. The resulting ratio is called Rf-value. As the chemicals being separated may be colourless, several methods exist to visualize the spots. Often a small amount of a fluorescent compound, usually manganese-activated zinc silicate, is added to the adsorbent that allows the visualization of spots under a backlight (UV$_{254}$). The adsorbent layer will thus fluoresce light green by itself, but spots of analyte quench this fluorescence, Iodine vapours are a general unspecific colour reagent, Specific colour reagents exist into which the TLC plate is dipped or which are sprayed onto the plate.Once visible, the R$_f$ value, or retention factor, of each spot can be determined by dividing the distance travelled by the product by the total distance travelled by the solvent (the solvent front). These values depend on the solvent used, and the type of TLC plate, and are not physical constants.
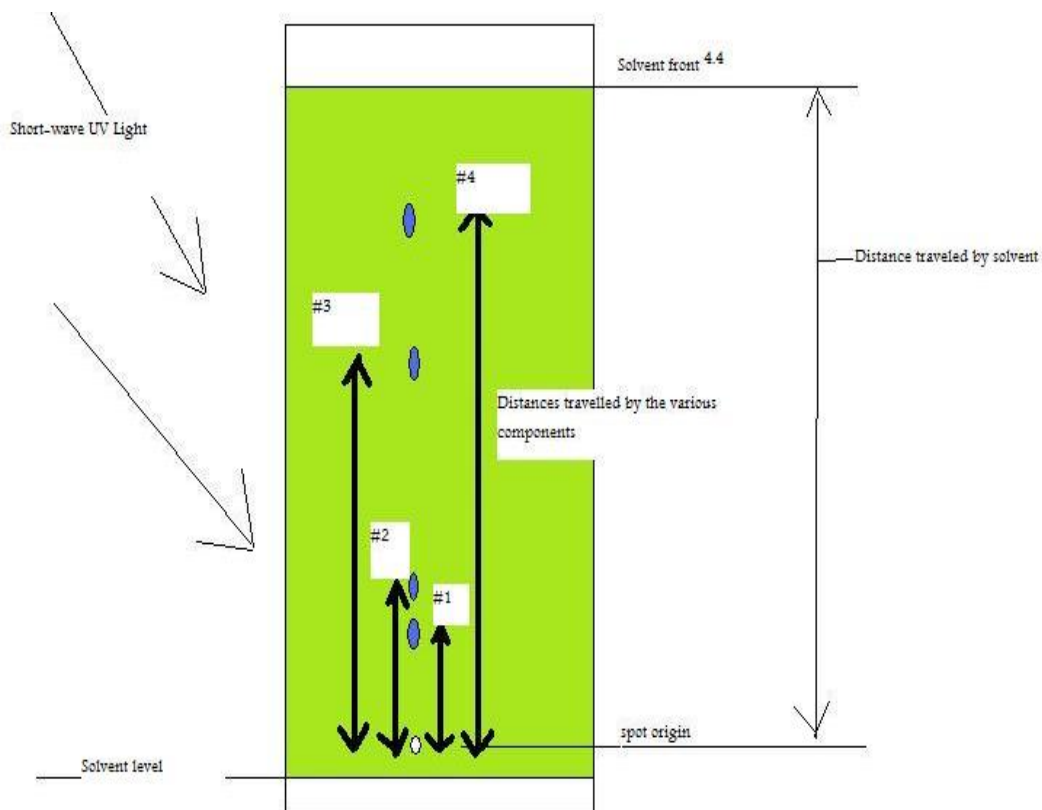
Below is a TLC plate under UV light:

Figure II.10:TLC plate under UV light

II.1.11. Applications [56, 59-64]:

Thin layer chromatography has been a useful tool in numerous applications of pharmaceutical importance.

II.1.11.a. TLC of amino acids:

TLC of amino acids is more difficult than TLC of inks, because amino acids are colourless. Therefore, one cannot see the spots with the naked eye once the plate is fully developed and dried. To see the spots, it is necessary to use either the ninhydrin or the black-light visualization techniques.

E.g., Amino acids, proteins and peptides [8]: A mixture of 34 amino acids, proteins and peptides has been successfully separated and isolated from urine using silica gel plates. All these substances were found to be ninhydrin positive. The development was carried out first with chloroform-methanol-20%ammonium hydroxide (2:2:1) and then with phenol-water.

II.1.11.b. Pharmaceuticals and drugs:

TLC is used in the identification, purity testing and determination of the concentration of active ingredients, auxiliary substances and preservatives in drugs and drug preparations, process control in synthetic manufacturing processes. Various pharmacopoeias have accepted TLC technique for the detection of impurity in a drug or chemical

E.g., Antibiotics: Penicillin's have been separated on silica gel 'G' by using the two solvents, acetone- methanol (1:1) and iso-propanol-methanol (3:7). As the detecting agent, the iodine-azide reaction was employed by spraying the dried plates with a 0.1 % iodine solution containing 3.5% of sodium aside.

II.1.11.c. Separation of multicomponent pharmaceutical formulations:

It is also used in separation of multicomponent pharmaceutical formulations.

II.1.11.d. Qualitative analysis of alkaloids:

It is used in qualitative analysis of alkaloids in control phase of both pharmaceutical formulations and vegetable drugs. TLC has been used for the isolation and determination of

alkaloids in toxicology where the 30-60 minute runs give a great advantage in comparison to the 12-24 hours required for paper chromatography. Purine alkaloids have been separated by TLC on silicic acid, silica gel and aluminium oxide. The spots are visualized by spraying first with an alcoholic iodine-potassium iodine solution followed by 25% HCl- 96% ethanol (1**:1**).

II.1.11.e. Clinical chemistry and Biochemistry:

For the determination of active substances and their metabolites in biological matrices, diagnosis of metabolic disorders such as phenylketonuria, cystinuria and maple syrup disease in babies. It serves as a useful tool in analysis of urinary constituent derived from lipids in analysis of many urinary constituents such as steroids, amino acids, porphyrins and bile acids. Urinary analysis by TLC is most effective when done in conjunction with other chromatographic processes, so that minor metabolites can be detected and resolved completely free of other components.

II.1.11.f. Cosmetology:

In the identification of dye raw materials and end products, preservatives, surfactants, fatty acids, constituents of perfumes.

II.1.11.g. Food Analysis:

For the determination of pesticides and fungicides in drinking water, residues in vegetables, salads and meat, vitamins in soft drinks, banned additives in Germany (e.g. sandalwood extract in fish and meat products), compliance with limit values (e.g. polycyclic compounds in drinking water, aflatoxins in milk and milk products). A typical separation of dyes in spinach looks like this:

II.1.12. Applications related to Organic Chemistry:

- It has been widely used for checking number of other separation processes. TLC has also been applied successfully in various purification processes, checking of distillation fractions and for checking the progress of purification by molecular distillation.

- TLC has been used as an analytical tool in organic chemistry due to its high speed of separation and its applicability in a large number of chemical compounds. Its important use is in the separation and isolation of individual components of a mixture, but in organic chemistry it has also been used for: Checking the purity of samples, as purification process, for identification of organic compounds, for studying various organic reactions, in characterizing and isolating a number of compounds such as acids, alcohols, glycols, amides, alkaloids, vitamins, amino acids, antibiotics, food stuffs and examination of reaction. The reaction mixture is examined by TLC to assess whether the reaction is complete or otherwise. The method is also used in checking other separation processes and purification processes like distillation, molecular distillation etc.

- High sensitivity of TLC is used to check purity of sample, because high sensitivity enables impurities to be observed in so called pure samples. With the help of TLC, it is possible to know whether a reaction is complete and had followed the expected course. The nature of by products can also be ascertained by using TLC. If the reaction does not proceed as desired or expected, then an examination of the behaviour of the spots with standard reagents may sometimes give information for the rapid identification of the products.

II.2. DPPH ASSAYS:

This method was developed by Blois [65]with the viewpoint to determine the antioxidant activity in a like manner by using a stable free radical α, α-diphenyl-β-picrylhydrazyl (DPPH; $C_{18}H_{12}N_5O_6$, M = 394.33). The assay is based on the measurement of the scavenging capacity of antioxidants towards it. The odd electron of nitrogen atom in DPPH is reduced by receiving a hydrogen atom from antioxidants to the corresponding hydrazine [66].

DPPH is characterized as a stable free radical by virtue of the delocalisation of the spare electron over the molecule as a whole (**Figure II.11**) so that the molecules do not dimerise, like most other free radicals. The delocalisation also gives rise to the deep violet colour, with an absorption in ethanol solution at around 520 nm.

On mixing DPPH solution with a substance that can donate a hydrogen atom, it gives rise to the reduced form with the loss of violet colour. Representing the DPPH radical by Z• and the donor molecule by AH, the primary reaction is:

$$Z^*+AH=ZH+A^*$$
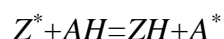
Where ZH is the reduced form and A• is free radical produced in the first step. The latter radical will then undergo further reactions which control the overall stoichiometry the previous reaction is therefore intended to provide the link with the reactions taking place in an oxidising system, such as the autoxidation of a lipid or other unsaturated substance; the DPPH molecule Z• is thus intended to represent the free radicals formed in the system whose activity is to be suppressed by the substance AH.
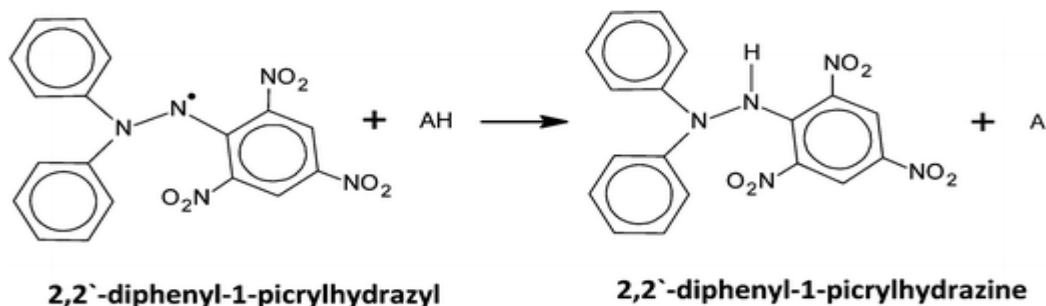

2,2`-diphenyl-1-picrylhydrazyl        2,2`-diphenyl-1-picrylhydrazine

Figure II.11:DPPH radical and its stable form

While DPPH can accept an electron or hydrogen radical to become a stable, diamagnetic molecule, it can be oxidized only with difficulty, and then irreversibly. DPPH shows a strong absorption band at 517 nm due to its odd electron and solution appears a deep violet colour, the absorption vanishes as the electron pairs off. The resulting decolourization is stoichiometric with respect to the number of electrons taken up.The alcoholic solutions of 0.5 mM are densely coloured and at this concentration, the Lambert-Beer law is obeyed over the useful range of absorption [65]

It is a rapid, simple, inexpensive and widely used method to measure the ability of compounds to act as free radical scavengers or hydrogen donors, and to evaluate antioxidant activity of foods. It can also be used to quantify antioxidants in complex biological systems, for solid or liquid samples. This method is easy and applies to measure the overall antioxidant capacity   and the free radical scavenging activity of fruit and vegetable juices [67]. This assay has been successfully utilized for investigating antioxidant properties of wheat grain and bran, vegetables, conjugated linoleic acids, herbs, edible seed oils, and flours in several different solvent systems including ethanol, aqueous acetone, methanol, aqueous alcohol and benzene [68] .It is a convenient method for the antioxidant assay of cysteine, glutathione, ascorbic acid, tocopherol and polyhydroxy aromatic compounds [69] for olive oil, fruits, juices and wines [70].

The method is unique in carrying out the reaction of the sample with DPPH in methanol/water, which facilitates the extraction of antioxidant compounds from the sample. Determination of antioxidant activity of various types of foods using DPPH is comparable to other methods.

Antioxidant analysis by other methods may be limited to those compounds soluble in the selected solvents. The advantage of this method is that DPPH is allowed to react with the whole sample and sufficient time given in the method allows DPPH to react slowly even with weak antioxidants. DPPH method may be utilized in aqueous and nonpolar organic solvents and can be used to examine both hydrophilic and lipophilic antioxidants [71]

DPPH assay is considered a valid accurate, easy and economic method to evaluate radical scavenging activity of antioxidants, since the radical compound is stable and need not be generated. Sanchez-Moreno et al. [70] , proposed a new methodology for the evaluation of antiradical efficiency towards DPPH, which is advantageous over other methods. It considers not only the antioxidant concentration but also the reaction time of scavenging reaction to reach the plateau. The results are highly reproducible and comparable to other free radical scavenging methods[72]. The antioxidant efficiency is measured at ambient temperature so that the risk of thermal degradation of the molecules tested is eliminated[72]. In optothermal window mode, the method can also be utilized for the evaluation of antioxidant efficiency of the compounds, which form opaque solution. It can also be used for online monitoring of changes in food containing natural antioxidants.

This method is limited because DPPH radical interacts with other radicals and the time response curve to reach the steady state is not linear with different ratios of antioxidant/DPPH [70, 73]. DPPH is sensitive to some Lewis bases and solvent types as well as oxygen DPPH can only be soluble in organic solvent and the interference of absorbance from the sample compounds could be a problem for the quantitative analysis. The absorbance of DPPH in methanol and acetone decreases under light 1998. DPPH method has limitations in reflecting the partitioning of antioxidants in the emulsion systems and is not useful for measuring the antioxidant activity of plasma, because proteins are precipitated in the alcoholic reaction medium.

II.3. FOURIER TRANSFORM INFRARED (FTIR) SPECTROSCOPY:

Infrared spectroscopy is one of the most common spectroscopic techniques used in the field of organic and inorganic chemistry. It is the study of absorption of an unknown sample placed in the path of an infrared beam at different infrared frequencies. The main goal of the IR spectroscopic analysis is to determine the different functional groups in the sample. Different functional groups absorb at characteristic frequencies of infrared radiation.

Thus IR spectroscopy is an important tool for structural analysis and compound identification. Light exhibits both wave and particle characteristics. Light waves are described as electric and magnetic fields oscillating at right angles to each other. The frequency (ϑ) is the number of wave cycles that pass through a point in one second. It is measured in Hertz (**Hz**). The wavelength (λ) is the length of one complete wave cycle. It is often measured in centimeter (cm). Wavelength and frequency are inversely related:

$$\vartheta = \frac{c}{\lambda} \qquad\qquad (17)$$

where **c** is the velocity of light (3 x 10^8 m/s).

Energy is related to wavelength and frequency by the following equation:

$$E=h.\vartheta = \frac{hc}{\lambda} \qquad\qquad (18)$$

IR absorption positions are generally presented as either wavenumbers $(\bar{\vartheta})$ or wavelengths(λ). Wavenumber defines the number of waves per unit length. Thus, wavenumbers are directly proportional to frequency, as well as the energy of the IR absorption. Wavenumber (unit cm^{-1}) is commonly used in modern IR instruments.

Infrared region refers to the part of the electromagnetic spectrum between visible and microwave regions. The electromagnetic spectrum is shown in **Figure II.12** . Infrared radiation covers a section of the electromagnetic spectrum from 13000 to 10 cm^{-1} or in terms of wavelengths from 0.78 µm to 1000 µm. Infrared radiation in this range is absorbed and converted into energy of molecular vibration by a molecule.[74]
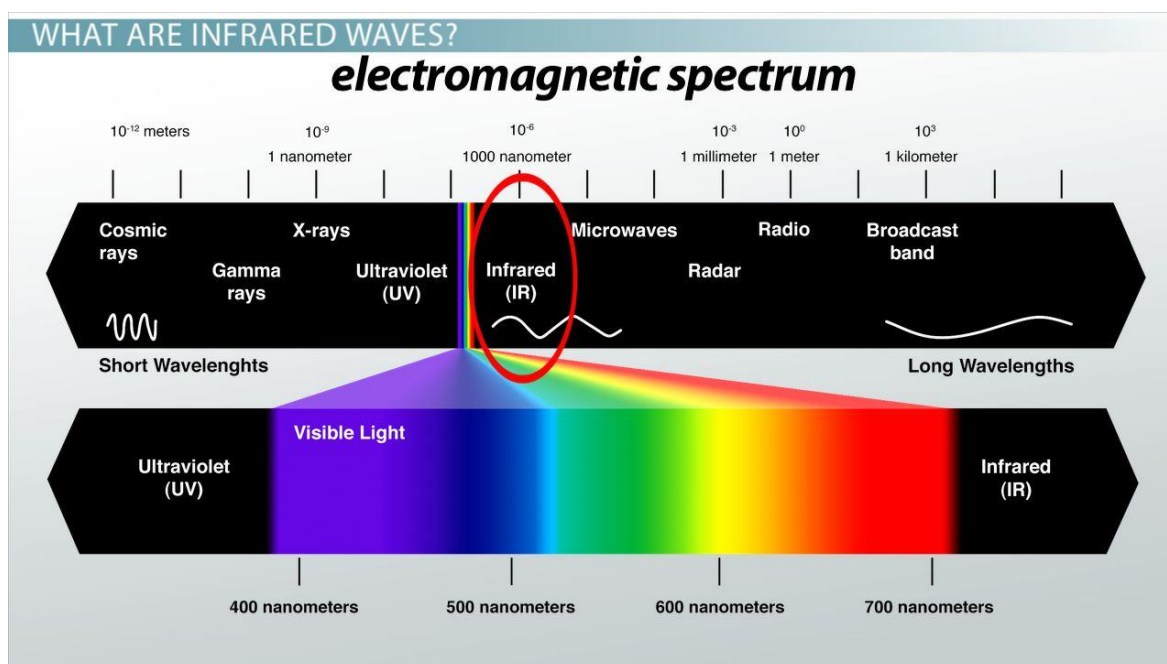
Figure II.12:Electromagnetic spectrum (picture downloaded from Study.com)

The infrared spectrometers can be divided into 2 groups:

- dispersive infrared spectrometer (IR)
- Fourier transform infrared spectrometers (FTIR).

In a dispersive IR spectrometer, a grating type monochromator is used to disperse the radiation of a polychromatic source into different spectral elements, which are then measured by detector, one element at the time. This makes sampling tedious and since only a small portion of the radiation is measured at each time, the signal intensity is rather weak. In an FTIR spectrometer an interferometer is used to generate an interferogram.

In an FTIR instrument, all wavelengths are measured simultaneously which results in faster sampling and in better signal to noise ratio as compared to dispersive instruments. The most commonly used interferometer is the Michelson interferometer, as shown in **Figure II.13**. The interferogram is subsequently Fourier transformed yielding the spectrum (**Figure II.14)** [75]:

Figure II.13:Construction of Michelson Interferometer
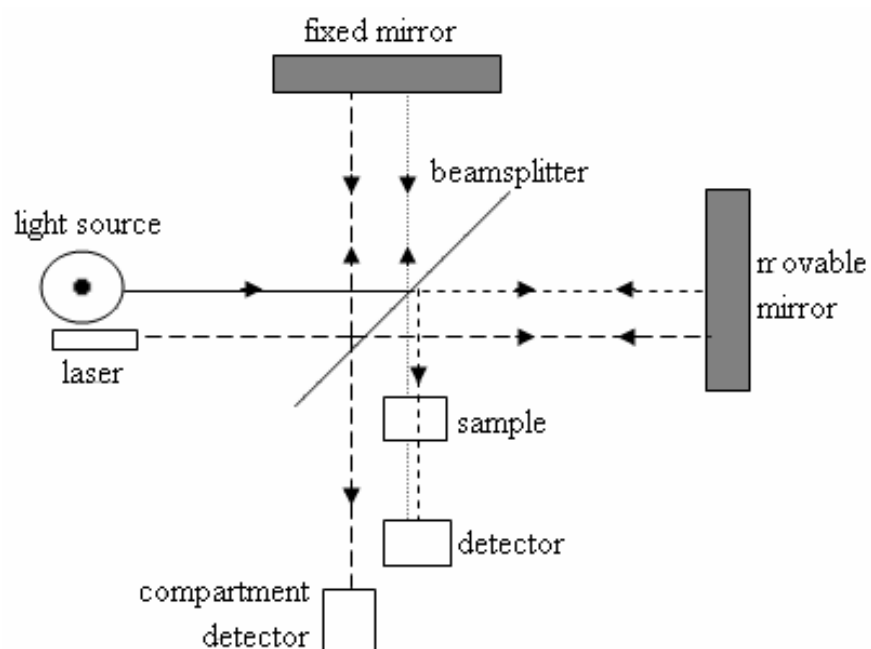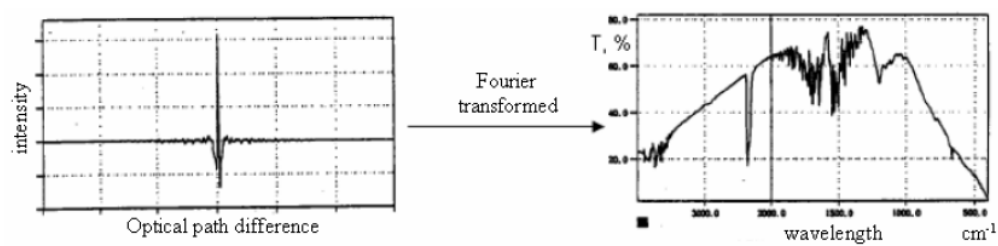

Figure II.14:Relation between interferogram and spectrum

References

1. Rasmussen, K. and S.R. Niketic, *The Consistent Force Field: A Documentation.* 1977: Springer.

2. Levine, I.N., D.H. Busch, and H. Shull, *Quantum chemistry*. Vol. 5. 2000: Prentice Hall Upper Saddle River, NJ.

3. Leach, A.R., *Molecular modelling: principles and applications*. 2001: Pearson education.

4. Heinrich, N., *A. Hinchliffe: Computational Quantum Chemistry, John Wiley & Sons, Chichester, New York, Brisbane, Toronto, Singapore 1988. 112 Seiten, Preis:£ 15.95.* Berichte der Bunsengesellschaft für physikalische Chemie, 1989. **93**(11): p. 1400-1400.

5. Cramer, C.J., *Essentials of computational chemistry: theories and models*. 2013: John Wiley & Sons.

6. Szabo, A. and N.S. Ostlund, *Modern quantum chemistry: introduction to advanced electronic structure theory*. 2012: Courier Corporation.

7. Hehre, W.J., *Ab initio molecular orbital theory*. 1986: Wiley-Interscience.

8. Hehre, W.J., R.F. Stewart, and J.A. Pople, *Self‐Consistent Molecular‐Orbital Methods. I. Use of Gaussian Expansions of Slater‐Type Atomic Orbitals.* The Journal of Chemical Physics, 1969. **51**(6): p. 2657-2664.

9. Whitley, D.C., *Drug Design Strategies Computational Techniques and Applications.* 2012.

10. Becke, A.D., *Density-functional exchange-energy approximation with correct asymptotic behavior.* Physical review A, 1988. **38**(6): p. 3098.

11. Stephens, P., et al., *Ab initio calculation of vibrational absorption and circular dichroism spectra using density functional force fields.* The Journal of Physical Chemistry, 1994. **98**(45): p. 11623-11627.

12. Grimme, S., *Accurate description of van der Waals complexes by density functional theory including empirical corrections.* Journal of computational chemistry, 2004. **25**(12): p. 1463-1473.

13. Salomon, O., M. Reiher, and B.A. Hess, *Assertion and validation of the performance of the B3LYP⋆ functional for the first transition metal row and the G2 test set.* The Journal of chemical physics, 2002. **117**(10): p. 4729-4737.

14. Ye, S. and F. Neese, *Accurate modeling of spin-state energetics in spin-crossover systems with modern density functional theory.* Inorganic chemistry, 2010. **49**(3): p. 772-774.

15. Deeth, R.J. and N. Fey, *The performance of nonhybrid density functionals for calculating the structures and spin states of Fe (II) and Fe (III) complexes.* Journal of computational chemistry, 2004. **25**(15): p. 1840-1848.

16. Pariser, R. and R.G. Parr, *A semi-empirical theory of the electronic spectra and electronic structure of complex unsaturated molecules. II.* The Journal of Chemical Physics, 1953. **21**(5): p. 767-776.

17. Pople, J.A., *Electron interaction in unsaturated hydrocarbons.* Transactions of the Faraday Society, 1953. **49**(0): p. 1375-1385.

18. Beveridge, D., *Approximate Molecular Orbital Theory.* MacGraw-Hill, New York, 1970.

19. Klopman, G. and R. Evans, *The neglect-of-differential-overlap methods of molecular orbital theory*, in *Semiempirical Methods of Electronic Structure Calculation*. 1977, Springer. p. 29-67.

20. Zerner, M., *Reviews in Computational Chemistry.* Vol. 2, Capítulo 8, pág. 313-365, KB Lipkowitz, DB Boyd Eds., VCH Publishers, Inc, 1991.

21. Dewar, M.J. and W. Thiel, *Ground states of molecules. 38. The MNDO method. Approximations and parameters.* Journal of the American Chemical Society, 1977. **99**(15): p. 4899-4907.

22. Dewar, M.J., M.L. McKee, and H.S. Rzepa, *MNDO parameters for third period elements.* Journal of the American Chemical Society, 1978. **100**(11): p. 3607-3607.

23. Dewar, M.J. and M.L. McKee, *Ground states of molecules. 50. MNDO study of hydroboration and borohydride reduction. Implications concerning cyclic conjugation and pericyclic reactions.* Journal of the American Chemical Society, 1978. **100**(24): p. 7499-7505.

24. Dewar, M.J., et al., *Development and use of quantum mechanical molecular models. 76. AM1: a new general purpose quantum mechanical molecular model.* Journal of the American Chemical Society, 1985. **107**(13): p. 3902-3909.

25.   Stewart, J.J., *Optimization of parameters for semiempirical methods II. Applications.* Journal of computational chemistry, 1989. **10**(2): p. 221-264.

26.   Stewart, J.J., *MOPAC: a semiempirical molecular orbital program.* Journal of computer-aided molecular design, 1990. **4**(1): p. 1-103.

27.   Stewart, J.J., *Optimization of parameters for semiempirical methods. III Extension of PM3 to Be, Mg, Zn, Ga, Ge, As, Se, Cd, In, Sn, Sb, Te, Hg, Tl, Pb, and Bi.* Journal of computational chemistry, 1991. **12**(3): p. 320-341.

28.   Jensen, F., *Introduction to computational chemistry*. 2017: John wiley & sons.

29.   Fabre, G., *Molecular interaction of natural compounds with lipid bilayer membranes: Towards a better understanding of their biological and pharmaceutical actions*. 2015, Université de Limoges; Univerzita Palackého [Olomouc, République tchèque].

30.   Fox, S.B., *"Design of Molecular Mechanics Modeling Techniques For Exploring Molecular Recognition Using Cyclodextrins.* 2003.

31.   Paton, R.S. and J.M. Goodman, *Hydrogen bonding and π-stacking: How reliable are force fields? A critical evaluation of force field descriptions of nonbonded interactions.* Journal of chemical information and modeling, 2009. **49**(4): p. 944-955.

32.   Jorgensen, W.L. and P. Schyman, *Treatment of halogen bonding in the OPLS-AA force field: application to potent anti-HIV agents.* Journal of chemical theory and computation, 2012. **8**(10): p. 3895-3901.

33.   Darden, T., D. York, and L. Pedersen, *Particle mesh Ewald: An N· log (N) method for Ewald sums in large systems.* The Journal of chemical physics, 1993. **98**(12): p. 10089-10092.

34.   Weiner, S.J., et al., *A new force field for molecular mechanical simulation of nucleic acids and proteins.* Journal of the American Chemical Society, 1984. **106**(3): p. 765-784.

35.   Cornell, W.D., et al., *A second generation force field for the simulation of proteins, nucleic acids, and organic molecules.* Journal of the American Chemical Society, 1995. **117**(19): p. 5179-5197.

36.   Brooks III, C.L. and M. Karplus, *Solvent effects on protein motion and protein effects on solvent motion: dynamics of the active site region of lysozyme.* Journal of molecular biology, 1989. **208**(1): p. 159-181.

37.   Karplus, M. and G.A. Petsko, *Molecular dynamics simulations in biology.* Nature, 1990. **347**(6294): p. 631.

38.   Lifson, S., A. Hagler, and P. Dauber, *Consistent force field studies of intermolecular forces in hydrogen-bonded crystals. 1. Carboxylic acids, amides, and the C: O. cntdot.. cntdot.. cntdot. H-hydrogen bonds.* Journal of the American Chemical Society, 1979. **101**(18): p. 5111-5121.

39.   Vinter, J.G., A. Davis, and M.R. Saunders, *Strategic approaches to drug design. I. An integrated software framework for molecular modelling.* Journal of Computer-Aided Molecular Design, 1987. **1**(1): p. 31-51.

40.   Mayo, S.L., B.D. Olafson, and W.A. Goddard, *DREIDING: a generic force field for molecular simulations.* Journal of Physical chemistry, 1990. **94**(26): p. 8897-8909.

41.   Momany, F., et al., *Energy parameters in polypeptides. VII. Geometric parameters, partial atomic charges, nonbonded interactions, hydrogen bond interactions, and intrinsic torsional potentials for the naturally occurring amino acids.* The Journal of Physical Chemistry, 1975. **79**(22): p. 2361-2381.

42.   van Gunsteren, W.F. and H.J. Berendsen, *Computer simulation of molecular dynamics: Methodology, applications, and perspectives in chemistry.* Angewandte Chemie International Edition, 1990. **29**(9): p. 992-1023.

43.   Allinger, N.L., *Conformational analysis. 130. MM2. A hydrocarbon force field utilizing V1 and V2 torsional terms.* Journal of the American Chemical Society, 1977. **99**(25): p. 8127-8134.

44.   Lii, J.H. and N.L. Allinger, *Molecular mechanics. The MM3 force field for hydrocarbons. 3. The van der Waals' potentials and crystal data for aliphatic and aromatic hydrocarbons.* Journal of the American Chemical Society, 1989. **111**(23): p. 8576-8582.

45.   Allinger, N.L., K. Chen, and J.H. Lii, *An improved force field (MM4) for saturated hydrocarbons.* Journal of Computational Chemistry, 1996. **17**(5-6): p. 642-668.

46.   Halgren, T.A., *Merck molecular force field. I. Basis, form, scope, parameterization, and performance of MMFF94.* Journal of computational chemistry, 1996. **17**(5-6): p. 490-519.

47.   Viswanadhan, V.N., et al., *Atomic physicochemical parameters for three dimensional structure directed quantitative structure-activity relationships. 4. Additional parameters for hydrophobic and dispersive interactions and their application for an automated superposition of certain naturally occurring nucleoside antibiotics.* Journal of Chemical Information and Computer Sciences, 1989. **29**(3): p. 163-172.

48.   Hill, T.L., *On steric effects.* The Journal of Chemical Physics, 1946. **14**(7): p. 465-465.

49.   Westheimer, F.H. and J.E. Mayer, *The theory of the racemization of optically active derivatives of diphenyl.* The Journal of Chemical Physics, 1946. **14**(12): p. 733-738.

50.   Barton, D. and J. Cox, *158. The application of the method of molecular rotation differences to steroids. Part IV. Optical anomalies.* Journal of the Chemical Society (Resumed), 1948: p. 783-793.

51.   Gasteiger, J. and M. Marsili, *Iterative partial equalization of orbital electronegativity—a rapid access to atomic charges.* Tetrahedron, 1980. **36**(22): p. 3219-3228.

52.   Benbrahim, I., *Etude par des méthodes quantiques et empiriques des relations SAR et QSAR dans des hétérocycles à intérêt médicinale*. 2017, Université Mohamed Khider-Biskra.

53.   Sousa, S.F., P.A. Fernandes, and M.J. Ramos, *Protein–ligand docking: Current status and future challenges.* Proteins: Structure, Function, and Bioinformatics, 2006. **65**(1): p. 15-26.

54.   Patrick, G.L., *An introduction to medicinal chemistry*. 2013: Oxford university press.

55.   Ettre, L., *Nomenclature for chromatography (IUPAC Recommendations 1993).* Pure and Applied Chemistry, 1993. **65**(4): p. 819-872.

56.   Bower, N.W., *Principles of Instrumental Analysis. 4th edition (Skoog, D. A.; Leary, J. J.).* Journal of Chemical Education, 1992. **69**(8): p. A224.

57.   Poole, C.F., *The essence of chromatography*. 2003: Elsevier.

58.   Bele, A.A. and A. Khale, *An overview on thin layer chromatography.* International Journal of Pharmaceutical Sciences and Research, 2011. **2**(2): p. 256.

59.   Kasture, A., et al., *Pharmaceutical Analysis-Instrumental Methods, Vol-2*. 2004, Pune: Nirali prakashan.

60.   Quach, H., R. Steeper, and G. Griffin, *Separation of plant pigments by thin layer chromatography.* Journal of chemical education, 2004. **81**: p. 385-7.

61.   Chatwal, G. and S. Anand, *Instrumental Methods of Chemical Analysis 2004*. 2004, Himalaya Publishing House.

62.   Beckett, A.H. and J.B. Stenlake, *Practical Pharmaceutical Chemistry: Part II Fourth Edition*. Vol. 2. 1988: A&C Black.

63.   Sagar, G.V., *Instrumental methods of drug analysis*. 2009: PharmaMed Press.

64.   Kirchner, J.G., *Thin-layer chromatographic quantitative analysis.* Journal of Chromatography a, 1973. **82**(1): p. 101-115.

65.   Blois, M.S., *Antioxidant determinations by the use of a stable free radical.* Nature, 1958. **181**(4617): p. 1199.

66.   Contrerasguzman, E. and F. Strong, *Determination of tocopherols (vitamin-E) by reduction of cupric ion.* Journal of the Association of Official Analytical Chemists, 1982.

67.   Sendra, J.M., E. Sentandreu, and J.L. Navarro, *Reduction kinetics of the free stable radical 2, 2-diphenyl-1-picrylhydrazyl (DPPH•) for determination of the antiradical activity of citrus juices.* European Food Research and Technology, 2006. **223**(5): p. 615.

68.   Yu, L., *Free radical scavenging properties of conjugated linoleic acids.* Journal of Agricultural and Food Chemistry, 2001. **49**(7): p. 3452-3456.

69.   Nishizawa, M., et al., *Non-reductive scavenging of 1, 1-diphenyl-2-picrylhydrazyl (DPPH) by peroxyradical: a useful method for quantitative analysis of peroxyradical.* Chemical and pharmaceutical bulletin, 2005. **53**(6): p. 714-716.

70.   Sánchez-Moreno, C., J.A. Larrauri, and F. Saura-Calixto, *Free radical scavenging capacity of selected red, rose and white wines.* Journal of the Science of Food and Agriculture, 1999. **79**(10): p. 1301-1304.

71.   Prior, R.L., X. Wu, and K. Schaich, *Standardized methods for the determination of antioxidant capacity and phenolics in foods and dietary supplements.* Journal of agricultural and food chemistry, 2005. **53**(10): p. 4290-4302.

72.   Gil, M.I., et al., *Antioxidant activity of pomegranate juice and its relationship with phenolic composition and processing.* Journal of Agricultural and Food chemistry, 2000. **48**(10): p. 4581-4589.

73.   Brand-Williams, W., M.-E. Cuvelier, and C. Berset, *Use of a free radical method to evaluate antioxidant activity.* LWT-Food science and Technology, 1995. **28**(1): p. 25-30.

74.   Manohar, S.N., *FTIR Spectroscopic Study of Atmospheric Molecules on Ice Surfaces.* 2008.

75.   Bykov, I., *Characterization of natural and technical lignins using FTIR spectroscopy.* 2008.

CHAPTER

3

EXPERIMENTAL

ASSAYS

Introduction:

Curcumin is a phytochemical found in the Indian spice turmeric, Curcuma longa. Because of the conjugated system of the molecule, curcumin gives the characteristic yellow colour of turmeric. Due to its strong colouring ability, curcumin is used in food and textile industries. It is also used as a preservative and the food additive number of curcumin is E100.

Turmeric does not only contain curcumin (compound P1), but also its analogues Demetoxycurcumin (compound P2), Bisdemetoxycurcumin (compound P3) and the water soluble protein turmerin. The biological and molecular properties of curcumin and its analogues are similar. It is suggested that in natural pathways the bisdemethoxycurcumin converts to Demetoxycurcumin, which in turn converts to curcumin (**Figure III.1**)[1]

The ratio between the analogues in an extract obtained from turmeric is curcumin ~75 %, Demetoxycurcumin ~ 16% and bisdemethoxycurcumin ~8%.

The antioxidant property of curcumin can prevent rancidity of foods and provide foodstuffs containing less oxidized fat or free radicals. The powerful antioxidant property of curcumin has an important role in keeping curry for a long time without it turning rancid. Curcuminoids are poorly soluble in the hydrocarbon solvents. Curcumin is an oil soluble pigment, practically insoluble in water at acidic and neutral pH, soluble in alkali. Preparations of water-soluble curcumin by incorporation into various surfactant micellar systems (acetone, methanol, and ethanol) have been reported[2].It is stable at high temperatures and in acids, but unstable in alkaline conditions and in the presence of light.
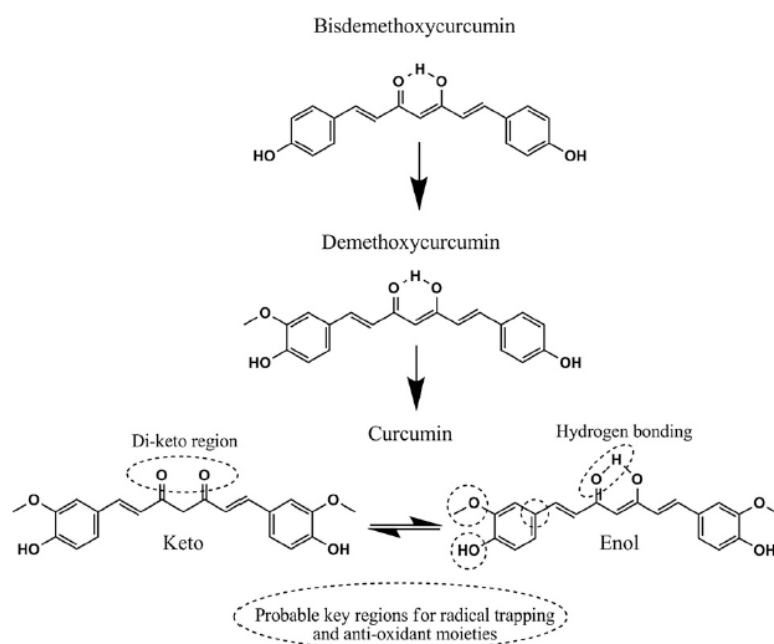

Figure III.1:The crucial sites for the antioxidant properties of the molecules and how the molecules transform from bisdemethoxycurcumin to curcumin.[1]

I. EXTRACTION AND SEPARATION OF CURCUMIN AND ITS DERIVATIVES:

The extraction and separation of curcuminoids were performed according to a previous research which explains the use of a certain methods and solvents [3, 4].

I.1. EXTRACTION:

To get good results from extraction, it is important to find a solvent that has the ability to extract curcumin together with the other two curcuminoids. As they are analogues, the polarity of the compounds is very similar and reaches from nonpolar to half polar, and therefore a half polar solvent was the most appropriate choice for the extraction procedure.

❖ **Products and materials:**
- Plant: **60 g** of turmeric Powder has been purchased from Herbalist
- Solvent used: Acetone (C_3H_6O)
- Materials: A Florence Flask as a container, stirrer
- A balance, an evaporating dish and a beaker for quantitative measurements, funnel, Support stand ... etc.

❖ *Process:*

60 g of turmeric powder was mixed in **400 ml** of acetone and stirred for 48 hours (not continuously). The solution was filtered using Suction filtration (Büchner filtration) , then passed through evaporation process to eliminate any solvent remains.(**Figure III.2).**
The obtained product was concentrated with a yield around **5.2 g**.

Figure III.2:extraction of Curcuminoids

To ensure that the experiment was going on a right path a TLC analysis was performed to confirm the identity and compositions ; showing a fingerprint with 3 clear spots (**Figure III.3**)
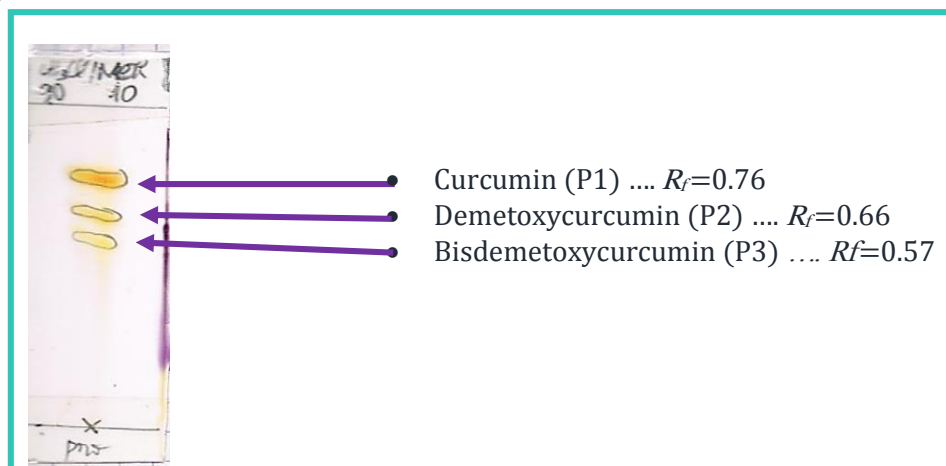

Curcumin (P1) .... R_f=0.76
Demetoxycurcumin (P2) .... R_f=0.66
Bisdemetoxycurcumin (P3) .... Rf=0.57

Figure III.3:The TLC Fingerprint of the extracted curcuminoids [eluent : Chloroform-methanol (95:5)]

The TLC process was as following : (**Figure III.4**)

1. Cut a large stock TLC plate from the box into rectangles with a Measured dimension in our first case for example it was 3x5 cm.
2. Mark the TLC plate with a pencil about 0.5 cm from the bottom and the same thing from the top, label these lines as starting material (prod)
3. Prepare the chromatography solvent or the eluent in our case its always

   Chloroform-methanol (95:5)
4. Prepare the curcumin solution after diluting the obtained extract in the same solvent because if the solution is too concentrated, the spots will streak and it will get no useful.
5. Take a small amount of solution by Submerging the tip of a glass pipette

   and the pipette will suck up a small amount .Lightly press the tip of the pipette to the intersection of one of the dashed lines and the horizontal line made previously on the silica side. This will cause the solution in the pipette to be sucked onto the silica, resulting in a small circle of solvent and compound .
6. Dry the TLC plate by Simply set the plate down and wait a minute or so for the solvent to evaporate off the plate.

7. Develop the plate. Using tweezers, gently place the TLC plate into the solvent jar, with the spotted end of the plate at the bottom close to the solvent. Submerge the bottom edge of the plate into the solvent, allowing the solvent to run up the plate, carrying the compounds along with it. Cover the jar with the lid. This will prevent solvent from evaporating and make the development stage much faster.

    Meanwhile the jar/system must be undisturbed otherwise it will get the band distorted, this is the stage where separation occurs. So we have to wait 2-3 minutes for the solvent to reach the top of the plate before removing it.

8. Remove the plate and dry it: Once the solvent comes close to reaching the upper edge of the plate, use tweezers to carefully remove it from the chamber and wait for the solvent to evaporate off the plate

9. Visualize the plate: since the Curcumin is already coloured there was no such a need for UV or any other procedures.

    After Confirming the existence of the three analogues, the concentrated extract was transferred to a column for separation process.
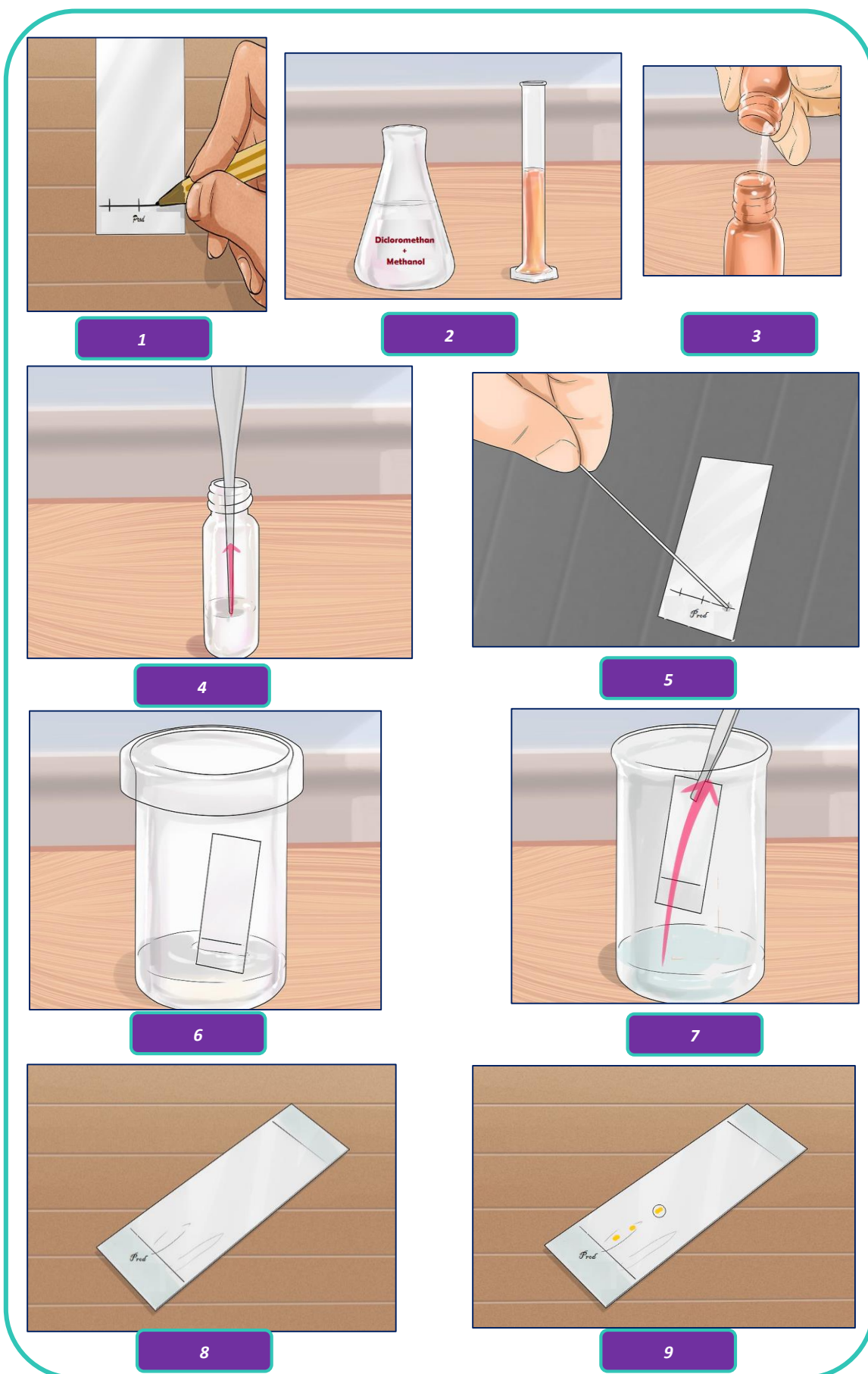
Figure III.4:TLC procedures (graphics were extracted from Wikihow website)

I.2. SEPARATION:

❖ *Raw Materials:*

- the concentrated extract
- Solvents: Chloroform ($CHCl_3$) – Methanol (CH_3OH)
- The column of chromatography
- An appropriate support stand
- thin layer chromatography Plate (TLC Plate)
- a TLC developing chamber
- Silica pot
- funnel
- Cotton , sand
- Beakers
- Pasteur pipettes
- propipettes,
- support and test tubes

❖ *Process:*

The realization of a column imposes to respect certain rules which will lead onto an effective separation.

A piece of cotton is placed at the bottom of the column, which is covered with eluent, in order to eliminate the air trapped in the cotton. Half a centimeter of sand is added above the cotton, so that the stationary phase cannot be leaked from the column. It will be considered here that the sand has no adsorbent properties.   Finally, the column is filled with the stationary phase by producing a suspension of silica in eluent which is Chloroform - methanol (95:5). The gel thus formed is introduced into the column through the funnel. Rinse with the eluent and let it flow.

Once the column filled, we add half a centimeter of sand at the top of the column above the silica surface, after making sure that the latter was flat. This layer makes it possible to make deposits and to add eluent without disturbing the silica surface, which would prevent a good separation. We regularly make sure not to dry the stationary phase, checking that there is still eluent at the sand.

✓ **Realization of the experiment:**

The level of eluent is brought to the level of the surface of the sand. It is then possible to carefully deposit dye solution curcuminoids at the top of the column with the Pasteur pipette so as not to disturb the silica surface.

The tap is opened so that curcuminoids reach the level of the silica. A few milliliters of eluent are added and the tap is re-opened to ensure that the entire solution is at the top of the silica column.

we can then add the eluent. The first milliliters should always be carefully added using the Pasteur pipette so as not to disturb the silica surface. Then we can add the eluent more quickly by pouring it directly into the column. (**Figure III.5**).

Figure III.5:Column chromatography in process

I.3. RESULTS AND DISCUSSION:

The extraction of curcuminoids from turmeric through the previous method was carried out. the method was relatively simple procedure and no complications occurred.

To evaluate the efficiency of the results obtained from extraction, a TLC analysis was considered, showing a fingerprint with 3 spots, indicates the existence of only three components that actually represents these major analogues of Curcumin (named curcuminoids):

- Curcumin (P1)
- Demetoxycurcumin (P2)
- Bisdemetoxycurcumin (P3)

And that gave us a good sign that the performed extraction was ideal.

On the other hand, the separation step was done by column chromatography. There were some difficulties ; Even though the solvents used in this experiment were the same as in previous studies[3], it did not give similar results. different solvents and solvent mixtures were tried on TLC in the hope to find a better mobile phase, which could separate the molecules better. As a result , and according to some other studies[4]we changed the elution phase (from Dichloromethane -methanol (**93:7**) to Chloroform -methanol (**95: 5**) and actually that improved a bit more the separation yields specially for the analogues (**p2**) and (**p3**) .

During the column development A TLC test was needed again to control the migration process and separate correctly each one of the analogues as its shown in the and procedure **Figure III.6** and TLC results **Figure III.7**

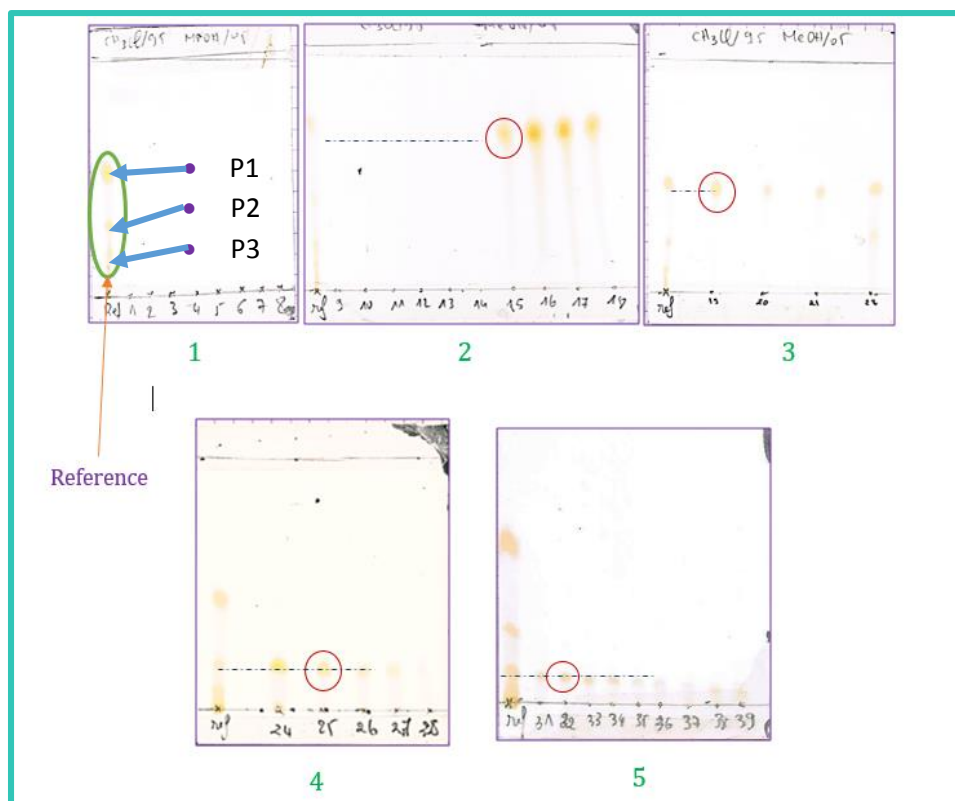*Figure III.6: Some TLC assays gathered from Column*

Figure III.7: TLC fingerprinting results (the first column)

➢ **Interpretation of the TLC results:**

The first plate shows the fingerprinting result of the extracted product before separation; nominated as the reference to follow-up the appearance of different analogues during column chromatography.

The next one (2 and 3) revealed the appearance of product 1 (Curcumin) with one spot which has the same level as the one referred in plate 1. meanwhile plate 4 and 5 have shown the appearance of **P2** and **P3** according to the level of the spots detected on each fingerprint. The extraction and separation procedures were repeated again as a hope to get a better results and obtain much more quantity for future tests; the same findings were observed as The TLC analysis in **Figure III.8** show .
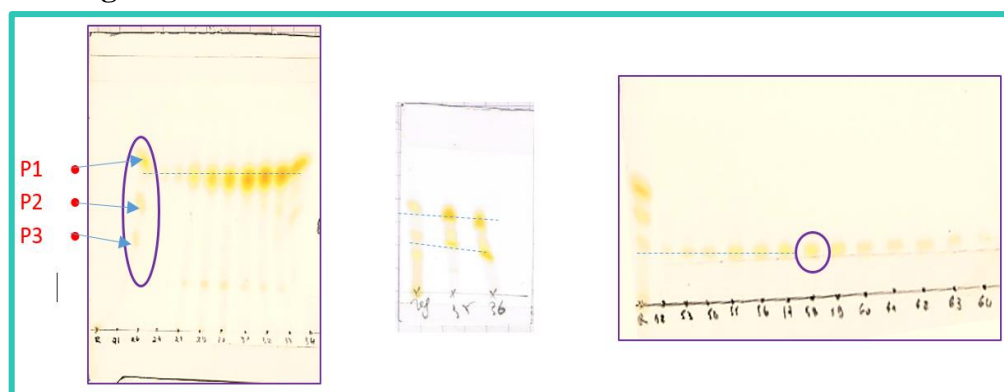

Figure III.8:TLC fingerprinting results (the second column)

All separated analogues from both columns have been assembled for further tests and analysis, after an evaporation process to eliminate the rest of the solvent used in column chromatography technique.

The characterization results were summarised in the table below:

Table III-1:Characterization results of curcuminoids before and after

Extract	Weight (g)	Coulure	Status
P1:Curcumin	0.8	Dark orange	Solid
P2: Demetoxycurcumin	0.135	Dark orange	Solid
P3: Bisdemetoxycurcumin	0.1	Dark orange	Solid

So according to these previous results, the experiment of the extraction and separation of the curcuminoids gave quite good findings.Without forgetting to mention that it has been shown in some literature that using the soxhlet method as an extraction process might give a better results and maybe increases the yield collected from extraction which might be considered in future.[2]

II. SPECTRAL CHARACTERIZATION OF CURCUMINOIDS:
II.1. FT-IR SPECTROSCOPY:

Fourier Transform Infrared Spectroscopy (FT-IR) is a popular tool for identifying and characterizing materials. FT-IR spectra of the ligands and simple complexes were recorded as KBr pellets with a Shimadzu, Model **FTIR-8400S** spectrophotometer in the 400-4000 cm^{-1} range.

The analysis were performed on the previous three isolated curcuminoids giving these spectrum shown in figures : **Figure III.9 ; Figure III.10 ; Figure III.11 ,** which were visualized using Spectragryph-Optical Spectroscopy Software, version 1.0. 7 [5]:
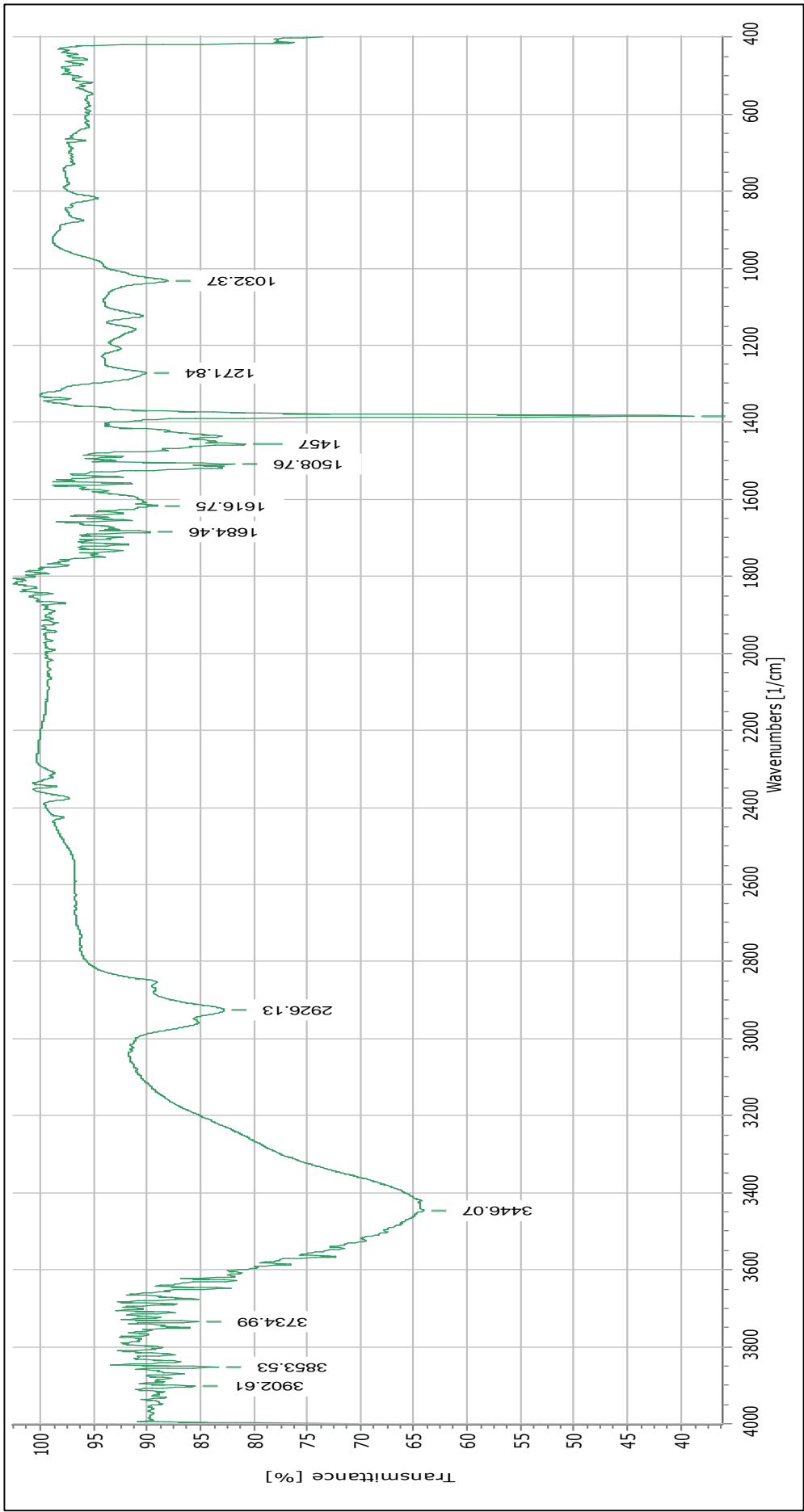
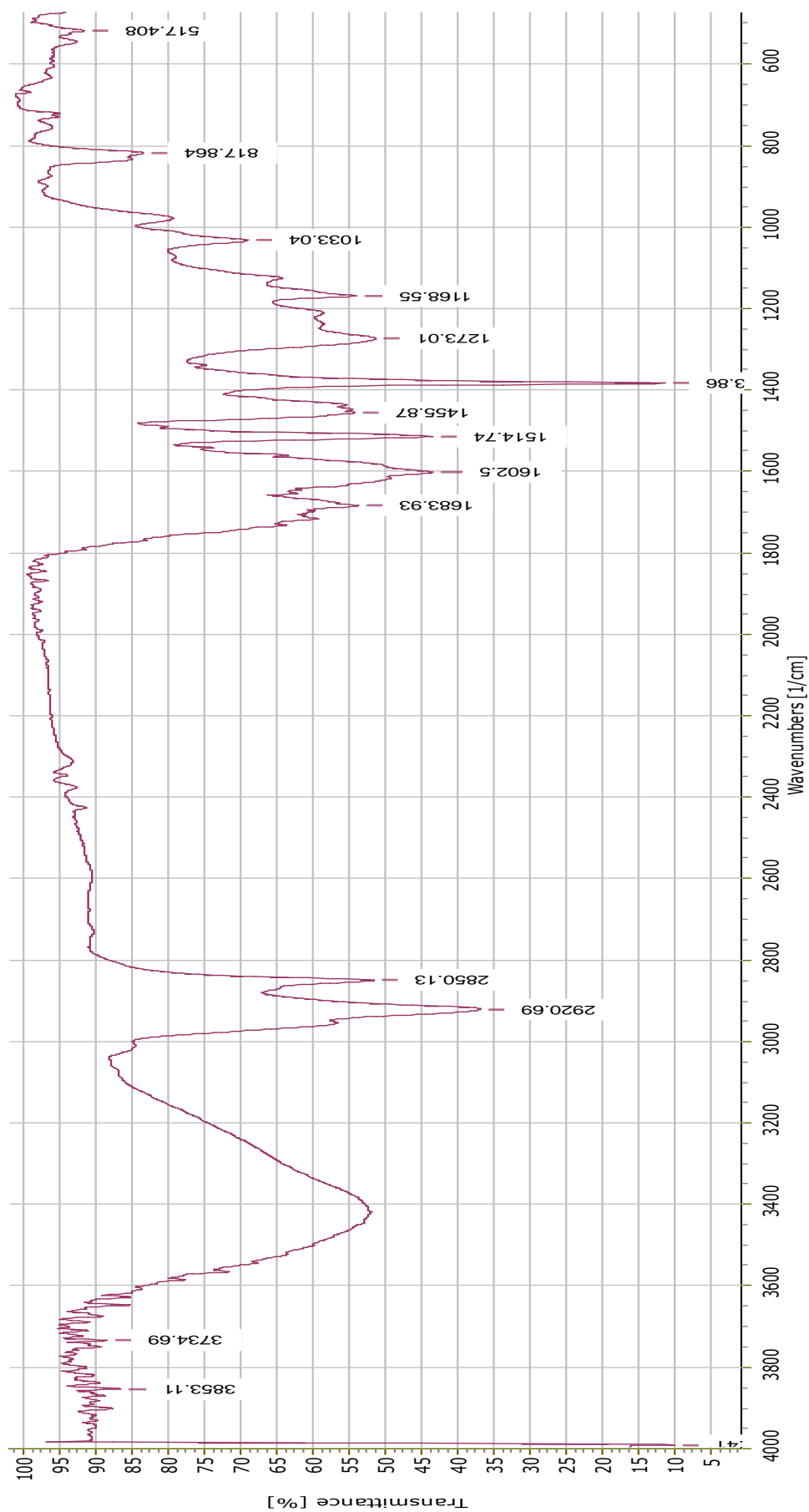*Figure III.9: FT-IR spectrum of P1(Curcumin)*

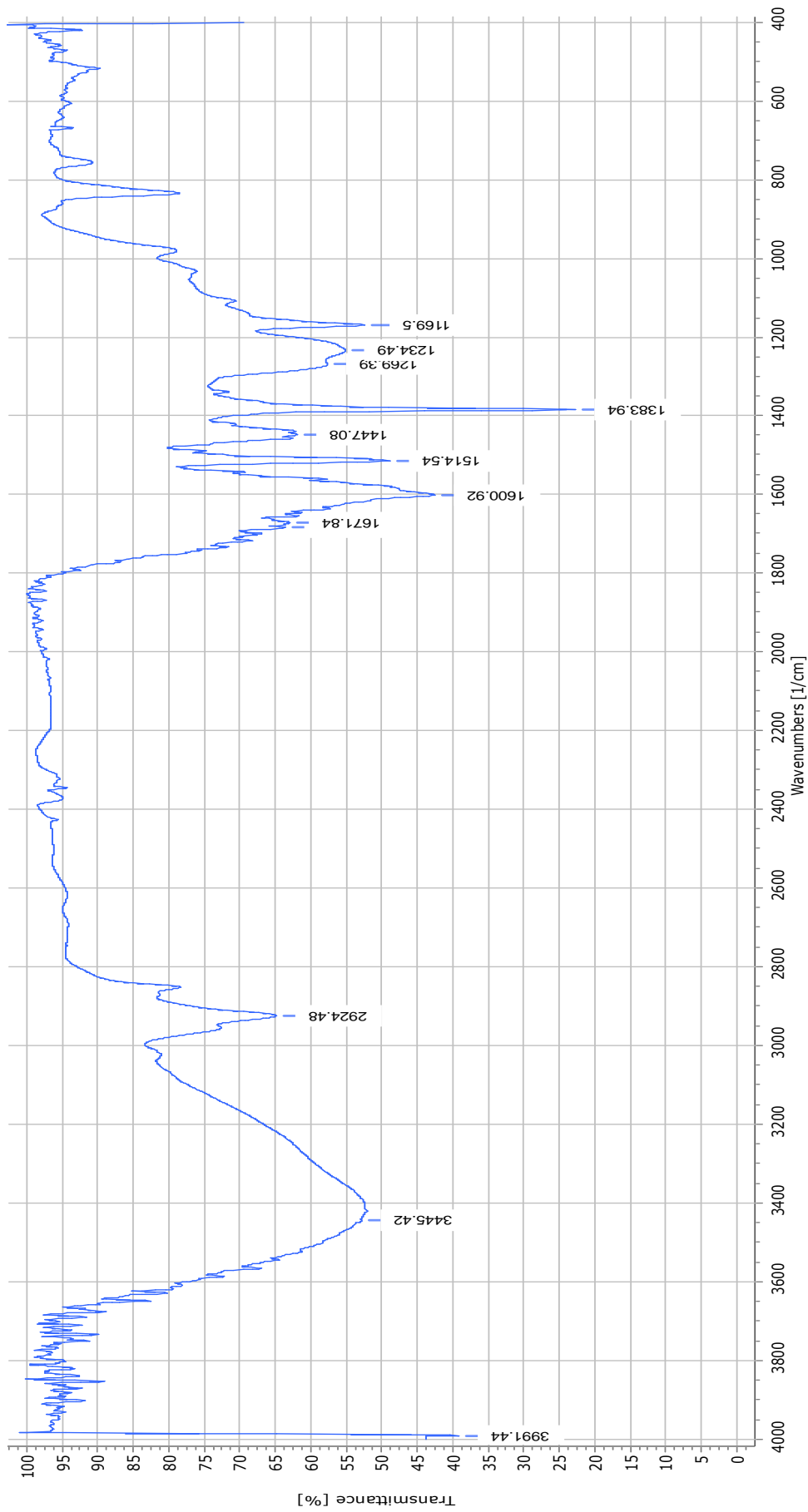*Figure III.10:FT-IR spectrum of P2 (Demetoxycurcumin)*

Figure III.11:FT-IR spectrum of P3 (Bisdemetoxycurcumin)

II.2. RESULTS AND DISCUSSION:

FT-IR spectra of curcuminoids shown in previous Figures, Assignments to the vibrational bands are presented in **Table III-2**.

The FTIR spectrum obtained for **P1** characterized with a band at 3446.07 cm^{-1}, this strong IR band is due to O-H stretching vibrations [3].The IR band at 2926.13 cm^{-1} and its doublet at 2852.34 cm^{-1} are due to asymmetric and symmetric stretching vibrations of the CH_2 group, the signature peaks at 1616.75 cm^{-1} indicates the benzene ring stretching vibrations meanwhile the picks 1508.76 cm^{-1} can be referred to C=O and C=C vibrations.

On the other hand the peak at 1475 cm^{-1} represents an olefinic C-H bending vibrations.[6].As observed in rest of FT IR fingerprinting; bands 1271.84 cm^{-1} assigned to C-O-H bending vibration and finally a peak at 1032.37 cm^{-1} indicates C–O–C stretching vibrations

The FTIR spectrum obtained for **P2** characterized with a band at 3421.1 cm^{-1}, this strong IR band is due to O-H stretching vibrations.The IR band at 2920.69 cm^{-1} and its doublet at 2850.13 cm^{-1} are also due to asymmetric and symmetric stretching vibrations of the CH_2 group. Peaks at 1602.5 cm^{-1} indicates the benzene ring stretching vibrations.

Meanwhile the picks 1514.74 cm^{-1} can be referred to C=O and C=C vibrations, and the olefinic C-H bending vibrations was detected at 1455.87 cm^{-1}. As observed in rest of FT IR fingerprinting; bands between 1273.01 cm^{-1} to 1033.04 cm^{-1} that clearly referred to the aromatic C–O-H Stretching Vibrations.

The FTIR spectrum obtained for **P3** characterized with a band at 3445.42 cm^{-1}, this strong IR band is as before due to O-H stretching vibrations.The IR band at 2924.48 $cm^{-1}$and its doublet at 2850.7 cm^{-1} are due to asymmetric and symmetric stretching vibrations of the CH_2 group. Two peaks at 1600.92 cm^{-1} indicates the benzene ring stretching vibrations meanwhile the picks 1514.54 cm^{-1} can be referred to C=O and C=C vibrations, and the olefinic C-H bending vibrations was detected at 1447.08 cm^{-1}.As observed in rest of FT IR fingerprinting; bands between 1269.39 cm^{-1} to 1234.49 cm^{-1} that clearly referred to the aromatic C–O-H Stretching Vibrations .

However, and according to previous spectral analysis we might say that the peak at 1169.5 cm^{-1} might refer to C–O–C stretching vibrations.[6]

3

The **Table III-2** summaries the obtained peaks which represent the characteristic functions

Table III-2: comparison between the obtained vibration's result for each curcurminoid (summary)

FT-IR			Assignements
P1	P2	P3	
3446.07	3421.10	3445.42	$U_{(O-H)}$ [O-H stretching]
2926.13 and 2852.34	2920.69 and 2850.13	2924.48 and 2850.7	$U_{(C-H)}$ [C-H asymmetric and symmetric stretching]
1616.75	1602.50	1600.92	$U_{(Benzene)}$ [benzene ring stretching vibrations]
1508.76	1514.74	1514.54	$U_{(C=O)}$, $U_{(c=c)}$[C=C stretching , C=0 stretching]
1475.00	1455.87	1447.08	δ_{CH3} [In plane CH3 deformation]
1271.84	1273.01 cm^{-1} to 1033.04		δ_{COH} [In plane C-OH bending.]
1032.37		1169.50	U (C-O-C) [C–O–C stretching vibrations]

for each molecule.

So according to the previous results and the table above its so clear that there is a high degree of resemblance in the obtained peaks rather than the demonstrated spectrum for each obtained analogue which is clearly due to the similarity of each curcuminoid's structure and the only difference could be observed in R$_{1,2}$ section as its shown in **Figure III.12** below :
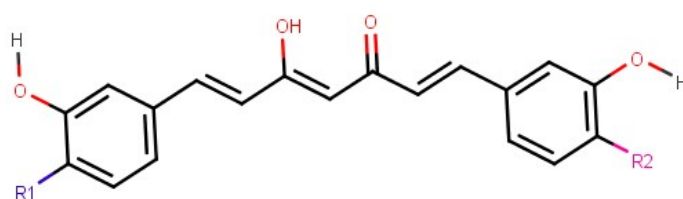
R$_1$: - OCH$_3$; R$_2$:- OCH$_3$ .... Curcumin

R$_1$:- H; R$_2$: -OCH$_3$ .... Demetoxycurcumin

R$_1$:- H; R$_2$: - H .... Bisdemetoxycurcumin

Figure III.12: General structure of curcuminoids (case of study)

A final summary for this FT-IR spectroscopy study; it has been shown that the gathered observations quietly reminiscent us to the other previous literature studies on curcumin which is a good reference that the experimental obtained curcuminoids and our research findings are so far acceptable. Although the IR study can't guarantee the full molecular structure but at least it gives a sign of chemical functions might be existed in a studied sample. As a further spectroscopic analysis approach it was planned to perform a Nuclear magnetic resonance study to insure that the obtained molecules fitting its chemical structure; Unfortunately, the amount (yield) of the obtained curcuminoids was not enough to proceed into such a study but it will be considered as a future analysis to perform.

III.   ANTIOXIDANT ANALYSIS:

III.1.   ANTIOXIDANT ASSAYS USING DPPH METHOD:

❖ **Raw Materials:**

▪ Methanol

▪ DPPH

▪ Balance

▪ Curcuminoids

▪ spectrophotometry at 517 nm

❖ **Process: [7]**

➕ **Preparation of the methanolic solution of DPPH with 0.2 mM:**

A quantity of **7.8 mg** of DPPH was dissolved in **100 ml** of methanol.

➕ **Preparation of the stock solution:**

With a balance **10 mg** has been weighted from the isolated curcuminoids and mixed
with **20 ml** of methanol. The final concertation of the stock solution should be **0.5 mg/ml**

➕ **Preparation of the different concentrations:**

On this step we prepare different solutions with gradually changed concentration from
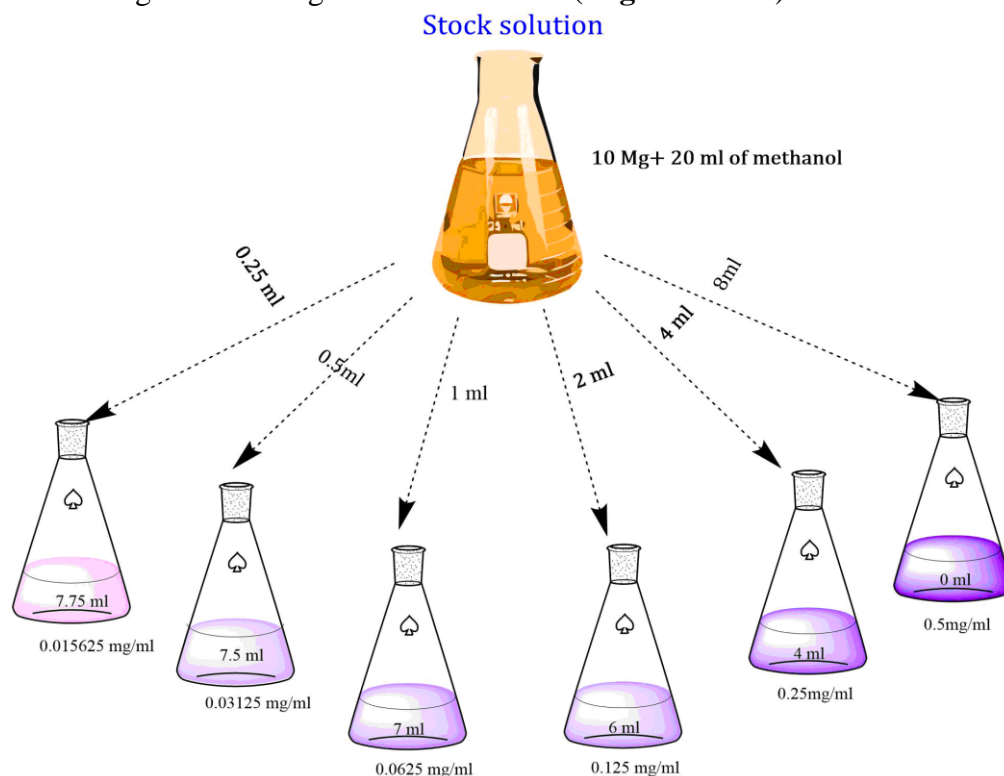0.015625 mg/ml to 0.5 mg/ml as its shown in (**Figure III.13**) .

Figure III.13: preparation of different concentrations of curcuminoids

DPPH Assays:

A **0.75 ml** of curcuminoids with different concentrations (as mentioned before) have been added to **0.25 ml** (250 µl) of methanolique solution of DPPH (0.2 mM) . after stirring, the mixture has been placed in darkness for 30 min to react properly, then the absorption was measured at 517 nm versus a negative witness of DPPH and methanol giving a numeric value of **0.837**.

- For every single concentration the absorption was measured three times.

Determination of the inhibition percentage:

The measurement of the absorption (or the optical density) was performed with spectrophotometry at 517 nm. Using the obtained inhibition percentage and the given formulas below (**Equation 19**), a graph was traced presenting the anti-radical activity in which the variation of the inhibition activity was correlated with the various concentrations of the tested products.

III.2.   RESULTS AND DISCUSSION:

The antioxidant activity which represents the capacity of a product to quench a free radical is estimated according to the DPPH decolouration in a solution mixed with methanol the activity is expressed as the inhibition activity of DPPH shown below (**Equation 19**):

$$IP = \frac{Abs\ C - Abs\ T}{Abs\ C}\ X\ 100$$

(19)

IP: inhibition percentage

Abs C: reference absorption at 517nm

Abs T: absorption of the curcuminoids solution at 517nm

Studying the variation of antiradical activity matched with the concentration of the product allows to determine the concentration representing 50% of the inhibition which is the required concertation of the tested products to reduce 50% of the DPPH radical.

IC50% is obtained graphically from the traced graph of inhibition percentage and different prepared concertation , the more the **IC50** is weak the more the studied product is efficient .[8]

The table below show the DPPH assays results:

Table III-3:Absorption results and inhibition percentage of DPPH for curcumin

[C] (µg/ml)	$C_0=500$	$C_1=250$	$C_2=125$	$C_3=62.5$	$C_4=31.25$	$C_5=15.625$
Abs (P1)	0.042	0.053	0.074	0.263	0.365	0.424
	0.043	0.051	0.069	0.264	0.361	0.435
	0.038	0.051	0.066	0.306	0.357	0.472
Inhibition percentage of DPPH %	95.101±0.32	93.827±0.14	91.676±0.48	66.825±2.93	56.869±0.48	46.993±3

Table III-4: Absorption results and inhibition percentage of DPPH for Demetoxycurcumin

[C] (µg/ml)	$C_0=500$	$C_1=250$	$C_2=125$	$C_3=62.5$	$C_4=31.25$	$C_5=15.625$
Abs (P2)	0.071	0.157	0.274	0.364	0.425	0.46
	0.078	0.158	0.248	0.366	0.426	0.453
	0.069	0.146	0.248	0.373	0.416	0.48
Inhibition percentage of DPPH %	91.318±0.56	81.641 ±0.6	69.334±1.79	56.073±0.56	49.542±0.65	44.524±1.67

Table III-5:Absorption results and inhibition percentage of DPPH for Bisdemetoxycurcumin

[C] (µg/ml)	$C_0=500$	$C_1=250$	$C_2=125$	$C_3=62.5$	$C_4=31.25$	$C_5=15.625$
Abs (P3)	0.153	0.246	0.365	0.423	0.48	0.466
	0.141	0.243	0.348	0.436	0.479	0.481
	0.141	0.246	0.344	0.431	0.428	0.483
Inhibition percentage of DPPH %	82.676±0.83	70.728±0.21	57.905±1.33	48.626±0.78	44.763±3.55	43.050±1.11

From the previous results we were able to trace the antiradical activity graph of the separated curcumin analogues as its shown in **Figure III.14.** In which each **Y** value of the graph is a numeric value calculated from **Equation 19,** but (**Abs T**) here is the mean value of three assays for one concentration obtained from the previous results ± standard deviation. Leading us to obtain graphically the corresponding values of **IC50** for each derivative.

The **IC50** value indicated in **Table III-6** shows that Curcumin has the lowest IC50 value comparing to the other two analogues , Demetoxycurcumin was second and bisdemethoxycurcumin as the highest third IC50 value .

From the previous remarks we can conclude that the antioxidant capacities of curcuminoids were found to decrease in the order:

Curcumin > Demetoxycurcumin > Bisdemethoxycurcumin.

These observations were also compared with some other experimental research [9, 10], and as a conclusion we might say that the gathered results were very representative and the antioxidant assays gave a correct interpretation at the end of this particular part of our research.
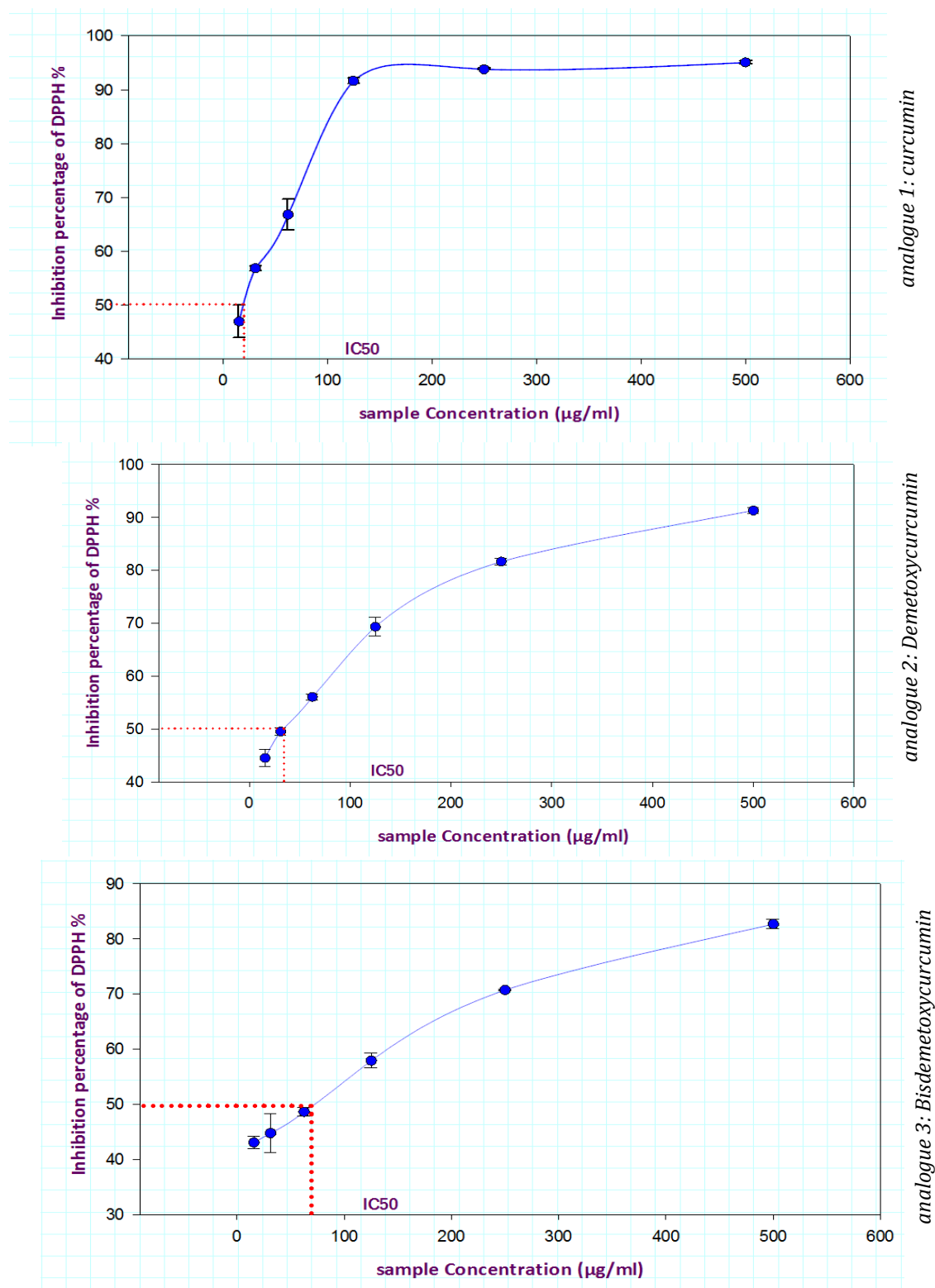
analogue 1 : curcumin

analogue 2: Demetoxycurcumin

analogue 3: Bisdemetoxycurcumin

Figure III.14:Antiradical activity of curcumin analogues

Table III-6: IC50 value of curcumin and its derivatives

Anti-oxidation	IC50(µg/ml)
Curcumin	19.35
Demetoxycurcumin	33.60
Bisdemethoxycurcumin	71.34

References

1. Irving, G.R., et al., *Curcumin: the potential for efficacy in gastrointestinal diseases.* Best practice & research Clinical gastroenterology, 2011. **25**(4-5): p. 519-534.

2. Kulkarni, S., et al., *Extraction and purification of curcuminoids from Turmeric (Curcuma longa L.).* International Journal of Pharmacology and Pharmaceutical Technology, 2012. **1**(2): p. 81-84.

3. Zetterström, S., *Isolation and synthesis of curcumin.* 2012.

4. Revathy, S., S. Elumalai, and M.B. Antony, *Isolation, purification and identification of curcuminoids from turmeric (Curcuma longa L.) by column chromatography.* Journal of Experimental sciences, 2011. **2**(7).

5. Menges, F., *Spectragryph-Optical Spectroscopy Software, version 1.0. 7.* Universität Konstanz: Obersdorf, Germany, 2017.

6. Chen, X., et al., *The stability, sustained release and cellular antioxidant activity of curcumin nanoliposomes.* Molecules, 2015. **20**(8): p. 14293-14311.

7. Kumar, A., et al., *Antioxidant efficacy and curcumin content of turmeric (curcuma-longa l.) flower.* International Journal of Current Pharmaceutical Research, 2016. **8**: p. 112-114.

8. Khoudali, S., et al., *Etude de l'activité antioxydante et de l'action anti corrosion de l'extrait méthanolique des feuilles du palmier nain (Chamaerops humilis L.) du Maroc.* J. Mater. Environ. Sci, 2014. **5**(3): p. 887-898.

9. Kedare, S.B. and R. Singh, *Genesis and development of DPPH method of antioxidant assay.* Journal of food science and technology, 2011. **48**(4): p. 412-422.

10. Jayaprakasha, G., L.J. Rao, and K. Sakariah, *Antioxidant activities of curcumin, demethoxycurcumin and bisdemethoxycurcumin.* Food chemistry, 2006. **98**(4): p. 720-724.

CHAPTER

4

THEORETICAL

ASSAYS

4

Introduction

Curcumin [(1E,6E)-1,7-bis(4-hydroxy-3-methoxyphenyl)-1,6-heptadiene-3,5-dione], the major curcuminoids component of rhizomes of Curcuma longa and other Curcuma species exhibits a wide range of biological activities including antioxidant, anti-inflammatory, anticancer, and antimicrobial properties. These activities are mediated through regulation of numerous biochemical targets encompassing inflammatory cytokines, transcription factors, anti-apoptotic proteins, adhesion molecules, antioxidant enzymes, ion channels and transporters. [1]

From previous chapter we concluded that Curcumin has a biological antioxidant activity that has been tested and verified in vitro, as a continuum to previous results we decided to go deeper and test if our extracted pure compounds; which are the curcuminoids, have another biological activity towards some other diseases, illnesses and even examine if curcuminoids structure could have some biological interactions in our human body same as some other existed drugs.

As a start, the ability of curcumin to regulate ion channels and transporters was recognized more than a decade ago and recent studies have revealed that many channels

and transporters are modulated by this molecule[2] . In this respect, curcumin was reported to activate/desensitize and antagonize the transient receptor potential channels TRPA1 and TRPV1[3, 4], respectively. These effects may contribute to the antinociceptive and anti-inflammatory properties of curcumin.

TRPV1 channel modulation by curcumin is, however, rather controversial and depends on disease condition.

Now, to investigate curcuminoids activity against these known biological targets; the **in vitro** assays were not a very appropriate method as it will take more time to accomplish rather than many difficulties that can face the research progression.

On the other hand, due to astronomical developments in computer hardware and associated achievements, quantum mechanical methods can now be directly applied for various scientific applications. And have become major tools in the study of molecular problems of structure, stability and reaction mechanism. For that reason, a theoretical study can help us in this case, using a virtual screening tests to investigate if curcuminoids are able to reach these active sites in the body, bind to its target macromolecule, and elicit the desired biological effect.

I. OPTIMIZATION AND THEORETICAL APPROACH OF CURCUMINOIDS:

At this point, we will focus on optimizing the molecular structures of Curcuminoids using different software, then visualize the theoretical IR spectrum and compare it with the obtained FT-IR spectrum from *chapter IV*.

I.1. STRUCTURE OF DIFFERENT MOLECULES:

Figure IV.1 represents the 2D structure of curcumin with both enolate (1) form and enol form (1') , Demetoxycurcumin (2) and bisdemethoxycurcumin (3) which were created and visualised using MarvinSketch and MarvinView [5].
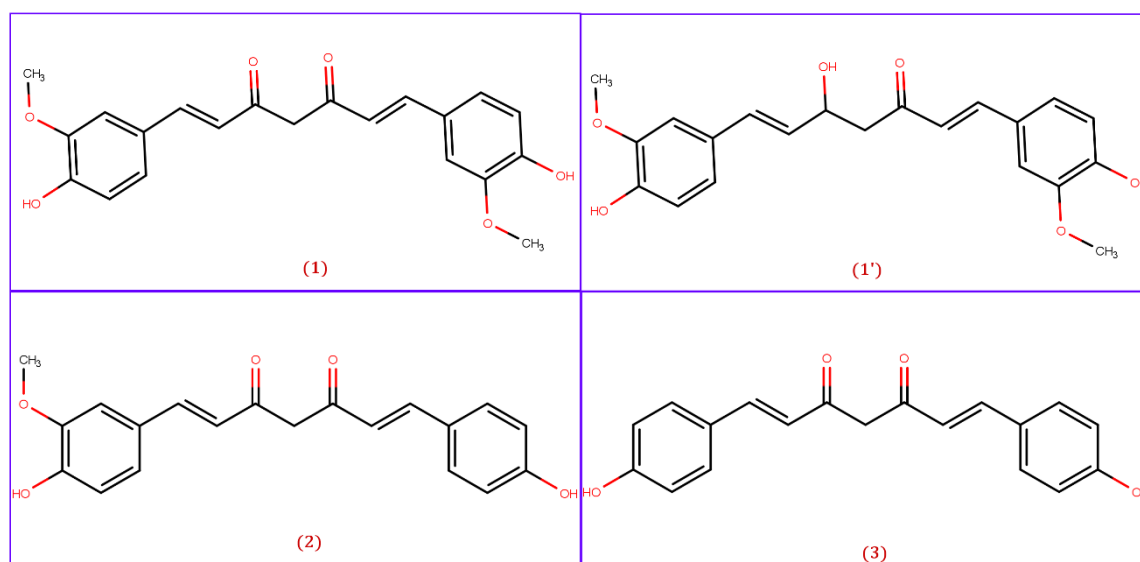

Figure IV.1:Different 2D structures of the studied curcuminoids

I.2. GEOMETRIC OPTIMIZATION OF DIFFERENT MOLECULES:

The theoretical study begins after creating the 3D conformation of the previous structures using HyperChem 8.0.10[6] by adding the Hydrogen to structures then perform a semi-empirical optimization using **AM1** method, the obtained conformations were saved as MDL MOL. The next step was optimizing the previous molecules using Gaussian 09 software, **DFT** as a calculation method with B3LYP as correlation and **6-311G** + (d,p) as a basis set[7] .The best obtained structure with the least energy values recorded after optimization are shown in figures below:
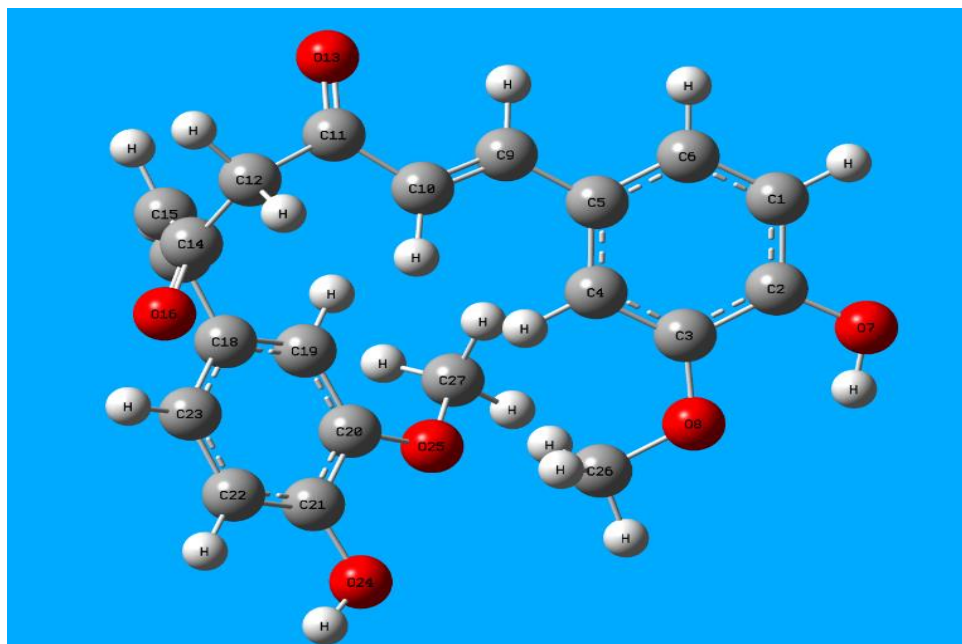
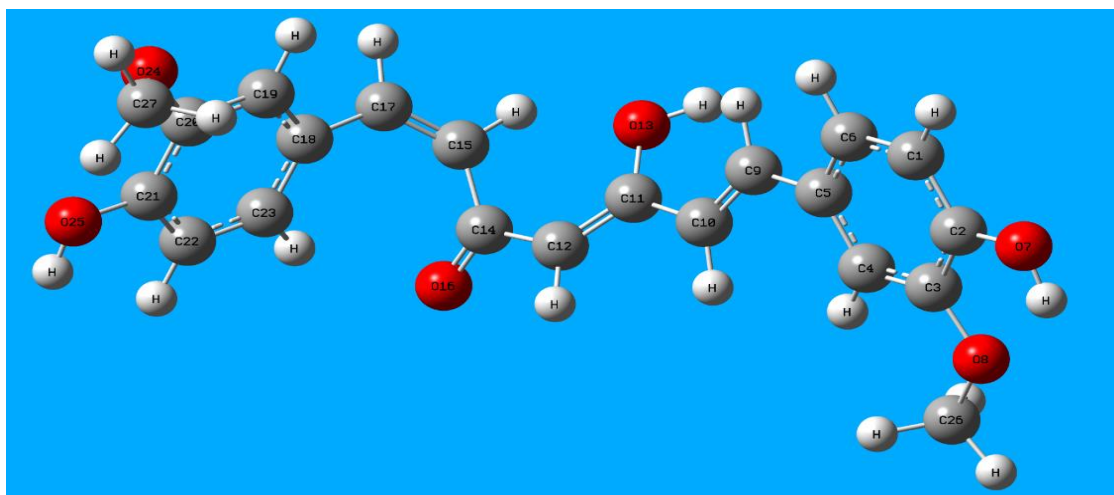*Figure IV.2:Curcumin structure after optimization (enolate)*

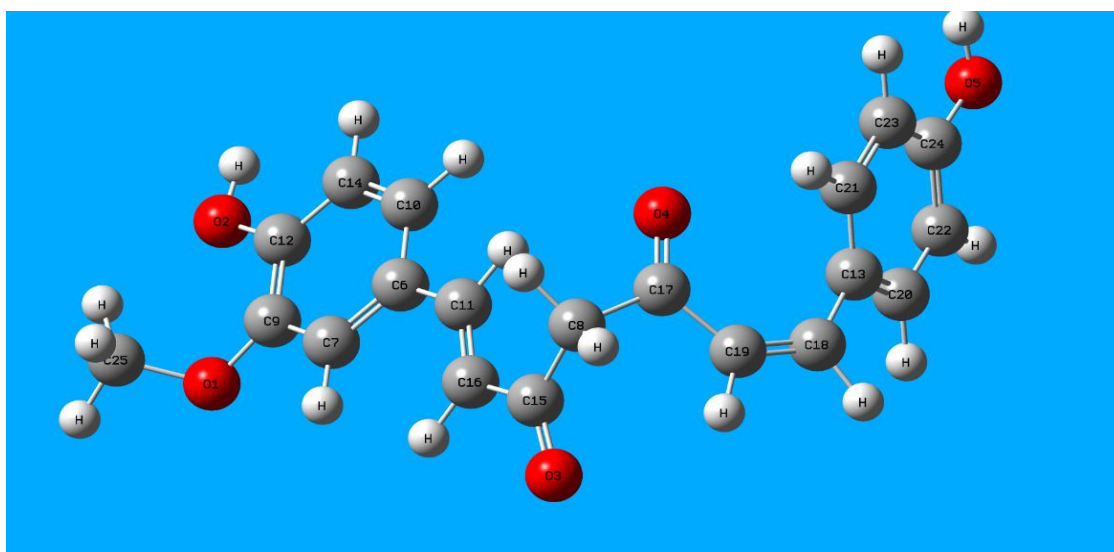*Figure IV.3:Curcumin structure after optimization (enol)*

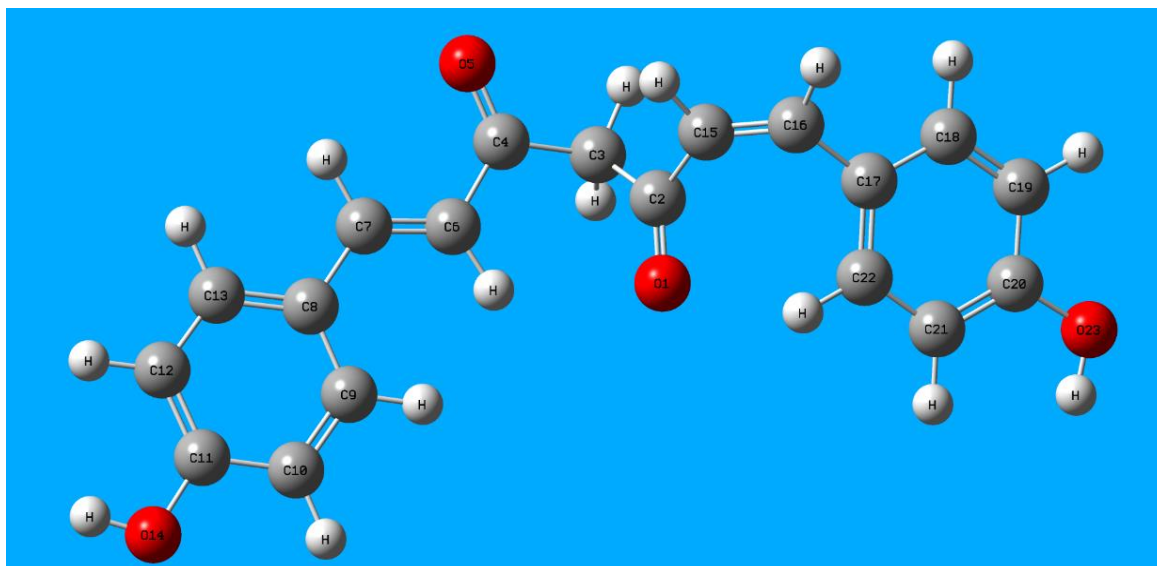*Figure IV.4: Demetoxycurcumin structure after optimization*

Figure IV.5:Bisdemethoxycurcumin structure after optimization

I.3. SPECTRAL VISUALIZATION:

Accompanied with previous optimization task in Gaussian software, a frequency analysis has been performed to get the theoretical IR-spectrum using the same optimization settings.

The calculated output file for Gaussian was converted into Avogadro 1.2.0 [8] to visualize the IR spectrum as shown in: **Figure IV.6;Figure IV.7;Figure IV.8; Figure IV.9**
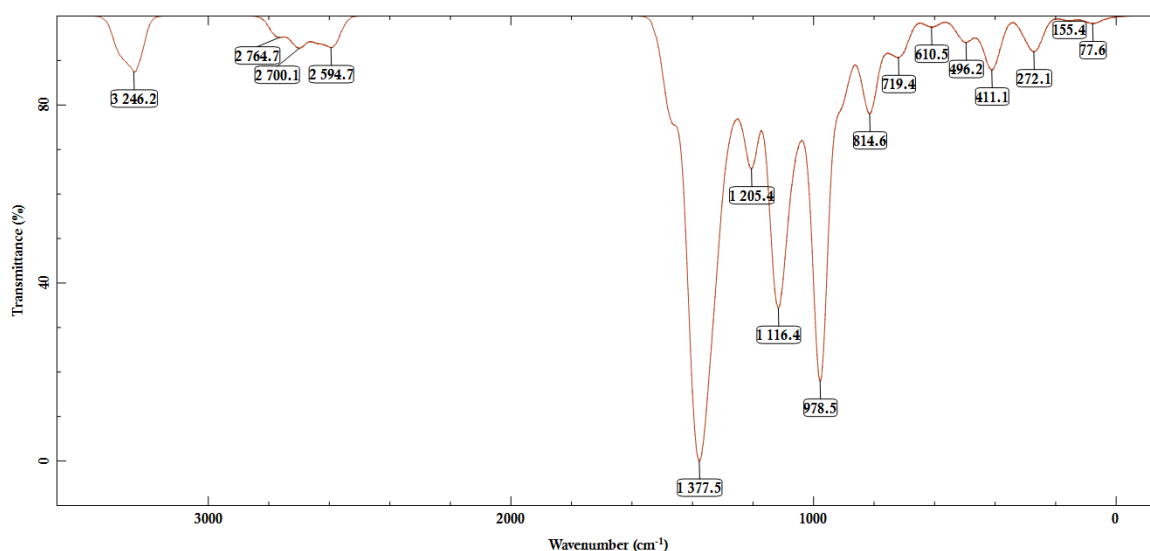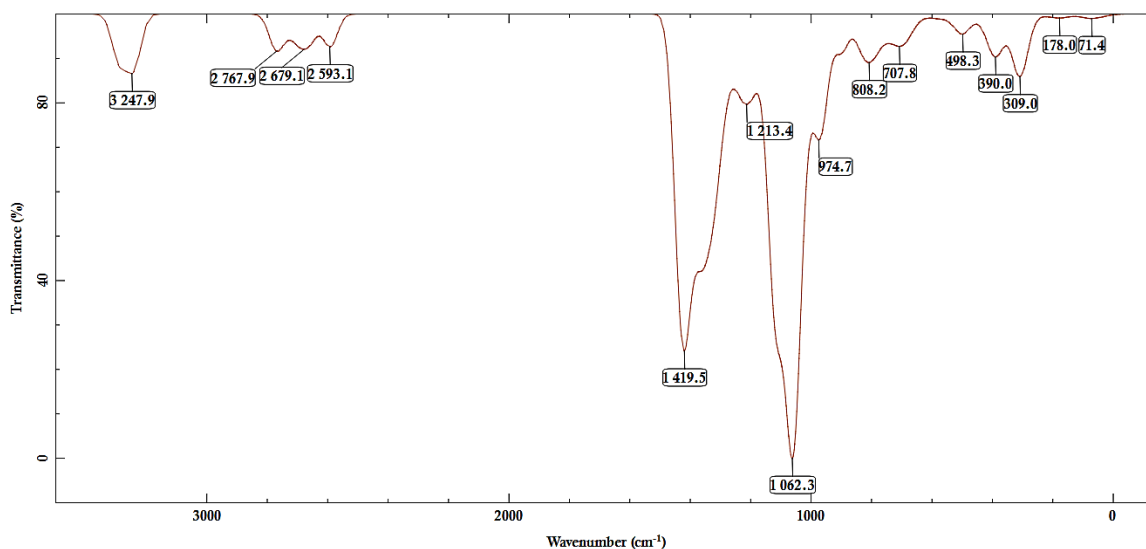

Figure IV.6: IR spectrum of curcumin (enolate)
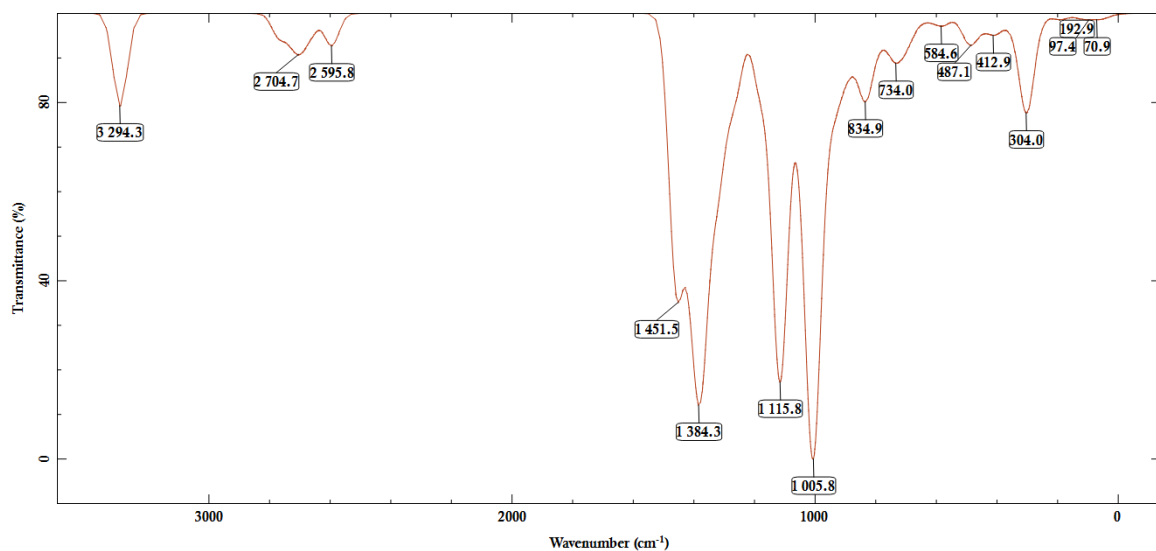
Figure IV.7: IR spectrum of curcumin (enol)

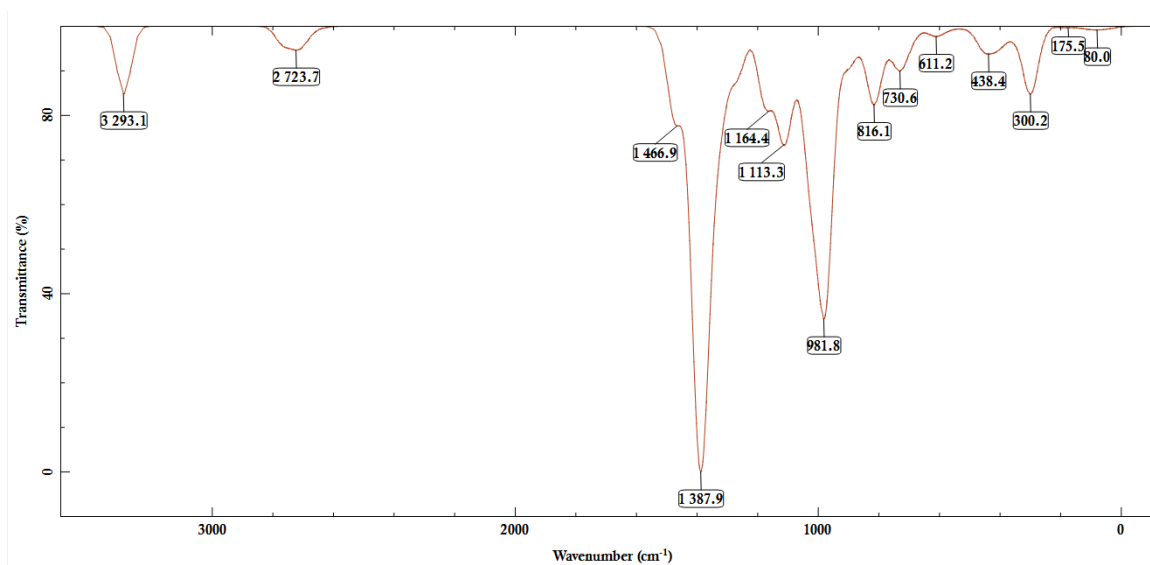*Figure IV.8: IR Spectrum of Demetoxycurcumin*

Figure IV.9:IR spectrum of Bisdemethoxycurcumin

103

I.4. RESULTS AND DISCUSSION:

In the previous chapter we only focused on studying the three curcuminoids without highlighting the different tautomers that can exist.

Since The IUPAC name of curcumin is 1,7-bis(4-hydroxy-3-methoxy phenyl)-1,6-heptadiene-3,5-dione (1E-6E) where the two aryl rings containing ortho-methoxy phenolic OH^- groups are symmetrically linked to a β-diketone moiety (**Figure IV.10**). The occurrence of intramolecular hydrogen atoms transfer at the β-diketone chain of curcumin leads to the existence of keto and enol tautomeric conformations in equilibrium.[9]
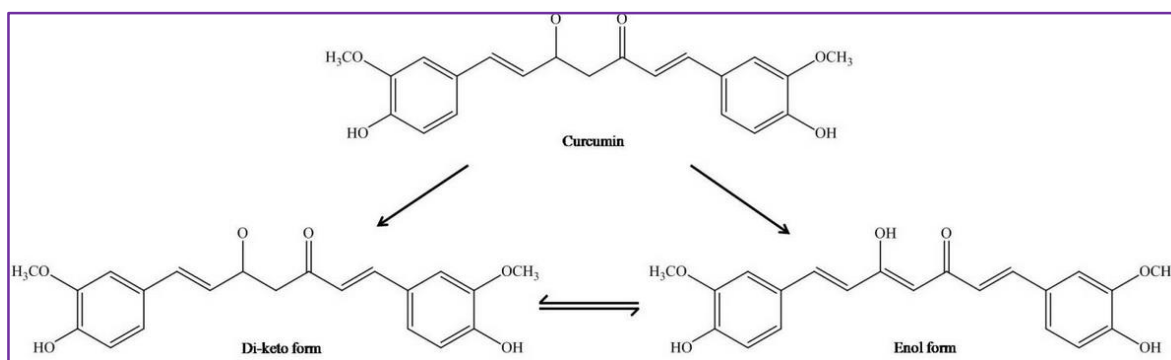

Figure IV.10:Chemical structure of curcumin existing in keto-enol tautomeric forms

As experimental assays either in vitro tests or separation and isolation processes, it is difficult to recover one of the tautomers. And the only available choice to obtain one specific curcumin tautomer for example is by synthesis [10].On the other hand, it is possible as a theoretical study to highlight both tautomers, for that reason we focused on studying the curcumin in both forms.

After creating the molecules and performing a semi empirical **AM1** optimization to prepare the molecular system, Gaussian software was the best distribution to handle the Quantum mechanics calculations with the best accurate results.

The table below summaries the after optimization energy

Table IV-1: After optimization energy calculated for curcuminoids

Molecule	Calculated Energy (U.A)
Curcumin(enolate)	-1263.918114
Curcumin(enol)	-1263.900997
Demethoxycurcumin	-1149.357357
Bisdemethoxycurcumin	-1034.808459

As its shown; the calculated energy for both forms of curcumin was remarkably very close which might be referred to the fact that they both are tautomers. Besides, the shown theoretical spectrum of curcumin (enol) visualised from Gaussian calculation is practically the same as the enolate form.

As a brief conclusion we might say that both forms are so similar in structured result's calculations. However creating the HOMO and LUMO frontal orbitals using the same software Gaussian ; shows that there is actually a huge difference in the LUMO orbital that could result in a different molecular interactions as shown in **Figure IV.11**

HOMO Orbital   LUMO Orbital

Curcumin (Enolate)

HOMO Orbital   LUMO Orbital
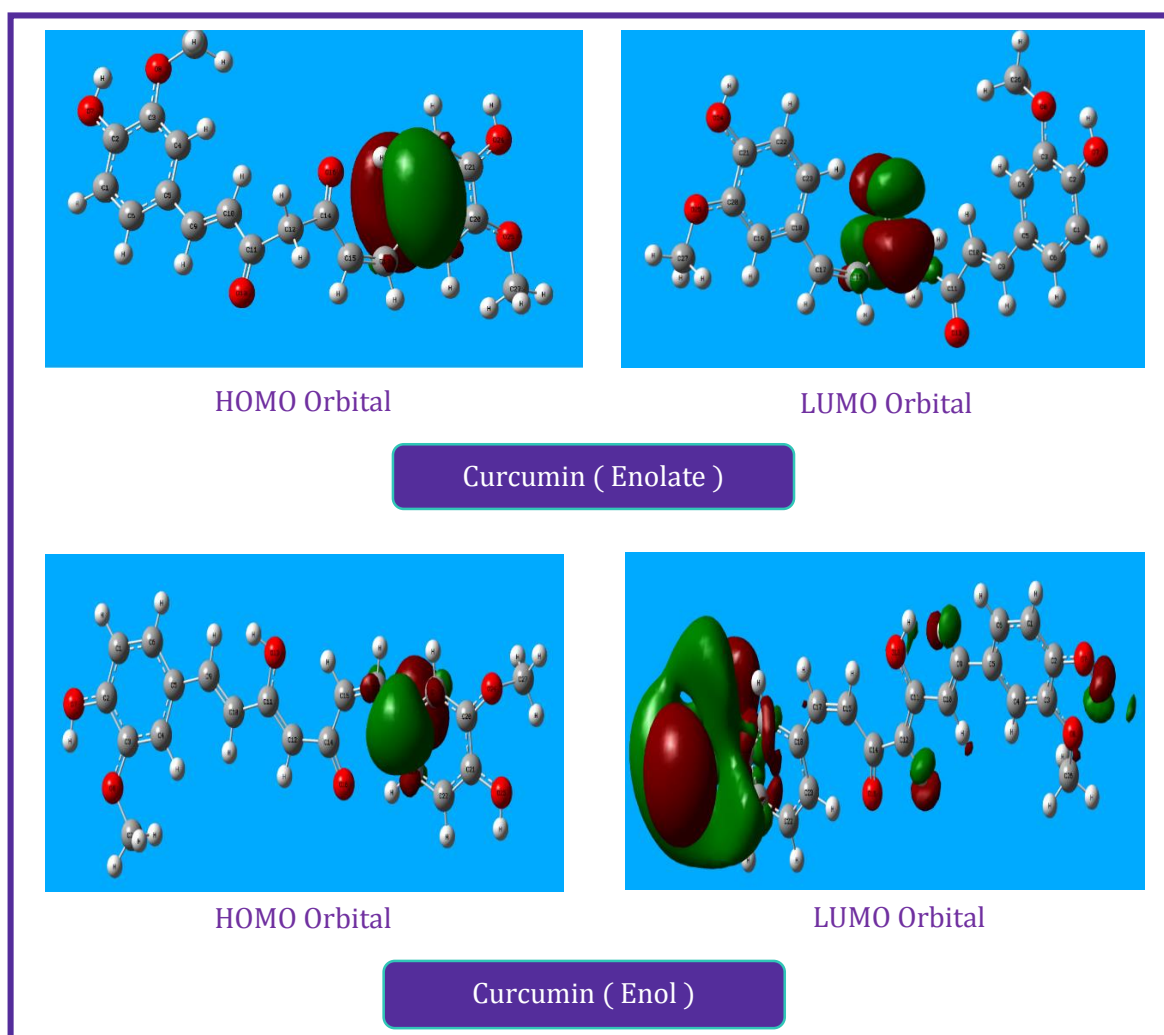
Curcumin (Enol)

Figure IV.11: Frontal orbitals of Curcumin (enol and enolate)

As a continuum to the spectral FT-IR analysis study in previous chapter we found that the theoretical calculated IR spectrums are too similar to the experimental ones; the representative peaks that refers to the characteristic functions of curcumin obtained from FT-IR analysis and its analogue were very much the same as the theoretical peaks.

II. CURCUMINOIDS AND TRPV1 IONIC CHANNELS INTERACTIONS INVESTIGATION:

II.1. PREPARATION OF THE TRPV1 PROTEIN:

II.1.1. Choosing the appropriate protein:

The structural information for the receptor are obtained by X-ray crystallography, NMR, or modelling techniques Since semi-flexible molecular docking algorithm is based on the ligand-receptor geometric complementarity, the 3D-structure of the receptor is of fundamental importance:

The more accurate the physical description of this structure, the more relevant, accurate and useful the predicted binding mode. The receptor structure should therefore be carefully checked regarding to two aspects.

First, it should correspond to a biological conformation that is relevant to the targeted biological mechanism. For instance, the presence of crystal contacts in X-ray structures should be verified, as well as the impact of the presence/absence of other interacting partners such as cofactors.

Second, the quality of the structure should be verified at an atomic level. For instance, the docking of a ligand is likely to fail if the region encompassing its native binding mode includes unresolved atoms; it also fails if the said region has a poor sequence identity with the template structure (if created by homology modelling), or encompasses flexible residues (reflected by a high B-factor if the structure has been determined by X-ray, or multiple conformations if determined by NMR). If such issues are identified, they have to

be addressed during the preparation of the structures for the docking. The structures are usually 'refined' before being used in the docking calculations with the aim to 'relax' the system towards a lower energy conformation, ideally the energy global minimum.[11]

Therefor ; in our study , we have downloaded the **TRPV1** structure in complex (**Figure IV.12**) with Capsazepine **(Figure IV.13)** from The Protein Data Bank (PDB) which is an archive contains a worldwide repository of information about the 3D structures of large biological molecules, including proteins and nucleic acids.
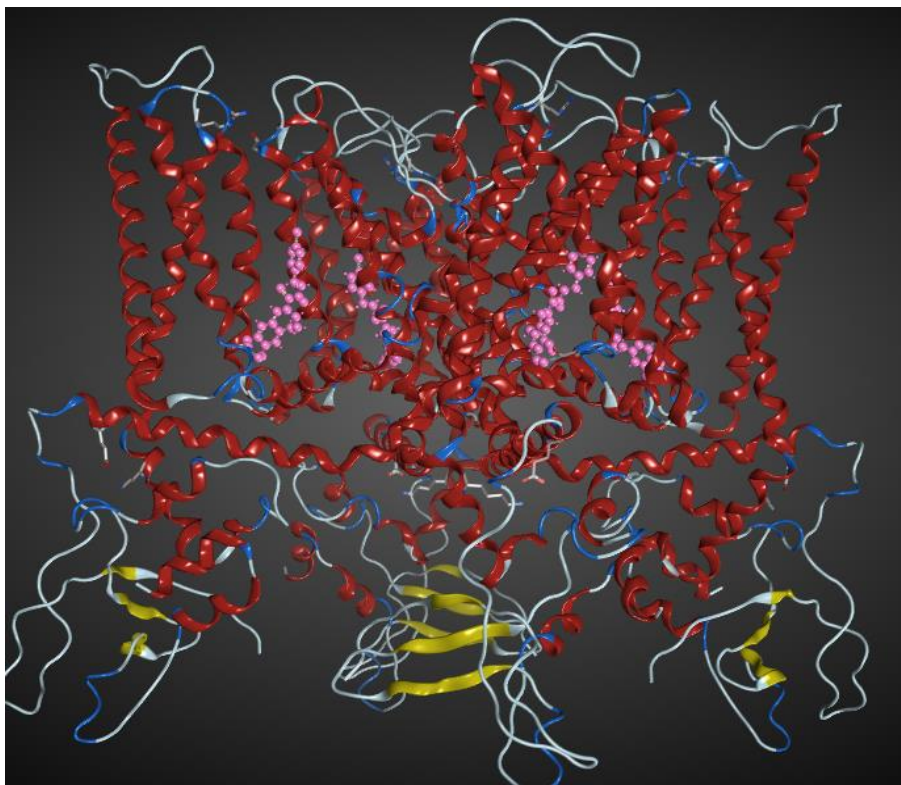
Figure IV.12: 3D structure of TRPV1 complexed with Capsazepine (5IS0)
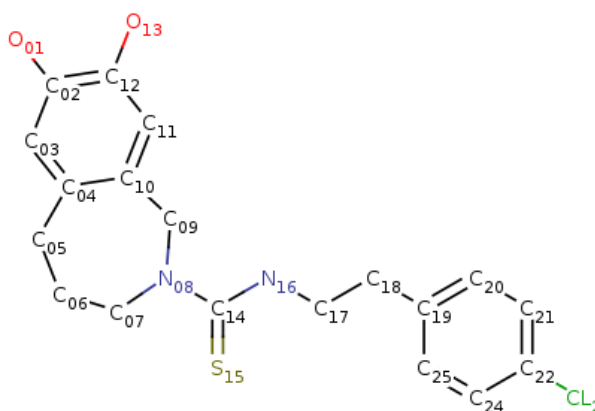
Figure IV.13: Capsazepine molecular structure (N-[2-(4-chlorophenyl)ethyl]-7,8-dihydroxy-1,3,4,5-tetrahydro-2H-2-benzazepine-2-carbothioamide) . C_{19} H_{21} Cl N_2 O_2 S

This particular protein holding **5IS0** ID was Reconstructed using ELECTRON MICROSCOPY method giving **3.43** Å Resolution , a **293344.78** total structure weight , **11808** counted atoms and **2544** residues [12].

II.1.2. ligand Capsazepine background:

Capsaicin and resiniferatoxin are natural products which act specifically on a subset of primary afferent sensory neurons to open a novel cation-selective ion channel in the plasma membrane. These sensory neurons are involved in nociception, and so, these agents are targets for the design of a novel class of analgesics. capsazepine.

This compound is the first competitive antagonist of capsaicin and resiniferatoxin to be described and is active in various systems, in vitro and in vivo. It has recently attracted considerable interest as a tool for dissecting the mechanisms by which capsaicin analogues evoke their effects. NMR spectroscopy and X-ray crystallography experiments, as well as molecular modeling techniques, were used to study the conformational behaviour of a representative constrained agonist and antagonist. [13]

Capsazepine (**Figure IV.13**), an analogue of capsaicin, was the first synthetic competitive antagonist of TRPV1 Compared with other TRPV1 antagonists, capsazepine has a relatively low potency on TRPV1. Capsazepine has been shown to inhibit capsaicin-induced TRPV1 currents in sensory neurons and to compete with RTX for binding.

Although capsazepine was shown to inhibit the behavioural nociceptive properties of capsaicin in vivo, its effect on heat- and proton-induced TRPV1 activation appears to be species-dependant.

In humans, capsazepine has been reported to inhibit TRPV1 activation by heat and protons. However, due to low metabolic stability and poor pharmacokinetic properties, capsazepine did not reach clinical development.

Capsazepine has also shown some effects on other channels, such as voltagegated calcium channels, nicotinic receptors and TRPM8. Although capsazepine has a low potency and exhibits unspecific binding,it has been used in many pharmacological studies and served as a pharmacological tool for comparing novel TRPV1 antagonists.[14]

## II.1.3. Structure preparation of the TRPV1:

The purpose of preparing 3D macromolecular structures is to correct structures and to prepare macromolecular data for further computational analysis.

Using Molecular operating environment software or **MOE** (release 2015.10) [15], the downloaded PDB file was loaded to the software interface then structure preparation task was launched which directly result in a structure correction and structure 3D protonation .

II.1.4. Cavity detection:

Proteins perform their biological functions in biological processes mainly by interacting with other molecules such as other proteins, small molecules, DNAs and RNAs. Usually not all the residues on a protein surface participate in these interactions. Thus, identification of these functional sites is of great importance to understanding the function of a protein and the mechanism of the interactions. In addition, knowledge of these functional sites can be used to guide the mutagenesis experiments. There exist a number of cavities or pockets on protein surface where small molecules bind. Therefore, identification of such cavities is often the starting point in protein–ligand binding site prediction for protein function annotation and structure-based drug design. Proper ligand binding site detection is a prerequisite for protein–ligand docking and high-throughput virtual screening to identify drug candidates in drug discovery processes.[16].Using MOE , four cavities were detected in TRPV1 protein as its shown in **Figure IV.14**
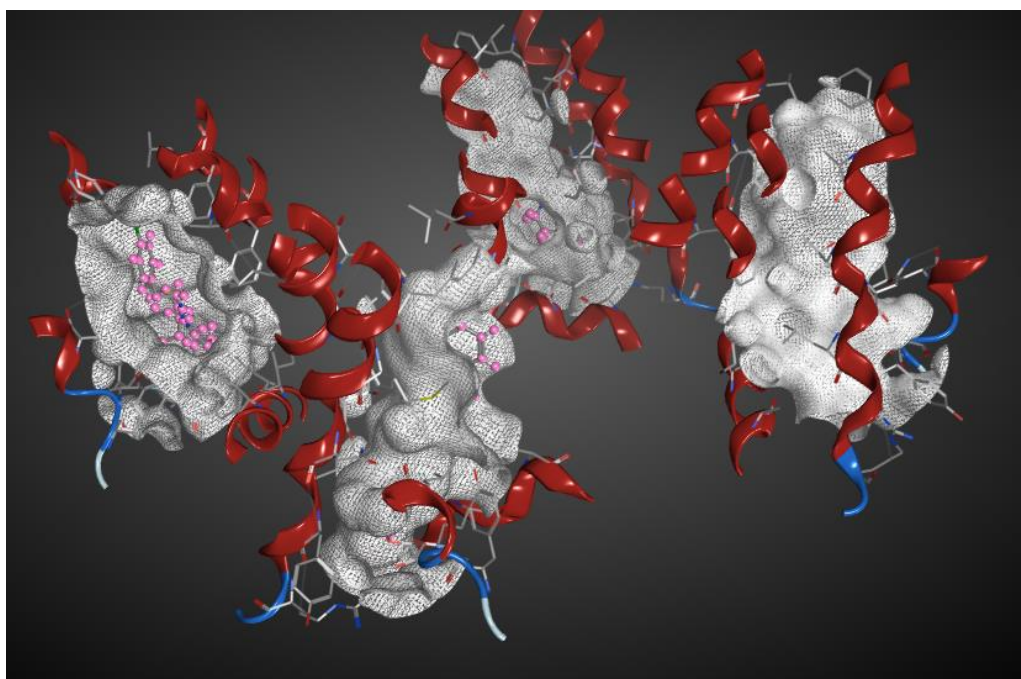
Figure IV.14:Isolated cavities detected from complex interaction with its ligand

Unfortunately, the MOE software doesn't simply calculate a cavity details without calculating all the pocket surface and volume at the same time. As a solution, to calculate the relative detailed information about these cavities were carried out using MVD (Molegro Virtual Docker) . [17]

The corresponding cavities were again detected and visualized using MVD and the obtained protein details are summarized in **Table IV-2**:

Table IV-2:surface and volume details of TRPV1 cavities

Cavity number	Surface $Å^2$	Volume $Å^3$
1	2154.24	764.928
2	2181.12	763.392
3	2109.44	747.008
4	2163.2	733.184

We clearly notice that the four cavities are complexed with the same ligand (Capsazepine) and all surface and volume results are too similar (as shown in table above) indicates that all these cavities are the same, which confirm that this protein contains four identical chains as shown in the protein data report is PDB website.

II.2. GEOMETRY OPTIMIZATION OF TRPV1:

Energy minimization is one of the most famous methods used to optimize bimolecular structures to obtain a stable system with a lower potential energy and a specific geometry.

With the same software (**MOE**) an energy minimization process has been applied to previous structure, using **Amber 10** as a forcefield method with default settings; the produced system had a total potential energy of: E_{Pot} = -26997.8 Kcal/mol

II.3. MOLECULAR DYNAMICS:

Molecular dynamics simulation addresses the problem of numerically solving the classical equations of motion for a system of N atoms in an effort to sample a thermodynamic ensemble, or trajectory, under specified thermodynamic conditions (e.g. constant temperature or constant pressure). Such a trajectory is important for two reasons.

Firstly, it provides configurational and momentum information for each atom, from which thermodynamic properties of the system can be calculated.

Secondly, the trajectory represents an exploration, or search, of the conformation space available to a particular system. The principle underlying conformation search using dynamics is that atoms in a dynamics simulation will eventually search their entire conformation space. The obvious problem with this approach is that the search space may be huge, and thus, it may take many thousands, millions, or even billions of steps to adequately and accurately sample the space.

Consequently, much research effort is spent on devising methods of accelerating the exploration without sacrificing accuracy.

Molecular dynamics simulations are often a sequence of simulation *stages* each of which is run under different temperature or pressure conditions; e.g. when heating or cooling a system. These sequences of stages are called *protocols* and are specified with a special protocol language. The protocol language is a sequence of stages, each with a name and parameters enclosed in braces. Parameters are of the form *name = value* where the *value* is either a number or a range interval, depending on the particular parameter. Ranged parameters are interpolated during the simulation stage. [15]

For our molecular dynamics simulation protocol, we have chosen the standard settings given by MOE with:

heat   [ps=100 T=(0,300)] ; equil [ps=100 T=300] ; prod [ps=500 T=300]

As a description of this protocol; the system will heat from 0 to 300 K followed by equilibration, production for 500 picoseconds and cooling to 0 Kelvin.

For calculation algorithm; **NAMD** was selected, which is an external **NAMD2** molecular dynamics engine. Downloaded as a program package and integrated to MOE ; the reason for choosing this particular algorithm is that it's the best free molecular dynamics simulator tool and has a higher efficiency compared to other algorithms.

The result ;1400 TRPV1 conformations were recorded during this simulation and the obtained system has now a lower energy at E_{pot} = -9247.17 Kcal/Mol **Figure IV.15**
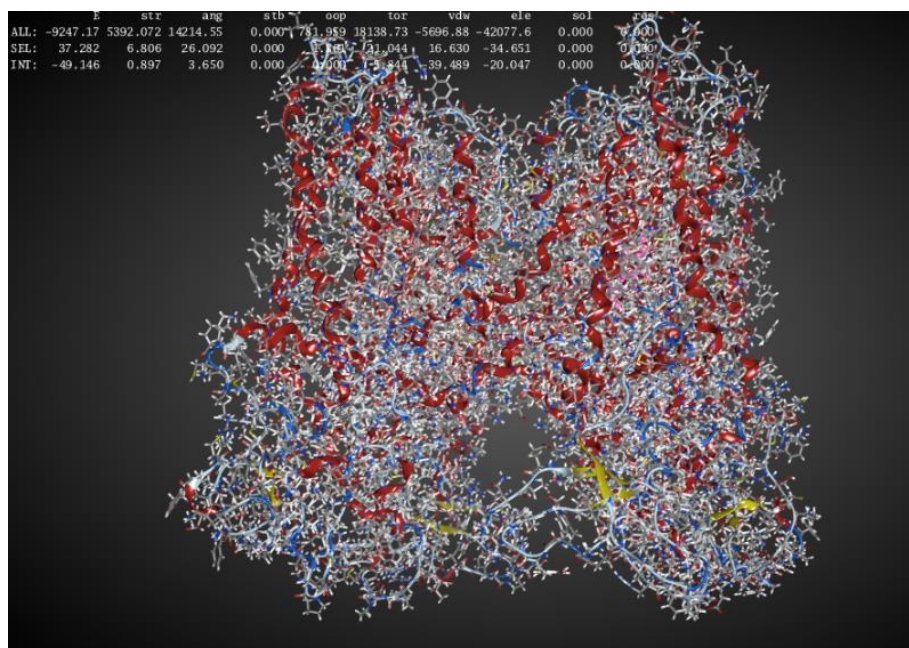
Figure IV.15:TRPV1 after molecular dynamics

II.4. FUTURE LIGANDS PREPARATION:

Before jumping onto the docking process; the future ligands or the database containing the investigated molecule, should now be prepared for docking; using a minimization and an optimization of geometry to obtain the least energy and a stable system. In our case, as shown in **(I.2)** all the concerned molecules were already been optimized.

II.5. MOLECULAR DOCKING APPROACH:

Docking is a computer simulation technique used to predict the preferred orientation of two interacting chemical species. Usually, this is the interaction of a small- to medium-sized molecule with a protein (molecular docking), but in recent years the concept has been expanded to protein-protein, protein-antibody, and protein-receptor interactions as well (macromolecular docking). Docking remains a critically important tool in the structure-based drug design process. In its most general sense, the docking process involves positioning various conformations (and potentially tautomeric forms) of one molecule with respect to another and determining the optimal interaction geometry and its associated energy.

The knowledge of the preferred orientation in turn may be used to predict the strength of association or binding affinity between two molecules using for example scoring functions.

The scoring function provides a way to rank placements of ligands relative to one another. Ideally, the score should correspond directly to the binding affinity of the ligand for the protein, so that the best scoring ligands are the best binders. Scoring functions can be empirical, knowledge based, or molecular mechanics based.

Scoring functions are fast approximate mathematical methods used to predict the strength of the non-covalent interaction between two molecules after being docked. Most commonly one of the molecules is a small organic compound such as a drug and the second is the drug's biological target such as a protein receptor [18, 19]

For the evaluation of a scoring function, an experimentally observed protein-ligand complex can be used as a positive control: Ideally, the generated ligand poses that are closest to the experimental structure should be ranked highest. In order to quantify the similarity between a native ligand and a generated ligand pose, the RMSD (Root-mean square deviation) can be calculated between both structures: The RMSD measures the average distance between atoms of two protein or ligand structures. The more the prediction of positioning is precise the higher the difference between both structure is small which will lead to a lower RMSD value. [20]

The table below (**Table IV-3**)shows how RMSD value can be interpreted:

Table IV-3: Referential RMSD values

RMSD	RMSD<1.5	1.5<RMSD<3.5	3.5<RMSD<6	6<RMSD
Structure	Perfect	Acceptable	inappropriate	Not acceptable

MOE's Dock application (the software we going to use) searches for favourable binding modes between small- to medium-sized ligands and a not-too-flexible macromolecular target, which is usually a protein. For each ligand, a number of placements called poses are generated and scored. If desired, the poses can be covalently bound to a receptor side-chain atom. The score can be calculated as either a free energy of binding including, among others contributions, solvation and entropy terms, or enthalpy terms based on polar interaction energies (including metal ligation) or as qualitative shaped-based numerical value.

The final highest scoring poses, along with their scores and conformation energies, are written to a database where they are ready for further analysis.[21]

II.5.1. Interactions protein-ligand (TRPV1- Capsazepine) :

After the last molecular dynamics process, the obtained stable system contains protein *TRPV1* complexed with Capsazepine (ligand of reference), this interaction could be measured for each cavity of the four available cavities using MOE and then visualized, but since all cavities are identical, one of these cavities was chosen for further studies to make interpretation much easier. The results of interaction between the ligand and the receptor is shown in **Figure IV.16** and **Figure IV.17**
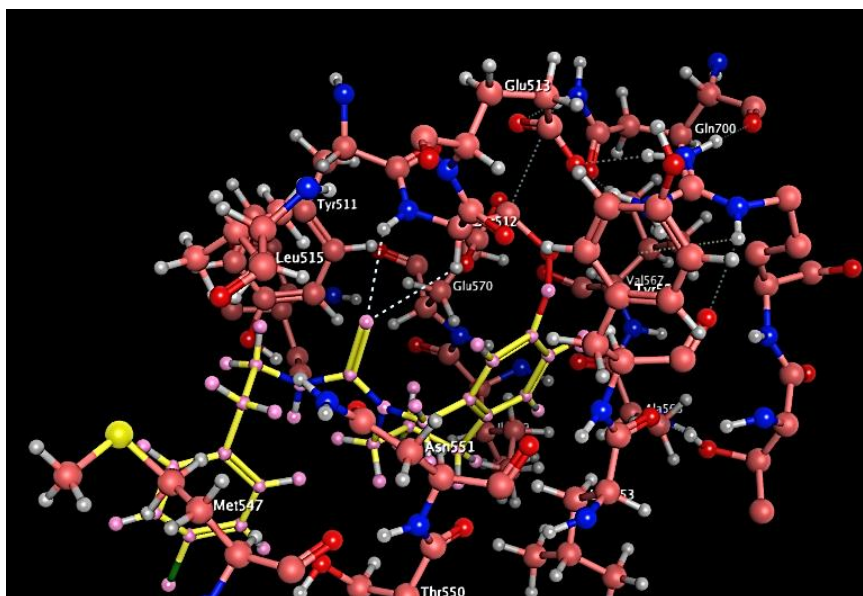

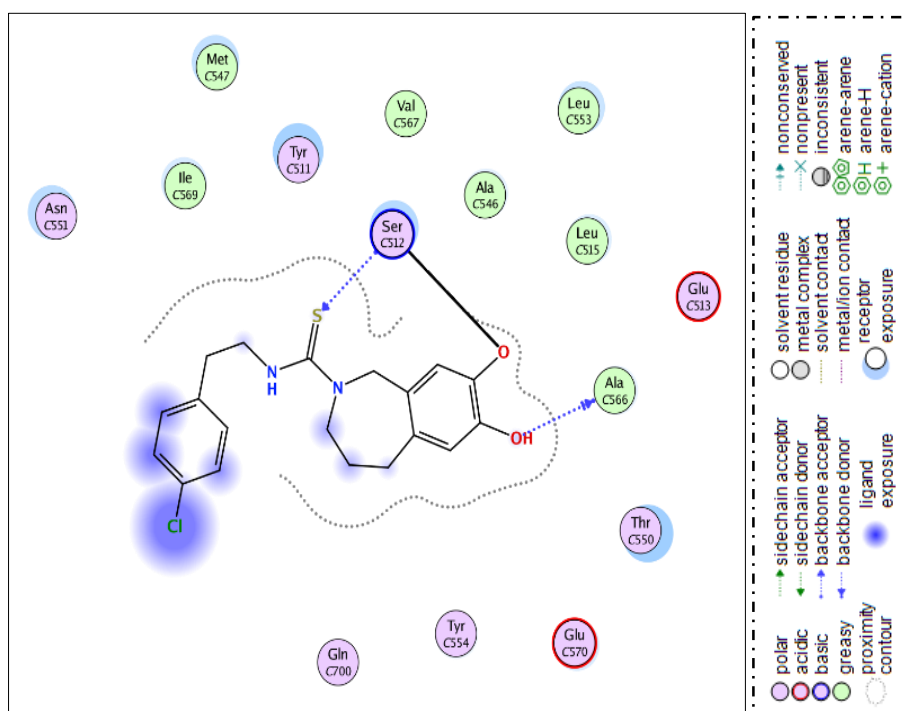*Figure IV.16:Ligand-receptor interactions visualisation (Capsazepine -TRPV1)*

Figure IV.17:Ligand-receptor interactions (Capsazepine -TRPV1) (schema)

With MOE, the RMSD and Scoring for the ligand of reference were recorded and the results are shown in the table below:

Table IV-4: RMSD and Scoring results of Capsazepine

Ligand	Scoring	RMSD
Capsazepine	-6.05513239	1.5911684

The importance of these previous results is that its considered as a reference for further docking evaluation, the closer the score of future ligand to reference is, the more it is acceptable as a potential alternative for the reference ligand.

II.5.2. Interactions protein-future ligand (TRPV1-curcuminoids) :

After creating a new database with all previously optimized curcuminoids, the Docking study was realised using MOE software with default settings; consequently, **Table IV-5** below summaries the Investigated database docking results.

Table IV-5: RMSD and Scoring results of Curcuminoids

Ligand	Score	RMSD
Capsazepine (reference)	-6.05513	1.5911684
Curcumin (enolate)	-6.4520	2.2610
Curcumin (enol)	-6.7976	1.5541
Demetoxycurcumin	-6.3688	1.6648
Bisdemethoxycurcumin	-6.0301	1.1846

The Observation noted from these values is that all Score values are too close to each other, with an acceptable RMSD results in general.

As a further approach to the interaction study, the interaction details for the curcuminoids with the residues of the active site were visualised (schematised and illustrated) with the obtained steric distance and reported for each complex as shown below:
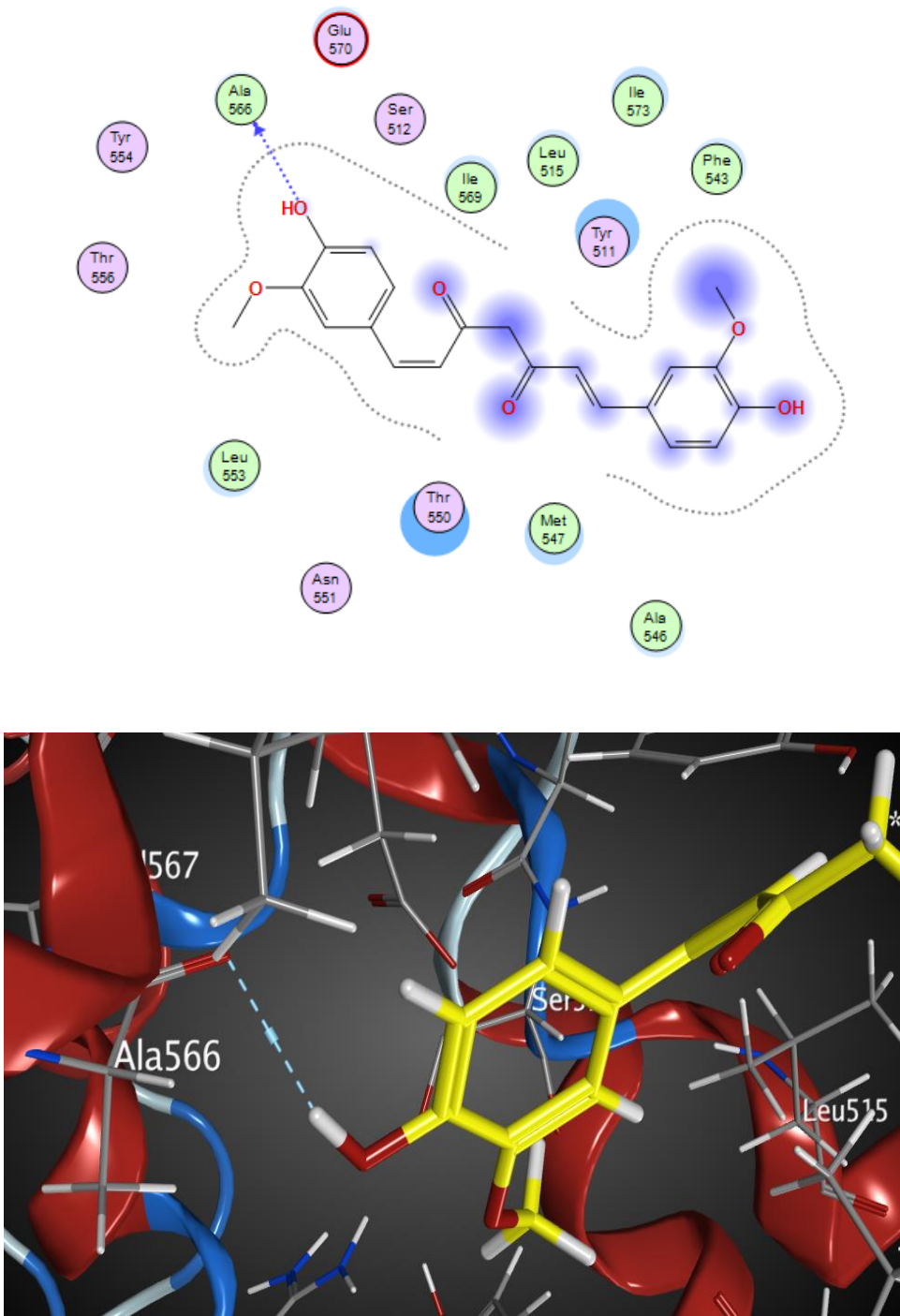
Ligand	Receptor	Interaction	Distance	E(Kcal/mol)
O$_{24}$	O ALA 566	H-donor	3.25	-0.8

Figure IV.18:Curcumin (enolate) interaction with TRPV1 report
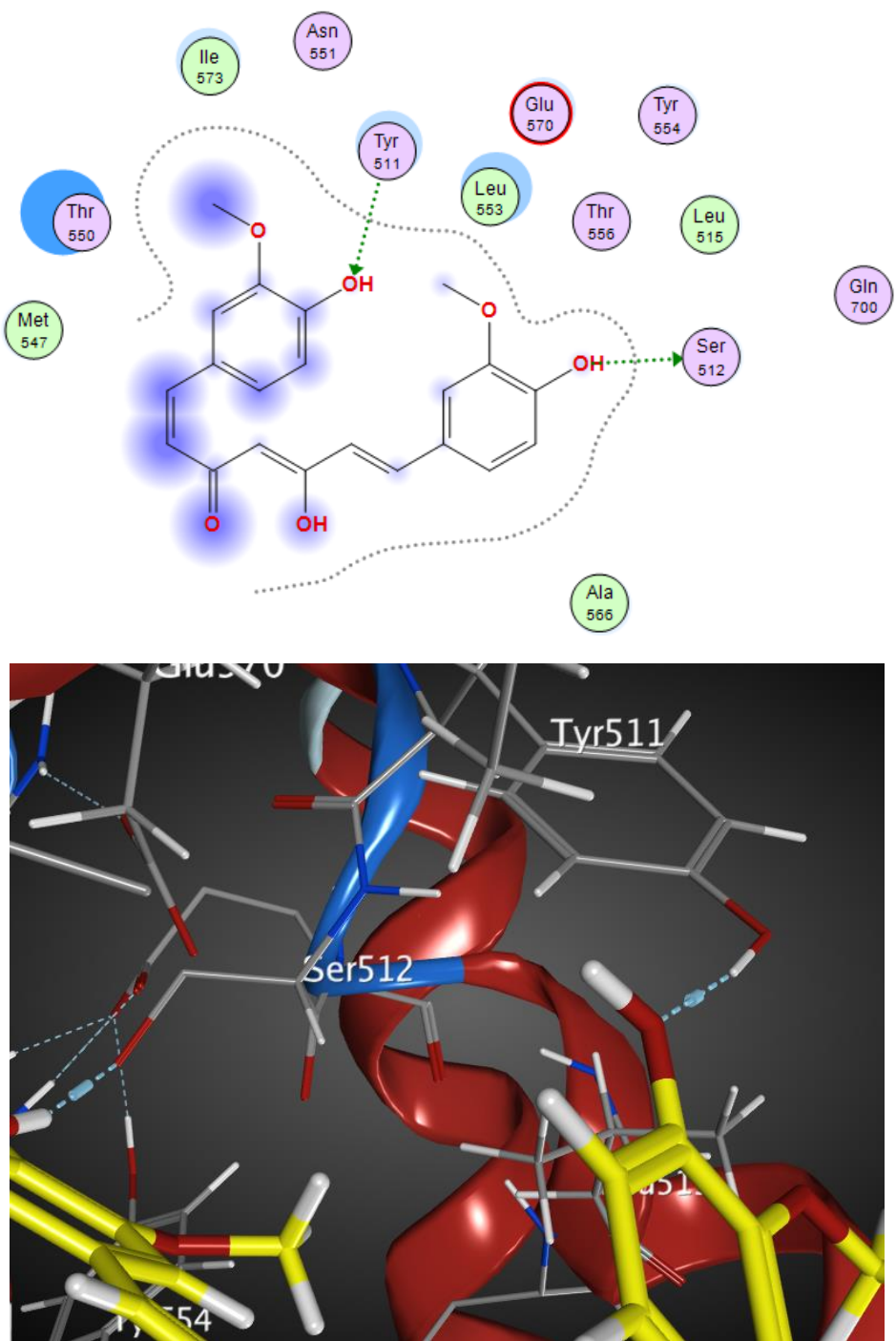
Ligand	Receptor	Interaction	Distance	E(Kcal/mol)
O_7	OG SER 512	H-donor	2.73	-1.6
O_{25}	OH TYR 511	H-acceptor	2.95	-1.0

Figure IV.19:Curcumin (enol) interaction with TRPV1 report
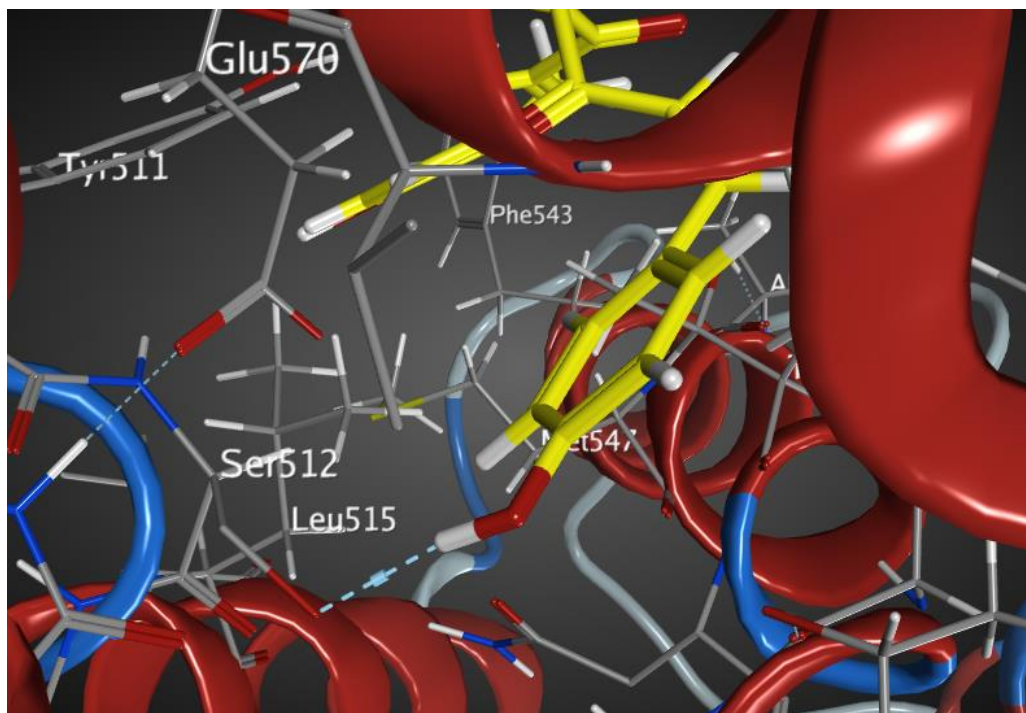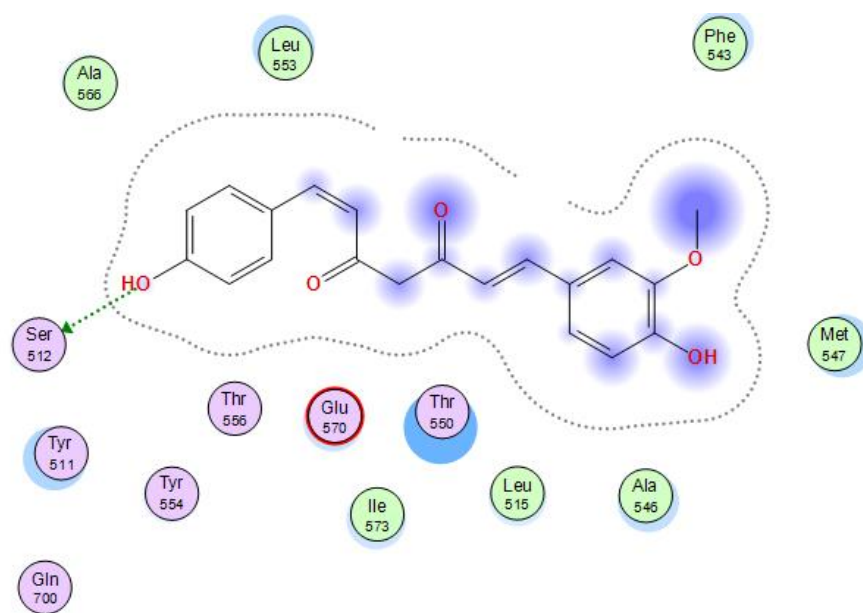
Ligand	Receptor	Interaction	Distance	E(Kcal/mol)
O_5	OG SER 512	H-donor	2.77	-1.4

Figure IV.20:Demetoxycurcumin interaction with TRPV1 report
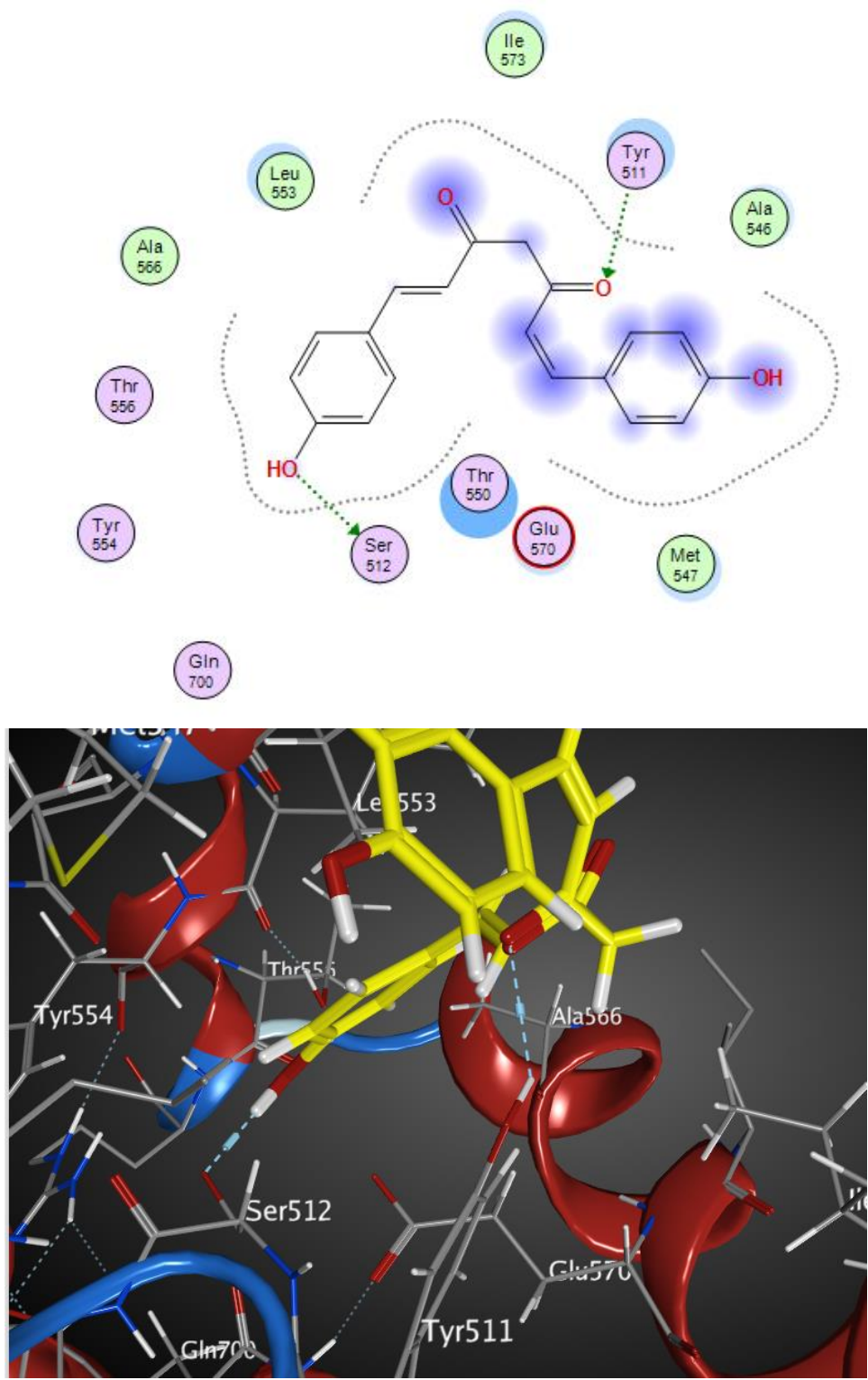
Ligand	Receptor	Interaction	Distance	E(Kcal/mol)
O_{14}	OG SER 512	H-donor	2.74	-1.6
O_1	OH TYR 511	H-acceptor	3.11	-0.7

Figure IV.21:Bisdemethoxycurcumin interaction with TRPV1 report

II.6. RESULTS AND DISCUSSION:

From previous docking reports and the obtained results, we found that all the investigated curcuminoids actually do interact with the active site of TRPV1; Curcumin (enol) and Bisdemetoxycurcumin surprisingly were attached to the same receptors (residues: **serine 512; Tyrosine 511**).

The distance values were too close between the three structures and the only one major difference was the ligand's atom within which the interactions were assigned to.

On the other hand, Demethoxycurcumin shows only one interaction with the residue **Serine 512,** which is the same residue as the other curcuminoids with the exception of Curcumin (enolate) ; interacted only with one residue : **Alanine 566**

Another notice, we know that curcumin has a vanilloid ring molecular moiety,which is the critical chemical structure for the regulation of TRPV1 as referred in this research[4, 22] .And as expected from this docking research all the investigated curcuminoids clearly indicated the importance of this structure as it was included in all interactions.

On a wider level, the docking study reveals that the distance between each curcuminoids and the binding sites was between [**2.74-3.25**] and all these interactions were a hydrogen bond type. As an interpretation, some studies show that the definition of a strong hydrogen bond is when the steric distance is between $2.5\,Å< \; D_{D\text{-}A} <3.1\,Å$.

Meanwhile a distance between $3.1\,Å< \; D_{D\text{-}A} <3.55\,Å$ is considered as a weak bond interaction[23]

So according to these study results we can say that all curcuminoids with exception of curcumin (enolate) create hydrogen bonds characterised as strong bonds.

The importance of these bonds is that the strong and weak hydrogen bonds are ubiquitous in protein–ligand recognition, and that with suitable computational tools very large numbers of strong and weak intermolecular interactions in the ligand–protein interface may be analysed reliably.[24]

Additionally, the reports show that all previous bond energy are weak, this weakness can lead to form a stable complex between ligand's atoms and the residues of the active site.

As a deeper docking study, we suggest that optimizing the enol form for Bisdemethoxycurcumin and Demetoxycurcumin might give a significant change, although there still no evidence that these two analogues have any inhibition or biological activity towards this selected protein.

Compared to curcumin previous results and researches indicate that curcumin inhibit visceral nociception via antagonizing TRPV1 and may be a promising lead for the treatment of functional gastrointestinal diseases.[3]

In conclusion, this study shows that the interaction between TRPV1 and the reviewed curcuminoids are possible and could be optimized and improved to obtain a better docking results that can lead onto discovering a new promising TRPV1 inhibitor.

References

1. Nalli, M., et al., *Effects of curcumin and curcumin analogues on TRP channels.* Fitoterapia, 2017.

2. Zhang, X., et al., *Effects of curcumin on ion channels and transporters.* Frontiers in physiology, 2014. **5**: p. 94.

3. Zhi, L., et al., *Curcumin acts via transient receptor potential vanilloid-1 receptors to inhibit gut nociception and reverses visceral hyperalgesia.* Neurogastroenterology & Motility, 2013. **25**(6).

4. Yeon, K., et al., *Curcumin produces an antihyperalgesic effect via antagonism of TRPV1.* Journal of dental research, 2010. **89**(2): p. 170-174.

5. Csizmadia, P. *MarvinSketch and MarvinView: molecule applets for the World Wide Web*. in *Proceedings of ECSOC-3, the third international electronic conference on synthetic organic chemistry, September 1ą30*. 1999.

6. HyperChem, R., *7.0 for windows, Hypercube*. 2002, Inc.

7. Rad, M.S., et al., *Fabrication of non-doped red organic light emitting diode using naturally occurring Curcumin as a donor-acceptor-donor (DAD) emitting layer with very low turn-on voltage.* Iranian Journal of Science and Technology, 2015. **39**(A3): p. 297.

8. Hanwell, M.D., et al., *Avogadro: an advanced semantic chemical editor, visualization, and analysis platform.* Journal of cheminformatics, 2012. **4**(1): p. 17.

9. Lee, W.-H., et al., *Curcumin and its derivatives: their application in neuropharmacology and neuroscience in the 21st century.* Current neuropharmacology, 2013. **11**(4): p. 338-378.

10. Ahmed, M., et al., *Curcumin: Synthesis optimization and in silico interaction with cyclin dependent kinase.* Acta Pharmaceutica, 2017. **67**(3): p. 385-395.

11. Domizio, D., *Development of methodologies for molecular docking and their applications.* 2009.

12. Gao, Y., et al., *TRPV1 structures in nanodiscs reveal mechanisms of ligand and lipid action.* Nature, 2016. **534**(7607): p. 347.

13. Walpole, C.S., et al., *The discovery of capsazepine, the first competitive antagonist of the sensory neuron excitants capsaicin and resiniferatoxin.* Journal of medicinal chemistry, 1994. **37**(13): p. 1942-1954.

14.   Abdel-Salam, O.M., *Capsaicin as a therapeutic molecule*. Vol. 68. 2014: Springer.

15.   ChemicalComputingGroup, M., *Molecular Operating Environment*. 2015.10, Chemical Computing Group Montreal, Quebec, Canada.

16.   Zhang, Z., et al., *Identification of cavities on protein surface using multiple computational approaches for drug binding site prediction.* Bioinformatics, 2011. **27**(15): p. 2083-2088.

17.   Molegro, A., *MVD 5.0 Molegro Virtual Docker.* DK-8000 Aarhus C, Denmark, 2011.

18.   Mohan, V., et al., *Docking: successes and challenges.* Current pharmaceutical design, 2005. **11**(3): p. 323-333.

19.   Lensink, M.F., R. Méndez, and S.J. Wodak, *Docking and scoring protein complexes: CAPRI 3rd Edition.* Proteins: Structure, Function, and Bioinformatics, 2007. **69**(4): p. 704-718.

20.   Lagarde, N., *Méthodes de criblage virtuel in silico: importance de l'évaluation et application à la recherche de nouveaux inhibiteurs de l'interleukine 6*. 2014, Paris, CNAM.

21.   Environment, M.O., *Chemical Computing Group ULC*. 2015.10, 1010 Sherbooke St. West, Suite #910, Montreal, QC, Canada, H3A 2R7, 2018. .

22.   Dulbecco, P. and V. Savarino, *Therapeutic potential of curcumin in digestive diseases.* World journal of gastroenterology: WJG, 2013. **19**(48): p. 9256.

23.   Imberty, A., et al., *Molecular modelling of protein-carbohydrate interactions. Docking of monosaccharides in the binding site of concanavalin A.* Glycobiology, 1991. **1**(6): p. 631-642.

24.   Panigrahi, S.K. and G.R. Desiraju, *Strong and weak hydrogen bonds in the protein–ligand interface.* Proteins: Structure, Function, and Bioinformatics, 2007. **67**(1): p. 128-141.

4

GENERAL

CONCLUSION

In this research we focused on studying and investigating curcumin and some curcumin analogues biological activity.

The experimental assays aimed to analyse in vitro, the antioxidant activity of curcuminoids.

Using selected experimental methods, it has been proven that extraction and separation can be processed using the presented protocol; as the TLC tests demonstrates the existence of the three intended curcuminoids (Curcumin;Demetoxycurcumin;Bisdemetoxycurcumin)

The protocol was then validated again using FT-IR spectroscopy which reinforces according to interpretations, the existence of the main important functions of the in case three analogues, and that was a powerful indicate that our work was rolling on the right pathway.

As a continuum, the antioxidant assays was remarkably very promising with the fact that the obtained results were so representative and much similar to some previous research, confirming according to **IC50** calculations; the capacity of curcumin in general to elicit an antioxidant activity. without forgetting to mention that the examined curcuminoids have different capacities as following:

Curcumin > Demetoxycurcumin > Bisdemethoxycurcumin.

In general, the experimental part was significantly very acceptable, and some slightly future changes may improve our findings to get a better result.

The theoretical approach on the other hand, highlights curcuminoids as a potential TRPV1 inhibitors using docking study as an investigation tool to validate this theory.

The optimization using Gaussian shows that there might be a difference between both curcumin tautomers in LUMO orbitals and that can influence the way each molecule interacts.

The docking study as well, shows that the interactions can be achieved between both curcuminoids and TRPV1 channels.

All the studied structures were as results show, very impressive compared to the ligand of reference; Capsazepine.

The docking interactions report, indicates that most of the molecules are bound to the same residue ; **SERIN** ,these interactions are characterised with hydrogen donor bonds which can influence the capability of the investigated molecules to create a protein-ligand complex .

In our case, all these bonds were strong bonds and that means the formed complex is generally stable.

So as a result we can say that the investigated curcuminoids can play a high role inhibiting the TRPV1 and might be a very promising future drug towards this specific target.

Abstract

The aim of this thesis is to evaluate and investigate some of turmeric biological activities using two different studies:

The experimental assay focused on evaluating the antioxidant capacities of some curcuminoids by utilizing the scavenging properties of hydroxyl radical and 1,1-diphenyl-2-picrylhydrazyl (DPPH) free radical; to obtain these curcuminoids, an extraction process was carried out, column chromatography was needed to separate each one of the analogues, then characterized by Fourier-transform infrared spectroscopy (FT-IR).

The theoretical approach investigates same curcuminoids docked with The Transient Receptor Potential cation channel subfamily V member 1 or **TRPV1** protein (PDB ID: 5IS0) to predict their putative interactions and review its inhibition capabilities towards the selected active site and compare the results to the ligand of reference (Capsazepine) After running a DFT calculations to minimize and optimize all the curcuminoids in scope.

Keywords: Antioxidant, Capsazepine, DFT, Docking, DPPH, extraction, FT-IR, separation, TRPV1, Turmeric

Résumé

Le but de cette étude est d'évaluer et d'étudier l'activités biologiques du curcuma en utilisant deux approches différentes :

L'essai expérimental a porté sur l'évaluation des capacités antioxydantes de certains curcuminoïdes en utilisant les propriétés de piégeage de radicaux hydroxyle et radicaux libres de 1,1-diphényl-2-picrylhydrazyl (DPPH); ces curcuminoïdes sont obtenus par un procédé d'extraction, suivi d'une séparation par chromatographie sur colonne pour séparer chacune des analogues. Les analogues sont caractérisés par Spectroscopie infrarouge à transformée de Fourier (IR-TF).

L'approche théorique de ces curcuminoïdes et leur complémentarité avec un récepteur transitoire canal cationique potentiel de sous-famille V 1 ou protéine de TRPV1 (ID PDB : 5IS0) a pour le but de prédire les interactions putatives et examiner ses capacités d'inhibition vers le site active sélectionné. Les résultats obtenus sont comparés avec le ligand de référence (capsazepine) après une exécution d'un calcul DFT pour minimiser et optimiser tous les curcuminoïdes portée.

Mots-clés : Antioxydant, Capsazepine,Curcuma, DFT, Docking, DPPH, FT-IR, séparation TRPV1